Universiteit Utrecht

MASTER THESIS

A journey through transport phenomena and holographic interactions in Weyl semimetals

VASILEIOS VLACHODIMITROPOULOS

Supervisors
Prof. dr. ir. Henk Stoof
Phd Vivian Jacobs

Utrecht | October 2015

"Al fin y al cabo,
somos lo que hacemos
para cambiar lo que somos"

Eduardo Galeano

Contents

Abstract

Following the discovery of topological insulators (TI) in 2005, a quest has begun in condensed-matter physics, for the discovery of more exotic topological phases of matter. One such example are Weyl semimetals (WSM), materials whose valence and conduction bands touch at a singular point in momentum space. Although these states of matter come with a number of interesting features, in this thesis we focus on their transport properties. More specifically, we concentrate on the ability of WSMs to support an electric current in the direction of an applied magnetic field, a phenomenon that came to be known as the chiral magnetic effect (CME). On the way, we come across a crucial interpretation issue, whose resolution will require bringing together physicists working on tremendously different energy scales. After establishing a consistent and physically acceptable theoretical framework, we briefly turn our attention to the current experimental status of CME. The thesis concludes with the construction of a simple holographic dual theory to WSM, through which we hope we could gain some insights into the interacting regime of WSM. Interactions are potentially of particular importance in experimental attempts to identify WSM and CME. Therefore, a model that successfully takes these effects into account is urgently on demand.

Chapter 1

Introduction

Most people remember from their high school years the 3 elementary states of matter, namely gas, liquid and solid, where each state is characterised by an increasing level of order in the system. Gases consist of particles freely moving in the available volume. In liquids, atoms[1] demonstrate some degree of interaction among themselves, and they tend to take the shape of the container they are placed in. Lastly, solids have a definite shape and in many cases their atoms are located in well-defined sites of some lattice structures, in which case we talk about crystals. Later on, we learn that materials, and solids in particular, can be further classified according to their response to an applied potential difference. This classification lead to insulators, materials that do not respond with an electric current to the external voltage[2], and conductors or metals, where an electric current appears parallel to the applied electric field.

In university, this difference was demystified. The simple, yet prevailing model is that of band theory. Electrons in solids occupy discrete energy levels, called energy bands, and they do so successively up to a maximum energy level called the Fermi level or Fermi energy[3]. Conductivity was related to the ability of electrons to move either within a band or from one band to the other. When the Fermi level is located between the two energy bands that are separated in energy the material will be called an insulator. Electrons cannot move within the lower band, because all states are occupied, and in order to move to the higher energy band an energy intake equal to the energy difference of the two bands, the energy gap, is required. On the other hand when the Fermi level lies inside an energy band, the material is a conductor. Electrons within a band can occupy nearby states and a current can develop easily.

As the energy gap becomes smaller but remains non-zero, we go into the regime of semiconductors. Their remarkable electronic properties have led to a tremendous growth in technological advancements following the invention of transistor in 1947 by Bardeen, Brattain and Shockley [1]. A further, internal, classification in the semiconductor family can be made according to which is the carriers of the electric current. Therefore, when the doping is such that electrons are the majority carriers and holes are the minority ones, we have n-type semiconductors. In the reverse case we refer to the material as p-type semiconductor. Finally, in the absence of any doping we end up with an intrinsic semiconductor and electrons and holes are treated on equal footing. The last member of the list, and the one that we will be occupied with for the rest of the thesis, arises when the two bands touch at a single point at the Fermi level. This type of behaviour is called semi-metallic and it will give rise to some remarkable properties fundamentally different from the previous ones. A schematic visualisation of this classification

[1] In this context the word is "atoms" is used in the philosophical sense, and refers to the smallest constituent particles that comprise the liquid and the solid. They can be atoms in the physicist's sense, molecules, ions, etc.

[2] Of course assuming a small external perturbation

[3] Rigorously speaking, the two concepts coincide only at zero temperature. However, since the main result of our analysis is calculated at $T = 0$, we shall use the two terms interchangeably.

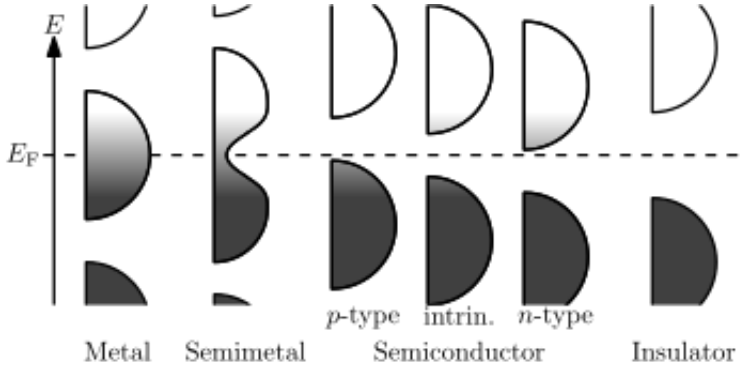

Figure 1.1: Filling of the electronic density of states in various types of materials at equilibrium. Here the vertical axis is energy while the horizontal axis is the Density of states for a particular band in the material listed. In metals and semimetals the Fermi level E_F lies inside at least one band. In insulators and semiconductors the Fermi level is inside a band gap; however, in semiconductors the bands are near enough to the Fermi level to be thermally populated with electrons or holes.

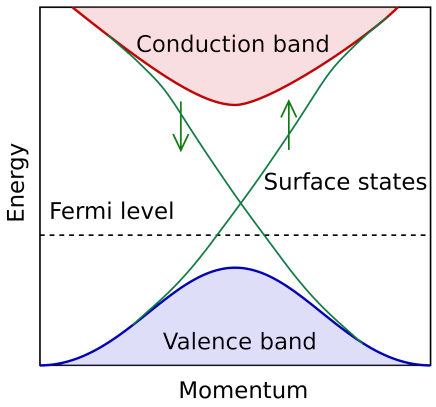

Figure 1.2: Band structure of a Topological Insulator. The dispersion relation of the bulk conduction and valence bands are plotted in red and blue colour respectively. Contrary, the dispersion relation relation of the surface states is plotted in green with the arrows indicating the spin polarization. Evidently, the material is an insulator in the bulk, with the Fermi level lying in the gap between the valence and the conduction bands. At the same time, the surface states cross it, leading to a conducting behaviour on the boundary.

can be seen in Fig. (1.1) [4].

This was the situation until the beginning of the 21^{st} century and each solid was thought to belong in one of the above categories. Then in 2005 Mele and Kane paved the way for a new era in condensed matter physics with the discovery of topological insulators (TI)[2]. This novel state of matter, elongated the above list with the first member of the subcategory that came to be known as topological phases of matter. What is special about TIs is an interesting coexistence of an insulating bulk with conducting surface states on their boundary. In simple words, the bulk bands are separated by an energy gap within which the Fermi level lies, and at the same time there exist states whose wavefunctions are localised on the surface of the material and whose corresponding energy bands cross the Fermi level. Fig. 1.2 depicts the situation quite accurately.

An intuitive way of thinking of a TI goes as follows[5]. The internal structure of a TI is such

[4]Borrowed from wikipedia.org

[5]The example was taken from a talk given by M.Z. Hasan.

that a surface electron sees no energy gap and can therefore move freely on the surface. On the contrary, in the "vertical" direction towards the bulk, there is a potential barrier that prevents such motion. Although a detailed analysis of TI goes beyond the scope of this thesis, it is important to note that these conducting states are protected by symmetry against perturbations. The existence of an associated quantity that can take only integer values, and therefore cannot change its value continuously, i.e. under a small perturbation, is the most important feature, common in all phases of matter that claim to be topological. But TI was only the beginning for a whole new quest in the scientific community that goes under the banner of condensed matter physics. It was the quest for phases of matter whose properties have their roots in topology and therefore can demonstrate great robustness against perturbations.

An immediate, naive generalisation of the concept of TI would be a topological conductor (TC), i.e. a state of matter that is conducting in the bulk and also supports conducting surface states. But does this sentence even make sense? A TC would be either a trivial state of matter, i.e. a conductor in the ordinary sense, or its surface states would simply decay into the bulk. Remember the intuitive picture with the surface electron on the boundary of a TI. In the case we are discussing now, there is no barrier in the "vertical" direction to prevent the electron from diving into the bulk. Therefore, a TC doesn't seem a very realistic option.

However, it seems that TCs exist and the crucial condition for their existence lies in the topologically non-trivial structure of their momentum space. To be precise, these materials are not conductors in the strict sense in the bulk. Rather they have two energy bands touching at a singular[6], people used to call it *diabolical*, point in momentum space. Eventually, the term that is used from scientists to describe such materials is *topological semimetals*.

It is this type of physical systems that we will try to understand in this thesis, using some conventional, field-theoretic tools but also some other that we borrowed from our high-energy partners working on string theory!

1.1 Into the Weyl

We now turn our attention on a particular type of semi-metals. The crucial, distinctive feature of these systems, is their linear dispersion relation around the band touching point. To see how this can happen, assume that we set up a $2-$band Hamiltonian for the system whose two eigenvalues cross at a point in momentum space. Then, if the linearised Hamiltonian, about the crossing point, reads

$$H(\vec{k}) = \pm v_f \vec{\sigma} \cdot \vec{k}, \tag{1.1}$$

then the system we describe is termed Weyl semimetal (WSM)[7]. In eq. (1.1), $\vec{k}$ measures momenta around the touching point. This is simply the Weyl equation describing massless, chiral fermions of spin$-1/2$. What this means is that the electrons around the Fermi point of a system described by the initial, non-linearised, Hamiltonian behave effectively as pseudo-relativistic chiral fermions! The "pseudo" term suggests that the quasiparticle's velocity is a few orders of magnitude less than the speed of light. Indeed, this quantity is a parameter of our effective model and can be determined experimentally.

Even at this starting point we can have some signs of the robustness of this system that as we shall shortly see has an underlying topological origin we have long been praising for. A crucial aspect of robustness lies in the dimensionality of the system. In 2 dimensions the Hamiltonian can be explicitly written as

[6]The singularity of the band touching point will be better understood in the next sections when we introduce the concept of Berry phase.

[7]In general the Hamiltonian would read $H(\vec{k}) = \pm \sum_{ij} v_{ij} \sigma^i k^j$.

$$H(\vec{k}) = \pm v_f(\sigma^x k_x + \sigma^y k_y). \tag{1.2}$$

In this case, the system has two bands that disperse like $\epsilon(\vec{k}) = \pm\sqrt{k_x^2 + k_y^2}$ and therefore there is a touching point of the two bands at the so called Weyl point [8] at $k_x = k_y = 0$. A perturbation of the system proportional to any of the two already used Pauli matrices, simply shifts the Weyl point in momentum. Similarly, any "mass term" perturbation, i.e. a term proportional to the identity matrix, simply shifts the point in energy. However, a perturbation proportional to the third Pauli matrix opens up a gap and therefore destroys the Weyl touching point.

On the contrary, in three dimensions the Hamiltonian reads

$$H(\vec{k}) = \pm v_f(\sigma^x k_x + \sigma^y k_y + \sigma^y k_y), \tag{1.3}$$

with a band touching point at $k_x = k_y = k_z = 0$ and all Pauli matrices used up. In this case any possible perturbation can be decomposed into the three already used Pauli matrices and the unit matrix. Therefore, it can only lead to shifts in the location of the Weyl point in momentum space but never to a gap opening. What the above discussion has shown is that Weyl point are robust against perturbations in 3 dimensions but not in 2! Therefore, we have seen that dimensionality is an important characteristic of topological semimetals.

The second crucial property that need to be fulfilled, for a Weyl point to exist, is that either time reversal (TR) or inversion (I) symmetry must be broken. TR symmetry inverts both momentum and spin, so that for a TR symmetric system $E_\sigma(\vec{k}) = E_{-\sigma}(-\vec{k})$. Thus, if a Weyl point exist at momentum $\vec{k}_w$ with a given chirality, then there exist another Weyl point at $-\vec{k}_w$ with the same chirality. On the contrary, I symmetry affects only the momentum leading to $E_\sigma(\vec{k}) = E_\sigma(-\vec{k})$. Hence, if a Weyl point exists at momentum $\vec{k}$ then there exist another Weyl point at $-\vec{k}$ with opposite chirality. As a result, breaking of TR symmetry leads to two Weyl cones being separated in momentum, while I symmetry breaking leads to a separation in energy[9]. Instead, a TR and I symmetric system has two doubly degenerate bands touching at a 4-fold degenerate point in momentum space that we shall call a Dirac point. The low-energy excitations of such a solid will be determined by the massless Dirac equation in 3 dimensions which reads

$$H_{Dirac}(\vec{k}) = \hbar v_f \begin{pmatrix} \vec{\sigma}\cdot\vec{k} & 0 \\ 0 & -\vec{\sigma}\cdot\vec{k} \end{pmatrix}. \tag{1.4}$$

We see that this 4×4 Hamiltonian is by no means stable to arbitrary perturbations. Therefore, robustness of a Dirac point in $d = 3$ dimensions is strongly dependent on the survival of both TR and I symmetries in the system.

Before moving further with the theoretical analysis of WSM, it is worth mentioning that as of 2015, WSM are no longer a mere mathematical artifact. On the contrary, experimental groups have managed to successfully identify a WSM behaviour in TaAs compounds [3, 4].

1.2 Topological character of WSM

We believe that it is clear by now, that WSM belong to the category of topological phases of matter. The robustness of the touching point against perturbations that we just described is definitely a good indication of the topological origin of WSM. However, in this section, we can be more concrete and define a topological invariant associated to the Weyl node. The quantity that will provide us with this topological invariant is Berry phase.

[8] Note the change of name from Fermi to Weyl point.

[9] The notion of separation we are referring to, will be made clear in chapter 2 when we break inversion symmetry of the system.

In 1984 Berry proposed that for systems that undergo a cyclic, adiabatic change, their state vector does not necessarily return to its original value but may acquire an extra geometrical phase factor [5]. This extra phase came to be known as the Berry phase and is given by the formula

$$\gamma_n = i \int_{\mathcal{C}} d\vec{R} \langle n(\vec{R}) | \nabla_{\vec{R}} | n(\vec{R}) \rangle = \int_{\mathcal{C}} d\vec{R} \cdot \mathcal{A}(\vec{R}), \tag{1.5}$$

where $\mathcal{A}(\vec{R}) \equiv i\langle n(\vec{R})|\nabla_{\vec{R}}|n(\vec{R})\rangle$ is the so called Berry curvature. The name suggests some connection to the electromagnetic gauge field and we will shortly see that this is indeed the case. In eq. (1.5), $\vec{R}$ denotes an abstract vector consisting of a number of quantities parametrising the system, $|n(\vec{R})\rangle$ is the state of the system for the a given value of the vector $\vec{R}$ and γ_n the Berry phase that the system gets after $\vec{R}$ has completed a cyclic evolution in parameter space that is described via the closed path $\mathcal{C}$. Under this perspective, the term *geometric* can be attributed to the geometrical properties of the parameter space. If the path in $\vec{R}$-space is trivial then the state vector does not acquire an extra phase. If on the other hand the system will "enclose a peculiar point[10]" after a cyclic, adiabatic change, then the state of the system will change by this extra Berry phase.

A few years later, in 1989, Zak applied Berry's formula in the context of condensed matter systems [6]. In fact, due to the periodicity of the Brillouin zone (BZ), Berry's phase finds a natural realisation in solid state physics. Here the role of the abstract parameter vector $\vec{R}$ is played by the momentum wavevector $\vec{k}$ which characterises the Bloch state of the system. In this context, we can define the Berry connection $\mathcal{A}(\vec{k})$ and the corresponding Berry curvature $\vec{B}(\vec{k})$ as

$$\begin{aligned} \mathcal{A}(\vec{k}) &= -i \sum_n \langle u_{n,\vec{k}} | \nabla_{\vec{k}} | u_{n,\vec{k}} \rangle \\ \vec{B}(\vec{k}) &= \nabla_{\vec{k}} \times \mathcal{A}, \end{aligned} \tag{1.6}$$

where the role of the arbitrary state vector $|n(\vec{R})\rangle$ is now played by the Bloch state $|u_{n,\vec{k}}\rangle$.

Let us see more explicitly, what this means for our case. The Hamiltonian for both chiralities can be written in the form $H = \kappa v_F \vec{k}.\sigma$, where $\kappa = \pm$ denotes the chirality of the node. By construction, this Hamiltonian has two eigenstates of the form

$$|+\rangle = \begin{pmatrix} \cos\frac{\theta}{2} e^{-i\phi} \\ \sin\frac{\theta}{2} \end{pmatrix} \qquad\qquad |-\rangle = \begin{pmatrix} \sin\frac{\theta}{2} e^{-i\phi} \\ \cos\frac{\theta}{2} \end{pmatrix}, \tag{1.7}$$

with corresponding eigenenergies $E_+(p) = \kappa v_f p$ and $E_-(p) = -\kappa v_f p$. This means that the $|+\rangle$ state is a positive energy eigenstate for the right chiral fermion while the $|-\rangle$ state is a positive energy eigenstate for the left one. In the above notation, θ and ϕ denote angles in momentum space.

Then, replacing eq. (1.7) in Berry's formulas in eq. (1.6), we see that the positive energy eigenstates for the two chiralities lead to an expression for the Berry curvature of the form

$$\vec{B}(\vec{k}) = \kappa \frac{1}{2k} \hat{k}. \tag{1.8}$$

Therefore, the Berry curvature of a Weyl point of positive (negative) chirality has the same form as a magnetic monopole (antimonopole) in momentum space. It is in this sense that a Weyl point "emits magnetic flux in momentum space". Calculating the total flux around each Weyl point, we find that each Weyl node is associated with a ± 1 quantum of Berry flux, in units of 2π, the sign of which depends on the chirality of the node, namely

[10] Both terms are used in a loose sense at this moment.

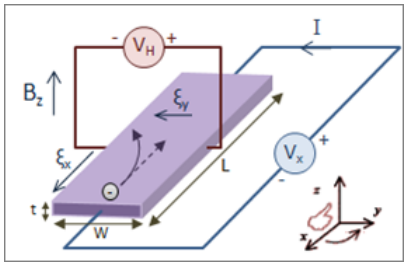

Figure 1.3: AHE denotes the appearance of a potential difference, V_H, in the direction transverse to an applied electric field, V_x, in the presence of a perpendicular magnetic field, B_z.

$$\int_S \vec{B}(\vec{k}) \cdot d\vec{S} = \kappa 2\pi \tag{1.9}$$

What the above analysis has shown us, is that a Weyl point is a topological object in momentum space; it is a point from which Berry flux emanates or sinks into. It is precisely this topological character that ensures stability and robustness of Weyl nodes against perturbations. Nonetheless, there is a way in which a Weyl point can be destroyed. This possibility arises when two Weyl nodes of opposite chirality annihilate each other when they meet in momentum space.

As a concluding remark, the situation is completely analogous to electrons in real space. Electrons are monopoles of electric field and by charge conservation these monopoles can only disappear if they meet with a monopole of opposite charge. Similarly, WSM are monopoles of Berry flux in momentum space, and the stability these configurations exhibit in the space where they live, ensures that the corresponding physical system is also stable against perturbations.

1.3 Topological electromagnetic responses

The second topological feature of a Weyl semimetal, and the one that we will be mostly concerned with in this thesis, is its topological response to an external electromagnetic field. The topological character of the response lies in the fact that it is directly related to the position of the Weyl nodes in momentum space and is insensitive to any other parameters of the system. There are two distinct responses that can be directly related to the topologically non-trivial nature of Weyl nodes: the anomalous Hall effect (AHE) and the chiral magnetic effect (CME). Although we shall be mostly interested in the latter, it is instructive to have a feeling of the underlying physics behind both effects.

1.3.1 Anomalous Hall Effect

In 1879, Edwin Hall observed a voltage difference in the direction transverse to the electric current induced by applied electric field, in the presence of an external magnetic field in the direction perpendicular to the current, Fig. 1.3. This off diagonal components in the conductivity tensor came to be known as the Hall effect. Shortly after his first discovery, he reported that the effect was nearly ten times stronger in ferromagnetic iron than in non-magnetic conductors. This latter much stronger effect in intrinsically magnetic materials was termed the anomalous Hall effect. Although the experimental discovery of the effect was made towards the end of the 19th century, it took scientist nearly 100 years to come up with the right theoretical description. The main reason for this delay lies in the fact that a proper model for AHE required concepts related to topology and geometry, such as the Berry phase, whose proper definition came about only quite recently.

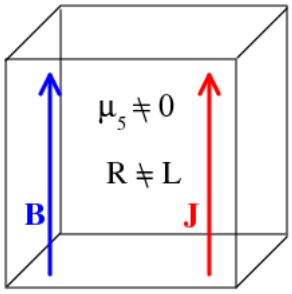

Figure 1.4: In systems with chiral charge imbalance, i.e. $\mu_5 \neq 0$, an collinear electric current is expected to appear as a response to an external magnetic field.

A controversial part in the story of AHE has been the relative importance of the two terms that constitute the effect. On the one hand, there are intrinsic properties of the electronic structure that contribute to the so called intrinsic AHE. On the other, impurity scattering gives rise to extrinsic AHE. In general ferromagnetic metals, both contributions are of the same magnitude and therefore an experimental separation of the two is a rather difficult and subtle matter. However, as Burkov pointed out [7], extrinsic contributions to the AHE are absent in the case of WSM and only the intrinsic ones survive. The latter is found to be proportional to the separation of the two nodes in momentum space and is nearly insensitive to deformations of the Fermi surface. The formula that gives the AHE current can be found to be

$$j^{\nu} = \frac{e^2}{2\pi^2} b_{\mu} \epsilon^{\mu\nu\alpha\beta} \partial_{\alpha} A_{\beta}, \tag{1.10}$$

where b_{μ} is the vector separating the two Weyl nodes in momentum space and A_{μ} is the applied gauge field.

1.3.2 Chiral Magnetic Effect

Athough AHE has great physical importance, it is not a novel feature of WSM. The truly and inherently unconventional properties of this new class of topological mater came with the theoretical discovery of CME. This effect is expected to occur in chiral systems with a chiral charge imbalance, and denotes the appearance of an electric current along the direction of an externally applied magnetic field. This behaviour is captured in Fig. 1.4. The proportionality constant between the response current and the applied magnetic field is termed CME conductivity and, as we shall prove in chapter 2, is found to be

$$\vec{j} = \frac{e^2}{2\pi^2} \mu_5 \vec{B}, \tag{1.11}$$

where $2\mu_5$ is the chiral chemical potential imbalance or equivalently the separation of the Weyl points in energy[11].

As we can see, the resulting expressions indeed depend only on the separation of the Weyl points in momentum space as we have anticipated and therefore verify their topological origin. We will devote a great part of the thesis discussing CME, therefore we shall refrain from making any further comments at this point.

[11] To make connection with the notation of chapter 2, if $\mu_R = b_0$ and $\mu_L = -b_0$ are the chiral chemical potentials, then $\mu_5 = \frac{\mu_R - \mu_L}{2} = b_0$. Thus the two symbols will be used interchangeably.

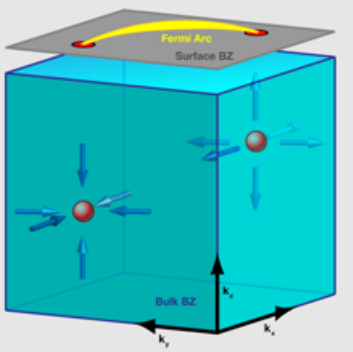

Figure 1.5: The bulk Brillouin zone is depicted in light blue colour where the two Weyl nodes are present. The arrows indicate the direction of the Berry curvature and denote the monopole (arrows pointing outwards) and the anti-monopole (arrows pointing inwards). The surface Brillouin zone is depicted in grey colour. The projections of the Weyl nodes onto the surface Brillouin zone, are connected with a conducting surface arc, called the Fermi arc.

1.4 Topological surface states - Fermi Arcs

The last property of WSMs we will comment on, and is also related to their topological nature, has great significance in the attempts to experimentally identify them. As we have stated before, a crucial characteristic of topological states of matter is the existence of topologically protected surface states. In the case of topological insulators, the bulk gap leads to protected conducting surface states whose existence is ensured by the gap of the bulk. In the case of WSM, the bulk is also conducting because of the touching point of the two bands and naively one would expect that no surface states exist. Such an expectation sounds reasonable because surface modes might merge with the bulk ones leading to a collapse of the notion of a surface state.

Nonetheless, due to the topological properties of momentum space, surface states can indeed survive. The general picture is vividly captured in Fig. 1.5. There one can see both the bulk and the surface Brillouin zones of a WSM. In the bulk, the two momentum space monopoles that correspond to each Weyl fermion are clearly distinguished. As we have commented, Berry flux emanates from one and dives into the other. However, in the surface Brillouin zone, the projections of the two monopoles are connected via a line of conducting states that are highly localised on the surface of the WSM. Therefore, in the case of WSM we no longer have closed Fermi surfaces, rather open Fermi arcs and these can be experimentally seen.

1.5 Free electrons are not enough

So far, we have dealt with fermionic systems with band touching points, and the interesting effects their topologically non-trivial momentum space gives rise to. All the analysis that we previously described is based on the concept of band theory whose main assumption is that the electrons in the solid are non-interacting. Such an assumption, even if justified in some cases, limits significantly the accessible physical systems that we can model. Interactions might give rise to fundamentally different physics that free the free approximation cannot capture. Therefore, we want to find a tool to describe the interaction mechanisms in solids and in Weyl semimetals in particular.

Perturbation theory has been so far a very successful tool for such a description. Yet, its validity is ensured, provided that the interaction model contains a sufficiently small parameter around which we can perform a Taylor expansion. If for example, our system can be described by a field theory action and the interaction term is added via a small coupling constant, then the partition function $\mathcal{Z}$ can be expanded in this sense. Thus, Feynmman diagrams provide a

very effective tool to obtain expectation values of the various operators of interest. So, in the weak coupling regime, interactions have been included in a properly working paradigm.

On the contrary, strongly interacting systems cannot always be modelled and described in a systematic way. In this case, Taylor expansion of the partition function is no longer possible as the coupling constant of the interaction term is not small and therefore the expansion breaks down; in short, a diagrammatic treatment of strongly coupled field theory is not valid. It is precisely this strongly coupled regime of interacting Weyl fermions that we will try to approach. Maybe it is trivial to note that leaving the weak coupling regime, does not come for free. Neither does it suggest that we can describe any type of strong interaction. On the contrary, in order to make further progress we need to specify the nature of the interactions and construct a mathematical framework that best suits for their description.

The first assumption that we make, is that the fermionic interactions can be modelled via coupling the free fermion to a quantum critical system, i.e. a system around a quantum critical point (QCP). To keep matters simple, we assume that such a system can be expressed in terms of a single complex scalar field Φ. If the interactions were small, the Φ field could have been pertubatively integrated out and an effective potential for the free fermion would easily arise. If, as in the case we are considering, the interactions are strong and the above scheme failed, then we further simplify the problem, assuming that the QCP is described by a strongly coupled conformal field theory (CFT).

This assumption is usually realistic since the main property of systems at the phase transition point is their scale invariance, dictated by a divergent correlation length, which is a crucial feature of a CFT. However, the conformal group has additional symmetries which are not always obeyd by a system at QCP. Believing that scale invariance is a good enough starting point, we then set off to determine correlation functions of conformal operators, having certain conformal dimensions, which are the main objects of a CFT. Even now, our task is not easy in any sense, principally because we have no clue about the generating functional or the microscopic composition of the operators of the theory. What we only know is their conformal dimension and symmetry properties.

Hence, to sum up, although we have reduced the problem of the interacting Weyl semimetal, to the calculation of n-point functions of *some* operators of *some* strongly coupled CFT, we don't know *neither* the operators *nor* the theory in which these unknown operators live! The situation doesn't seem quite encouraging, does it?!

1.5.1 AdS/CFT correspondence

Quite remarkably string theory is here to save the day and show us the way out of this apparent dead in that we put ourselves into[12]! The way out that we shall follow, has its roots in the holographic principle proposed by Gerard 't Hooft and Leonard Susskind, suggesting that information of a string theory in a bulk spacetime can be encoded on its boundary [8, 9]. Stepping on this proposal, Juan Maldacena conjectured in 1997 that string theories in spacetimes with constant negative curvature, Anti deSitter (AdS), are in some sense equivalent to CFTs defined on their boundary, which is of one dimension less [10]. The canonical example of Maldacena's conjecture is the duality between type II-B superstring theory defined on $AdS_5 \times S_5$ and an $\mathcal{N} = 4$ supersymmetric Yang-Mills theory in 3+1 dimensions. Nonetheless, proposals have been made for other theories as well.

In the appropriate limit of the correspondence, the string theory side of the duality reduces to classical gravity described by Einstein's theory while the field theory side corresponds to the strong coupling with large-N_c (i.e. large "color") and large 't Hooft coupling limit. Although a rigorous proof of the correspondence is still missing, Maldacena's conjecture has survived a large number of numerical tests and therefore expectations that we are on the right track are

[12] After all nobody forced us to take the assumptions we took!

high.

Instead of getting into the cumbersome mathematical details of the conjecture, that will take us away from our path, we shall give two physically intuitive arguments that support the conjecture. The first one, is related to the degrees of freedom (dof) of the theory. Dofs of a system are counted by its entropy. In a QFT the entropy is an extensive quantity meaning that it scales with the volume. On the contrary, in a theory of gravity, the entropy is bounded by the entropy of a black hole surrounding the volume, the Bekenstein bound, and which scales with the area of the black hole [11, 12]. Therefore, entropy in a theory of gravity in d dimensions scales in the same way as a field theory defined in a $(d-1)$-dimensional spacetime.

The second argument in support of the correspondence, lies in symmetry. A conformal field theory is characterised by conformal invariance i.e invariance under conformal transformations. These transformations form a group, the so called conformal group, which is isomorphic to $SO(d_{cft}+1,1)$, where d_{cft} denotes the dimension of the spacetime where the CFT lives in. Similarly, the AdS spacetime is characterised by a set of transformations that leave the metric invariant. One can easily see that the AdS symmetry group is also isomorphic to $SO(d_{ads},1)$, where it was assumed that the AdS spacetime is $d_{ads}+1$-dimensional. Therefore, the symmetry group of a CFT living in a d-dimensional spacetime, is isomorphic to the symmetry group of an AdS space of one dimension higher.

Hoping that the two previous arguments were sufficient to motivate the reader, the moral strory of the correspondence goes like this: ignoring all fancy, mathematical details, the basic tool that 't Hooft, Susskind and Maldacena[13] have given us, is that a strongly coupled conformal field theory "is" dual to **some** theory of classical gravity. In essence, the main idea of AdS/CFT correspondence is captured in the following compact yet elegant formula[14]

$$\langle e^{\int d^d x \mathcal{O}\phi}\rangle_{CFT} = \exp(\frac{i}{\hbar} S_{bulk}[\chi \to \phi]). \tag{1.12}$$

On the left hand side of eq. (1.12) we have the generating functional for correlation functions of an operator $\mathcal{O}$, sourced by the field ϕ. On the right hand side, S_{bulk} is **a** gravity action evaluated on the solution of the equations of motion that reduce χ to its boundary value. What the AdS/CFT correspondence suggests, via eq. (1.12), is that correlation functions of a composite operator $\mathcal{O}$ of a CFT in d dimensions, can be calculated by an appropriate $d+1$ gravity action put on-shell. Miraculously[15] or not, the AdS/CFT seems to be exactly the missing part of the strongly coupled CFT puzzle. What Maldacena basically told us, boils down to this:

> *"You have an unknown CFT theory, with unknown composite operators whose n-point functions you want to calculate? No problem! Just come up with a suitably chosen gravity theory and you will be just as good!"*

The real challenge of the AdS/CFT program lies in the phrase "suitably chosen". So far there is no unique and universal way to determine the correct gravity dual of a strongly coupled CFT. Instead, it is up to the theorist's experience and physical intuition to come up with the best model. Eventually, the experiment will be the final judge of every possible theory of nature, whenever the time is ready for an AdS/CFT model with experimentally falsifiable results.

1.5.2 Semi-holography

In our approach we make an attempt to go a step further towards that direction. What we are interested in is to calculate the interacting Green's functions of elementary fermionic op-

[13] Among numerous other scientists with great contribution to the field.

[14] Rigorously, eq. (1.12) is valid only for a massless field, but the prescription is valid in essence both for massive and fermionic fields.

[15] Actually no miracle has happened. It was AdS/CFT that we had in our minds when making all these assumptions on the nature of the interactions.

erators and eventually the conductivity they give rise to. The main reason we are after the former quantity is that its imaginary part, i.e. the spectral function, is directly measurable in experiments, e.g. using angle-resolved photoemission spectroscopy (ARPES) for solid-state systems or radio-frequency spectroscopy when studying ultra-cold atoms. A crucial property of the spectral function that makes it rather useful and appealing is the fact that it satisfies a sum rule of the form

$$\int_{-\infty}^{\infty} d\omega \rho(\vec{k}, \omega) = 1, \tag{1.13}$$

making it easy to determine whether there were excitations in the system that were not properly taken into account. In addition, the above sum rule is a perfectly suitable criterion to check whether our constructed spectral function corresponds indeed to a single fermionic operator.

However, the above sum rule holds for single-particle Green's functions[16], while the AdS/CFT correspondence provides n-point functions of composite operators. To reconcile this incompatibility, we shall employ a variation of the holographic principle that came to be known under the term *semi-holography*. This approach was first introduced by Faulkner and Polchinski in [13] and was further applied in the case of non-Fermi liquids [14], in heavy-ion collisions [15] as well as strange metallic behaviour [16].

What the semi-holographic prescription suggests is that the strongly coupled CFT, whose gravity dual we are after, is coupled to another QFT that is treated in a conventional field theoretic manner. This approach allows for a more powerful and effective bottom-up approach to the correspondence. Schematically, this approach can be seen in the following action

$$S = -i\hbar c \int d^d x \bar{\psi} \gamma^\mu \partial_\mu \psi + ig \int d^d x (\bar{\psi} \mathcal{O} + \bar{\mathcal{O}} \psi) + S_{CFT}[\bar{O}, O]. \tag{1.14}$$

The first term denotes a the free term of the Dirac fermion ψ, which is coupled to the operator $\mathcal{O}$ of the strongly coupled CFT with coupling constant g. The last term denotes the action describing the CFT itself. Effectively, the coupling of the CFT operator $\mathcal{O}$ to the Dirac fermion will generate a self energy term modifying the free Green's function. This modification is proportional to the two-point function of the operator $\mathcal{O}$, i.e.

$$\Sigma(\vec{k}, \omega, T) \propto g^2 \langle \bar{\mathcal{O}} \mathcal{O} \rangle_{CFT}. \tag{1.15}$$

To conclude, and as an appetizer for what will be more thoroughly discussed in chapter 4, we mention that what we will do to introduce interactions into WSMs boils down to this. First, we construct a gravity theory that is the dual of the field theory describing the WSM and then, we introduce an extra field leaving in this world and being coupled to it, to some extend. This model reduces on its boundary, to an interacting fermion and this boundary description will provide us with the interacting Green's function[17].

1.6 Disclaimer

This introduction had no intention of being exhausting, and therefore couldn't have been exhaustive! Instead, the intention was to cover in a concise and physically intuitive way the primary features of the topics that will be further discussed in the rest of the thesis. At the same time, the author is not claiming on any ground that has reinvented the wheel. On the contrary, he was heavily influenced by many excellent reviews on the topics that are covered. This introduction followed their steps and tried to include their main points, hopefully, in an

[16] This is because the sum rule of eq. (1.13) is a direct consequence of the anti-commutation relations of the single fermion creation and anihilation operators

[17] We are confident that all that will be made more clear after we introduce the field theory description of WSM in chapter 2 and even more in chapter 4, where a more thorough description of the holographic model is given.

explanatory level for the level of a Master student. For deepening his/her knowledge, through examination of the original work, the reader could consult [17, 18], in the area of TIs, while a beautiful journey in the topology of quantum vacua is elegantly presented in [19] and in the classical [20]. More specifically, thorough and well written reviews on Weyl semimetals can be found in [21, 22, 23, 24] and partly in [25].

At the same time, on the AdS/CFT part, there was some focus on the intuitive plausibility of the conjecture and the reasons that we thought it would be a useful tool to be used in the description of WSM. Nice reviews on the correspondence abound in the literature. Some prominent examples with application in the AdS/CondensedMatter program can be found in [26, 27, 28]. Any reader interested in diving deeper into a more mathematical analysis of the concepts we briefly discussed, is eagerly encouraged to consult the rich and pedagogical literature that can be found therein.

As a last remark, it must be heavily stressed that this thesis is critically influenced and builds upon relevant work that was carried out in the Institute for Theoretical Physics in Utrecht University, such as [29, 30, 31].

1.7 Thesis Outlook

The rest of the thesis is organised as follows. In Chapter 2, we introduce a phenomenological model that incorporates the splitting of the two Weyl fermions in energy. There, we present the first of the two results of this thesis, which is a re-derivation of the already known formula for CME. The novel element in this derivation, is the use of spectral functions which enables application of the derived formula in the case of interacting fermions, whose propagator is obtained via the AdS/CFT correspondence in Chapter 4.

In Chapter 3, we attempt a resolution of the conceptual problem related to the nature of CME, that was already apparent in the derivation we did in Chapter 2. Such resolution is achieved via a thorough examination of the related literature that approaches CME both from a high energy perspective, as in our case, but also from a condensed matter approach, where a full band structure model is considered. After a reconciliation is achieved, the chapter ends with a short discussion on the recent experimental status of CME.

In Chapter 4, we move on with the description of interacting Weyl semimetals using the AdS/CFT correspondence. After the model is introduced, plots of the resulting spectral functions resembling Weyl fermions split in energy, are presented for different values of the model parameters Short comments on the dependence of the results on these parameters are then put forward.

The thesis concludes with Chapter 5, where a short Outlook is presented. On the one hand, we comment on further steps to be taken, directly related to the present work, as well as more general ones related to a way towards a more accurate holographic model of Weyl semimetals. On the other, we comment on possible open questions regarding the nature of WSM, as seen from a condensed matter point of view.

Chapter 2

CME Part I: A controversial formula

2.1 Introduction

In this chapter we move on to the main theme of this thesis, which is no other than the Chiral Magnetic Effect or CME. We start our approach to the phenomenon by building a field theory model that describes two Weyl fermions separated in energy space. This splitting is done in a phenomenological way, simply with the introduction of an additional term in the free Dirac action that explicitly breaks inversion (I) symmetry. Then, after perturbing the system with a magnetic field in the x direction, we calculate the system's response in the linear regime. What we find is an electric current parallel to the magnetic field whose magnitude, in the DC and uniform limit, is proportional to the energy separation between the two nodes. Therefore, we conclude the, theoretical, existence of CME. Nonetheless, the result we arrive at, will depend on the limiting procedure we use. The physical implications of this dependence will occupy us in the next chapter.

Up to a point our analysis will remain rather general and only after a general formula for the CME conductivity is obtained in terms of the spectral functions of the system under study, will we make explicit use of the free nature of the model. This generality in the description of CME, allows us to generalise the results to interacting Weyl fermions once their corresponding propagators are known. It is exactly at this point where the field theory approach meets the AdS/CFT results we obtain in Chapter 4. We will comment more on this point in the outlook.

2.2 WSM Green's functions

Our starting point is the free, massless Dirac Lagrangian

$$\mathcal{L}_D = \bar{\psi}\left(-i\hbar\partial\!\!\!/\right)\psi, \tag{2.1}$$

where from now on we set $c = 1$. Eq. (2.1) results in two 2-fold degenerate dispersion relations touching at a 4-fold degenerate Dirac point as can be seen in Figure 2.1(a). To describe a WSM we need to break this degeneracy by separating the two nodes either in momentum, as in Figure 2.1(b), or in energy, as in Figure 2.1(c). In our case we discuss WSM with broken inversion (I) symmetry, which amounts to two Weyl cones separated in energy. There are two reasons why we are interested in this scenario. Firstly, it is the one that gives rise to the unique phenomenon of CME which as we will see in chapter 3 has directly observable effects. Secondly, having our minds set towards the interacting regime, a holographic model that incorporates the energy splitting is a feasible thing to do. On the contrary, a gravity dual theory of a WSM with momentum cone-splitting is still under investigation.

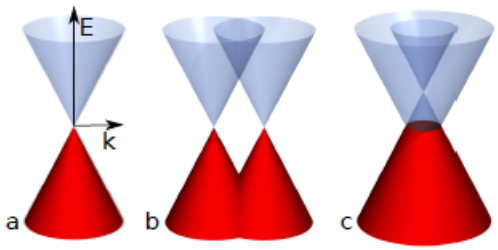

Figure 2.1: (a) In the presence of TR and I symmetries, two doubly degenerate bands touch at a 4-fold degenerate point. (b) TR symmetry breaking leads to momentum cone-splitting. (c) I symmetry breaking leads to energy cone-splitting. The figure is borrowed from [32].

There is a straightforward, phenomenological way to construct a Lagrangian that incorporates such a splitting. It simply requires the introduction of an extra term, proportional to $\bar{\psi}\gamma^0\gamma^5\psi$ to the free Dirac Lagrangian density. The proportionality factor b_0, that we shall assume positive without any loss of generality, denotes the magnitude of the splitting. Then the free WSM Lagrangian will read

$$\mathcal{L}_{WSM} = \bar{\psi}\left(-i\hbar\not{\partial} + \hbar b_0\gamma^0\gamma^5\right)\psi. \tag{2.2}$$

Before moving any further, a notational clarification is in order. Although the Lagrangian (2.2) is written in a general form, to avoid confusion, we state that in the rest of the thesis the following realization of the Dirac matrices will be used, namely

$$\gamma^0 = \begin{pmatrix} 0 & -\mathbb{I} \\ \mathbb{I} & 0 \end{pmatrix}, \qquad \gamma^i = \begin{pmatrix} 0 & \sigma^i \\ \sigma^i & 0 \end{pmatrix}, \qquad \gamma^5 = \begin{pmatrix} \mathbb{I} & 0 \\ 0 & -\mathbb{I} \end{pmatrix}, \tag{2.3}$$

where

$$\mathbb{I} = \begin{pmatrix} 1 & 0 \\ 0 & 1 \end{pmatrix}, \qquad \sigma^1 = \begin{pmatrix} 0 & 1 \\ 1 & 0 \end{pmatrix}, \qquad \sigma^2 = \begin{pmatrix} 0 & -i \\ i & 0 \end{pmatrix}, \qquad \sigma^3 = \begin{pmatrix} 1 & 0 \\ 0 & -1 \end{pmatrix}. \tag{2.4}$$

To verify that the Lagrangian (2.2) indeed describes a WSM with cones separated in energy, let us have a closer look at the Green's function. Performing our analysis in the more convenient momentum space, by Fourier transforming the Dirac spinor as

$$\psi(x^\mu) = \int \frac{d^4k}{(2\pi)^4}\tilde{\psi}(k^\mu)e^{ik^\mu x_\mu}, \tag{2.5}$$

we see that the inverse Green function for the WSM is

$$G^{-1} = \gamma^0(\not{k} + \not{b}\gamma^5) = \begin{pmatrix} -k_0 - b_0 - k_i\sigma^i & 0 \\ 0 & -k_0 + b_0 + k_i\sigma^i \end{pmatrix}. \tag{2.6}$$

Inverting the above matrix we have

$$G(k) = \begin{pmatrix} G^+(k) & 0 \\ 0 & G^-(k) \end{pmatrix}, \tag{2.7}$$

with

$$G^+(k) = \frac{-(k_0 + b_0) + \vec{k}\cdot\vec{\sigma}}{(k_0 + b_0)^2 - |\vec{k}|^2}, \tag{2.8}$$

and

$$G^{-}(k) = \frac{-(k_0 - b_0) - \vec{k}\cdot\vec{\sigma}}{(k_0 - b_0)^2 - |\vec{k}|^2}. \tag{2.9}$$

In the above notation the $\pm$ signs denote the chirality of the fermion that each 2×2 Green's function describes. It will be convenient to further decompose the chiral fermion propagators in the basis of Pauli matrices, as

$$G^{\pm} = \mathcal{G}^{\pm}_{\mu}\sigma^{\mu} = \mathcal{G}^{\pm}_{0}\mathbb{I} + \mathcal{G}^{\pm}_{i}\sigma^{i}, \tag{2.10}$$

with coefficients that read

$$\mathcal{G}^{\pm}_{0} = -\frac{k_0 \pm b_0}{(k_0 \pm b_0)^2 - |\vec{k}|^2}, \tag{2.11}$$

and

$$\mathcal{G}^{\pm}_{i} = \pm\frac{k_i}{(k_0 \pm b_0)^2 - |\vec{k}|^2}. \tag{2.12}$$

Whenever we feel it is notationally convenient, we shall denote both chiralities with a chirality index α, taking values ± 1.

To see that indeed the propagator given in eq. (2.8) indeed describes a Weyl fermion that is shifted upwards in energy, we simply need to look at its poles. As we know, the poles of the free Green's function define the dispersion relation of the particle. Hence, the poles of (2.8) read[1]

$$\begin{aligned} (k_0 + b_0)^2 - k^2 &= 0 \\ (-\omega + b_0)^2 - k^2 &= 0 \\ \omega &= \pm k + b_0, \end{aligned} \tag{2.13}$$

which indeed describes a linear dispersion shifted in energy by b_0. Similarly, the dispersion relation of a particle whose propagator is given by eq. (2.9) is

$$\begin{aligned} (k_0 - b_0)^2 - k^2 &= 0 \\ (-\omega - b_0)^2 - k^2 &= 0 \\ \omega &= \pm k - b_0, \end{aligned} \tag{2.14}$$

where in this case the shift is done downwards by the same amount. In eqs. (2.13) and (2.14) I converted the wavenumber k_0 in frequency ω via the relation

$$k_0 = -\frac{\omega}{c} = -\omega, \tag{2.15}$$

where we have made explicit use of the metric that we adopt, namely

$$\eta_{\mu\nu} = (-1, 1, 1, 1). \tag{2.16}$$

2.3 Linear response of a WSM

Now that we have constructed a field theoretical model that provides an effective description of our system, we want to check its response to an external electromagnetic perturbation. The way to incorporate the perturbation in the system, follows the standard steps of field theory.

The first thing to note is that the system possesses a global symmetry

[1] Whenever there is no ambiguity, we will use the notation $|\vec{k}|$ and k interchangeably to denote the norm of the spatial part of the wavevector.

$$\psi \to e^{i\alpha}\psi, \tag{2.17}$$

that according to Noether's theorem leads to a classically conserved current that reads

$$j^\mu = \bar{\psi}\gamma^\mu\psi. \tag{2.18}$$

Next, we assume that the system is perturbed under the influence of an external electromagnetic field that is conveniently described by a $U(1)$ gauge field that we denote as A_μ. Ignoring the kinetic term of the gauge field, which is of no concern in the present analysis, we couple the gauge field to the current j^μ with a coupling constant e. In essence, the gauge field will act as the source of the fluctuations of the current around its equilibrium value[2], that we suppose is zero, i.e. $\langle j_\mu \rangle \Big|_{A_\mu=0}$. With that in mind, the perturbed Lagrangian reads

$$\mathcal{L} = \bar{\psi}\left(-i\hbar\partial\!\!\!/ + \hbar b_0\gamma^0\gamma^5\right)\psi + ej^\mu A_\mu = \bar{\psi}\left(-i\hbar\partial\!\!\!/ + \hbar b_0\gamma^0\gamma^5\right)\psi + e\bar{\psi}\gamma^\mu\psi A_\mu, \tag{2.19}$$

and what we are after, is the expectation value $\langle j^\mu \rangle$.

Our approach will be based on linear response theory. In this regime, we assume that the disturbance in the system is sufficiently small, so that quadratic and higher order terms can be considered negligibly small. As a result, the response of the system is a linear function of the source which reads

$$\langle j^\mu(\vec{x},t)\rangle = \int d^d\vec{x}'dt'\chi^{\mu\nu}(\vec{x}',t';\vec{x},t)A_\mu(\vec{x}',t'), \tag{2.20}$$

where the proportionality constant is given by the Kubo formula

$$\chi^{\mu\nu}(\vec{x}',t';\vec{x},t) = -i\theta(t-t')\langle\left[j^\mu(\vec{x},t), j^\nu(\vec{x}',t')\right]\rangle. \tag{2.21}$$

Assuming spatial and temporal translational invariance, the linear response formula can be recast in momentum space as

$$\langle\tilde{j}^\mu(\vec{k},\omega)\rangle = \tilde{\chi}^{\mu\nu}(\vec{k},\omega)\tilde{A}_\nu(\vec{k},\omega). \tag{2.22}$$

Crucially, in the linear response regime, the system does not introduce new frequencies in the response. In essence, the appearance of new frequencies is a higher order phenomenon that is not captured in this approximation. This property is evident in eq. (2.22) where the response of the system is at the same frequency and momenta as its disturbance.

Specifically, we are interested in the system's response to an external magnetic field. Due to the spherical symmetry of the problem, and without loss of generality, we assume that the magnetic field points along the x-direction; i.e. $\vec{B} = B_x\hat{x}$. In order to express the magnetic field in terms of the gauge potential, we recall from electrodynamics that

$$B_l = \epsilon_{lmn}\partial_m A_n \to \tilde{B}_l = i\epsilon_{lmn}k_m\tilde{A}_n, \tag{2.23}$$

where the arrow denotes taking the Fourier transform on both sides of the equation, with k_m being the Fourier variable corresponding to spatial direction m.

Next, we gauge fix A_μ such that the only non-vanishing component of the gauge field is A_y and hence we can express the Fourier components of the magnetic field in terms of the gauge field components as[3]

$$B_x = -ik_z A_y, \tag{2.24}$$

or equivalently

[2] Its value when $A_\mu = 0$.

[3] For the rest of the chapter we will work exclusively in momentum space. Thus, and for notational economy, we will drop the tilde symbol over the Fourier coefficients.

$$A_y(\vec{k},\omega) = \frac{i}{k_z} B_x(\vec{k},\omega). \tag{2.25}$$

As a last step, recalling that we are interested in the electric current in the same direction as the applied magnetic field, we set in eq. (2.22), $\mu = x$ and keep only the $\nu = y$ term in the summation due to the gauge condition. Then, we get

$$\langle j^x(\vec{k},\omega)\rangle = \chi^{xy}(\vec{k},\omega) A_y(\vec{k},\omega) = \frac{i}{k_z}\chi^{xy}(\vec{k},\omega) B_x(\vec{k},\omega), \tag{2.26}$$

where $\chi^{xy}(\vec{k},\omega)$ is the $(\vec{k},\omega)$ Fourier mode of $\chi^{\mu\nu}(\vec{x}',t';\vec{x},t)$. Denoting the proportionality constant between the electric current and the magnetic field as σ^x we have that[4]

$$\sigma^x(\vec{k},\omega) = \frac{\langle j^x(\vec{k},\omega)\rangle}{B_x(\vec{k},\omega)} = \frac{i}{k_z}\chi^{xy}(\vec{k},\omega). \tag{2.27}$$

In general, the magnetoconductivity σ^x is a complex quantity. However, we will focus on its real part since the imaginary component describes transient and oscillatory phenomena that are not of primary interest to us in the present analysis. So what we are interested in is

$$\mathrm{Re}[\sigma^x(\vec{k},\omega)] = \mathrm{Re}[\frac{i}{k_z}\chi^{xy}(\vec{k},\omega)]. \tag{2.28}$$

To calculate $\chi^{xy}(\vec{k},\omega)$, we first define

$$\begin{aligned} \hbar\Pi^{\mu\nu}(q) &= \int d^4(x-y)\langle J^\mu(x) J^\nu(y)\rangle e^{-iq(x-y)} \\ &= e^2 \int \frac{d^4k}{(2\pi)^4} \mathrm{Tr}\left[G(k)\gamma^0\gamma^\mu G(k+q)\gamma^0\gamma^\nu\right], \end{aligned} \tag{2.29}$$

where in the above, Wick's theorem was used and disconnected Feynman diagrams were omitted as we are interested in the connected correlator. Going to imaginary frequency, both for the external electromagnetic field and for the internal fermionic one finds[5]

$$\hbar\Pi^{\mu\nu}(\vec{q},i\omega_b) = \frac{e^2}{\hbar\beta}\int \frac{d^3\vec{k}}{(2\pi)^3} \sum_{n=-\infty}^{+\infty} \mathrm{Tr}\left[G(\vec{k},i\omega_n)\gamma^0\gamma^\mu G(\vec{k}+\vec{q},i\omega_b+i\omega_n)\gamma^0\gamma^\nu\right]. \tag{2.30}$$

Then, by analytic continuation back to the real frequency domain, i.e.

$$i\omega_b \to \omega^+ = \omega + i\epsilon, \tag{2.31}$$

we see that the CME conductivity reads[6]

$$\sigma^x(\vec{q},\omega) = \frac{i}{q_z}\Pi^{\mu\nu}(\vec{q},\omega^+). \tag{2.32}$$

The analysis to arrive at eq. (2.32) was undoubtedly rather sketchy. Nonetheless, the steps we took are rather standard and can easily be found in any textbook that applies field theory techniques in condensed matter systems, such as [33, 34].

We first turn to the calculation of the trace that appears in the expression of eq. (2.30), i.e.

[4] Not to be confused with the Pauli matrix of course!

[5] Since the electromagnetic field is bosonic, its corresponding Matsubara frequency $i\omega_b$ will be of the same type. Similarly for the Matsubara frequency $i\omega_n$ corresponding to the fermionic field.

[6] To avoid confusion, let us note explicitly that upon analytic continuation, $i\omega_b \to \omega^+ = \omega + i\epsilon$, $\Pi^{\mu\nu}(\vec{q},i\omega_b)$ coincides with $\chi^{\mu\nu}(\vec{q},\omega)$.

$$\mathrm{Tr}\big[G(\vec{k}, i\omega_n)\gamma^0\gamma^i G(\vec{k}+\vec{q}, i\omega_n + i\omega_b)\gamma^0\gamma^j\big]. \tag{2.33}$$

Recalling

$$\gamma^0\gamma^i = \begin{pmatrix} 0 & -\mathbb{I} \\ \mathbb{I} & 0 \end{pmatrix}\begin{pmatrix} 0 & \sigma^i \\ \sigma^i & 0 \end{pmatrix} = \begin{pmatrix} -\sigma^i & 0 \\ 0 & \sigma^i \end{pmatrix}, \tag{2.34}$$

so that

$$G\gamma^0\gamma^i = \begin{pmatrix} G^+ & 0 \\ 0 & G^- \end{pmatrix}\gamma^0\gamma^i = \begin{pmatrix} -G^+\sigma^i & 0 \\ 0 & G^-\sigma^i \end{pmatrix}, \tag{2.35}$$

and

$$G\gamma^0\gamma^i G\gamma^0\gamma^j = \begin{pmatrix} G^+\sigma^i G^+\sigma^j & 0 \\ 0 & G^-\sigma^i G^-\sigma^j \end{pmatrix}, \tag{2.36}$$

we get

$$\mathrm{Tr}\big[G\gamma^0\gamma^i G\gamma^0\gamma^j\big] = \sum_\alpha \mathrm{Tr}\big[G^\alpha\sigma^i G^\alpha\sigma^j\big] = \sum_\alpha \mathcal{G}^\alpha_\mu\mathcal{G}^\alpha_\nu \mathrm{Tr}\big[\sigma^\mu\sigma^i\sigma^\nu\sigma^j\big]. \tag{2.37}$$

For notational convenience, the argument of G is implied by its order in the product[7]. We have also splitted the analytic part of the Green's function from its matrix part, using the decomposition $G^\alpha = \mathcal{G}^\alpha_\mu\sigma^\mu$, where $\sigma^\mu = (\mathbb{I}, \vec{\sigma})$.

First we further manipulate the analytic part of the Greens function. To that end, it is re-expressed in terms of the spectral function as

$$\mathcal{G}^\alpha_\mu(\vec{k}, i\omega_n) = \int_{-\infty}^{+\infty} d\omega \frac{\mathcal{A}^\alpha_\mu(\vec{k}, \omega)}{i\omega_n - \omega}. \tag{2.38}$$

Then

$$\begin{aligned}
\sum_n \mathcal{G}^\alpha_\mu\mathcal{G}^\alpha_\nu &= \sum_n \int d\omega^{'} d\omega^{''} \frac{\mathcal{A}^\alpha_\mu(\vec{k}, \omega^{'})}{i\omega_n - \omega^{'}} \; \frac{\mathcal{A}^\alpha_\mu(\vec{k}+\vec{q}, \omega^{''})}{i\omega_n + i\omega_b - \omega^{''}} \\
&= \int d\omega^{'} d\omega^{''} \mathcal{A}^\alpha_\mu(\vec{k}, \omega^{'})\mathcal{A}^\alpha_\nu(\vec{k}+\vec{q}, \omega^{''}) \sum_n \frac{1}{i\omega_n - \omega^{'}} \; \frac{1}{i\omega_n + i\omega_b - \omega^{''}} \\
&= \hbar\beta \int d\omega^{'} d\omega^{''} \frac{N_f(\omega^{'}) - N_f(\omega^{''})}{i\omega_b + \omega^{'} - \omega^{''}} \mathcal{A}^\alpha_\mu(\vec{k}, \omega^{'})\mathcal{A}^\alpha_\nu(\vec{k}+\vec{q}, \omega^{''}).
\end{aligned} \tag{2.39}$$

In the last line, the Matsubara summation over the fermionic Matsubara frequencies was implicitly performed, and in the resulting expression, only the external, bosonic Matsubara frequency associated with the photon field is left.

Now lets turn our attention to the matrix part.

$$\begin{aligned}
\sigma^\mu\sigma^i\sigma^\nu\sigma^j &= (\delta^\mu_0\mathbb{I} + \delta^\mu_k\sigma^k)\sigma^i(\delta^\nu_0\mathbb{I} + \delta^\nu_l\sigma^l)\sigma^j \\
&= \delta^\mu_0\delta^\nu_0\sigma^i\sigma^j + \delta^\mu_0\delta^\nu_l\sigma^i\sigma^l\sigma^j + \delta^\mu_k\delta^\nu_0\sigma^k\sigma^i\sigma^j + \delta^\mu_k\delta^\nu_l\sigma^k\sigma^i\sigma^l\sigma^j.
\end{aligned} \tag{2.40}$$

Then, checking each term separately, we get[8]

[7] I.e. $GG \equiv G(k)G(k+q)$

[8] In the calculations, when the σ -matrices "disappear", we have implicitly taken the trace using $\mathrm{Tr}[\sigma^i] = 0$ and $\mathrm{Tr}[\sigma^i\sigma^j] = 2\delta^{ij}$.

$$\sigma^i\sigma^l\sigma^j = (i\sum_c \epsilon^{ilc}\sigma^c + \delta^{il})\sigma^j = 2i\epsilon^{ilj}, \tag{2.41}$$

similarly

$$\sigma^k\sigma^i\sigma^j = 2i\epsilon^{kij} = -2i\epsilon^{ikj} \tag{2.42}$$

and

$$\begin{aligned}\sigma^k\sigma^i\sigma^l\sigma^j &= (i\sum_c \epsilon^{kic}\sigma^c + \delta^{ki})(i\sum_d \epsilon^{ljd}\sigma^d + \delta^{lj}) \\ &= -\sum_{cd} \epsilon^{kic}\epsilon^{lid}\sigma^c\sigma^d + \delta^{ki}\delta^{lj} + i\big(\sum_c \epsilon^{kic}\delta^{lj}\sigma^c + \sum_d \epsilon^{ljd}\delta^{ki}\sigma^d\big) \\ &= -2\sum_c \epsilon^{kic}\epsilon^{lic} + 2\delta^{ki}\delta^{lj} = -2\big(\delta^{kl}\delta^{ij} - \delta^{kj}\delta^{il}\big) + 2\delta^{ki}\delta^{lj}.\end{aligned} \tag{2.43}$$

Putting all the above together we see that

$$\begin{aligned}\mathrm{Tr}[\sigma^\mu\sigma^i\sigma^\nu\sigma^j] &= i2\epsilon^{ilj}(\delta^\mu_0\delta^\nu_l - \delta^\nu_0\delta^\mu_l) \\ &\quad + 2\Big[\delta^\mu_0\delta^\nu_0\delta^{ij} - \delta^\mu_k\delta^\nu_l\big(\delta^{kl}\delta^{ij} - \delta^{kj}\delta^{li} - \delta^{ki}\delta^{lj}\big)\Big].\end{aligned} \tag{2.44}$$

Then, replacing eq. (2.44) in eq. (2.30), and using the well known formula

$$\frac{1}{\omega + \omega^{'} - \omega^{''} + i\epsilon} = PV\big(\frac{1}{\omega + \omega^{'} - \omega^{''}}\big) - i\pi\delta(\omega^{+} + \omega^{'} - \omega^{''}), \tag{2.45}$$

we get[9]

$$\begin{aligned}\sigma^x(\vec{q},\omega) = \frac{2e^2}{\hbar q_z}\int \frac{d^3\vec{k}}{(2\pi)^3} d\omega^{'} d\omega^{''} \sum_\alpha \quad &\text{P.V.}\left(\frac{N_f(\omega^{'}) - N_f(\omega^{''})}{\omega + \omega^{'} - \omega^{''}}\right) \times \\ &(\mathcal{A}^\alpha_0(\omega^{'},\vec{k})\mathcal{A}^\alpha_z(\omega^{''},\vec{k}+\vec{q}) - \mathcal{A}^\alpha_z(\omega^{'},\vec{k})\mathcal{A}^\alpha_0(\omega^{''},\vec{k}+\vec{q})).\end{aligned} \tag{2.46}$$

Therefore, when a WSM, described effectively by the Lagrangian (2.2), is perturbed by a magnetic field along the x direction having momentum $\vec{q}$ and frequency ω, its magnetic conductivity is given by eq. (2.46)[10].

Nonetheless, what we are mostly interested in, is the DC and uniform limit response of the system. That is, its response at $\vec{q} = \vec{0}$ and $\omega = 0$. As a first comment, we see that the q_x and q_y components of the momentum vector can be set to zero without any problems. However, q_z appears in the denominator of eq. (2.46) and therefore taking it to zero might lead to divergences. The way to deal with this issue, is to expand the term containing the spectral functions of the system in power series in q_z and check if this approach can sort things out.

Moreover, there is a second issue that arises at this point. The ambiguity that we are facing has to do with the limiting procedure that we will use to get to the DC and uniform limit. Put differently, magnetoconductivity can be considered a multivariable function in frequency and momentum of the external magnetic field, i.e. $\sigma^x = \sigma^x(q_z,\omega)$. As it happens with functions of more than one variable, not all limits are uniquely defined. Instead, one might depend on which path in the multi-dimensional space we choose to approach the limiting point. Therefore,

[9] As we will focus only on the real part of the conductivity, σ^x will stand for the more rigorous $\mathrm{Re}[\sigma^x]$.

[10] After eq. (2.46), the principal value perscription will be implied and not explicitly noted.

different paths may lead to different results and, as a result, to different interpretations of the underlying physics. We will comment more on the implications of this possible non-analyticity of magnetoconductivity around the origin of the 2D plane (q_z, ω) in the next chapter. For now let us simply examine both limits and see if indeed the limiting procedure affects the result we arrive at.

2.4 Static limit

The first limit order we will examine, is the one that, as we will see, can give us a sensible result. Furthermore, a similar analysis uses the same limiting procedure to arrive at the same result [36]. Hence, the way to get a finite answer is if we first take the frequency of the external field to zero and then its momentum. That translates to first assuming a static, time independent magnetic field whose spatial variations are taken to zero only in the end. For apparent reasons, we will refer to this order as the static limit. Physically this amounts to studying an equilibrium property of the system and it is due to this interpretation that we will have to reconsider if this is indeed the physical limit order to take. Nonetheless, let us be naive in first instance and try to see where this road will take us.

The crucial technical point where this limit appears useful is in the product of the Fermi-Dirac distributions with the spectral functions. We see that, after taking $\omega^+ \to 0$ the first term in the product is symmetric under the exchange of the two frequencies we integrate over, i.e. $\omega^{'} \leftrightarrow \omega^{''}$. So we can exchange the frequencies in one of the two terms containing products of spectral functions in order for same components of the spectral function to have the same integration frequency. Due to the above mentioned symmetry, the Fermi-Dirac distribution term can again factor out of the sum[11]. Eventually, after we perform this trick we see that the conductivity (2.46) reads

$$\sigma^x(\vec{q}, \omega = 0) = \frac{2e^2}{\hbar q_z} \int \frac{d^3\vec{k}}{(2\pi)^3} d\omega^{'} d\omega^{''} \sum_{\alpha} \frac{N_f(\omega^{'}) - N_f(\omega^{''})}{\omega^{'} - \omega^{''}} \times (\mathcal{A}_0^{\alpha}(\omega^{'}, \vec{k})\mathcal{A}_z^{\alpha}(\omega^{''}, \vec{k} + \vec{q}) - \mathcal{A}_z^{\alpha}(\omega^{''}, \vec{k})\mathcal{A}_0^{\alpha}(\omega^{'}, \vec{k} + \vec{q})). \tag{2.47}$$

Before taking the uniform limit, let us denote the term involving the spectral functions as

$$I = \mathcal{A}_0(\omega^{'}, \vec{k})\mathcal{A}_z(\omega^{''}, \vec{k} + \vec{q}) - \mathcal{A}_z(\omega^{''}, \vec{k})\mathcal{A}_0(\omega^{'}, \vec{k} + \vec{q})) \tag{2.48}$$

where for notational convenience the chirality index α was dropped for now. Moreover the spectral functions can be rewritten as

$$\begin{aligned} \mathcal{A}_0(\omega^{'}, \vec{k}) &= g(\omega^{'}, |\vec{k}|) \\ \mathcal{A}_z(\omega^{''}, \vec{k}) &= f(\omega^{''}, |\vec{k}|)k_z \end{aligned} \tag{2.49}$$

where they still retain a general form. Using these two relations, I can be rewritten as

$$\begin{aligned} I &= g(|\vec{k}|)f(|\vec{k} + \vec{q}|)(k_z + q_z) - f(|\vec{k}|)k_z g(|\vec{k} + \vec{q}|) \\ &= k_z[g(|\vec{k}|)f(|\vec{k} + \vec{q}|) - f(|\vec{k}|)g(|\vec{k} + \vec{q}|)] + q_z g(|\vec{k}|)f(|\vec{k} + \vec{q}|) \end{aligned} \tag{2.50}$$

Next, we Taylor expand the f and g factors in eq. (2.50) in a power series in q_z. As we have commented before the q_x and q_y components of $\vec{q}$ can be set to zero easily. So using $\vec{q}$ in

[11] This is a technical trick that we will use again at later points without explicitly mentioning it.

eq. (2.50) we actually mean $\vec{q} = (0, 0, q_z)$. Working first abstractly, we see that for a general function $h(|\vec{k} + \vec{q}|)$ the following expansion holds[12]

$$\begin{aligned} h(|\vec{k} + \vec{q}|) = h(\lambda(q_z)) = h(q_z) &= h(q_z = 0) + q_z \frac{d}{dq_z} h(q_z)|_{q_z=0} + \mathcal{O}(q_z^2) \\ &= h(0) + q_z h^{'}(\lambda) \frac{d\lambda}{dq_z}|_{q_z=0} + \mathcal{O}(q_z^2) \\ &= h(0) + q_z h^{'}(|\vec{k}|) \frac{k_z}{|\vec{k}|} + \mathcal{O}(q^2), \end{aligned} \tag{2.51}$$

where

$$\lambda(q_z) = |\vec{k} + \vec{q}| = \sqrt{k_x^2 + k_y^2 + (k_z + q_z)^2} \tag{2.52}$$

and $h^{'}(\lambda)$ denotes the derivative of h with respect to λ.

Then, we have

$$\begin{aligned} &g(|\vec{k}|)f(|\vec{k} + \vec{q}|) - f(|\vec{k}|)g(|\vec{k} + \vec{q}|) \\ &= g(|\vec{k}|)(f(|\vec{k}|) + q_z f^{'}(|\vec{k}|)\frac{k_z}{|\vec{k}|} + \mathcal{O}(q_z^2)) - f(|\vec{k}|)(g(|\vec{k}|) + q_z g^{'}(|\vec{k}|)\frac{k_z}{|\vec{k}|} + \mathcal{O}(q_z^2)) \\ &= q_z \frac{k_z}{|\vec{k}|}(g(|\vec{k}|)f^{'}(|\vec{k}|) - f(|\vec{k}|)g^{'}(|\vec{k}|) + \mathcal{O}(q_z^2), \end{aligned} \tag{2.53}$$

and

$$q_z g(|\vec{k}|)f(|\vec{k} + \vec{q}|) = q_z g(|\vec{k}|)f(|\vec{k}|) + \mathcal{O}(q_z^2). \tag{2.54}$$

The crucial point to note here is that the 0th order terms of the expansion vanish identically and therefore there are no infinities appearing when taking the uniform limit. In the same limit, $\mathcal{O}(q_z^2)$ also vanish. So the only term contributing in the conductivity is the linear one. Explicitly,

$$\lim_{q_z \to 0} \frac{1}{q_z} I = k \cos^2\theta (g(k)f^{'}(k) - f(k)g^{'}(k)) + g(k)f(k), \tag{2.55}$$

where we have readopted the more convenient notation $k = |\vec{k}|$ and we also used that $k_z = k\cos\theta$.

Next, we focus on the integral over the 3D momentum space which can be decomposed as

$$\int d^3\vec{k} = \int_0^\infty dk k^2 \int_0^{2\pi} d\phi \int_0^\pi d\theta \sin\theta = 2\pi \int_0^\infty dk k^2 \int_0^\pi d\theta \sin\theta, \tag{2.56}$$

where in the last step the ϕ-integral was trivially performed since there is no such ϕ-dependence in the formulas. Then we turn our attention to the θ-integrals. The second term in eq. (2.55) does not depend on the angle θ either. Therefore the θ-integral can also be performed trivially giving an extra factor of 2. On the contrary, the first term has an extra $\cos^2\theta$ that after integration over a range of π will give

$$\int_0^\pi d\theta \sin\theta \cos^2\theta = -\int_0^\pi \frac{d\cos^3\theta}{3} = \frac{2}{3}. \tag{2.57}$$

Eventually, the DC and uniform limit of the Weyl fermion CME conductivity reads

[12] In the following analysis we focus on the momentum dependence and therefore we suppress the frequency argument.

$$\sigma^x(\vec{q}=0,\omega=0)=\frac{e^2}{\hbar\pi^2}\sum_\alpha\int_0^\infty dk\int_{-\infty}^{+\infty}d\omega^{'}d\omega^{''}k^2\frac{N_f(\omega^{'})-N_f(\omega^{''})}{\omega^{'}-\omega^{''}}$$
$$\times\left[\frac{k}{3}(g(k)f^{'}(k)-f(k)g^{'}(k))+g(k)f(k)\right]. \tag{2.58}$$

Eq. (2.58) is a central result for this thesis. It provides the general formula to calculate the CME conductivity of the system, provided that its spectral functions are known and are of the form of eq. (2.49).

This is an important formula on two grounds. Firstly, it can be used in the case of free fermions when the spectral functions are explicitly known. Thus we can first check the validity of this formula by comparing with the CME conductivity formula found in the literature. Secondly, it is a suitable framework to apply the AdS/CFT calculations we carry out in Chapter 4. The holographic model that we construct there, provides us with the holographically interacting Weyl fermions' propagator, whose imaginary part is precisely the spectral function we need. Therefore, we can use eq. (2.58) to obtain a holographic CME conductivity.

2.5 Free fermions

As a first check of eq. (2.58), we will try to apply it in the free fermion case, where a closed formula already exists in the literature and was obtained via different approaches and arguments [35, 36, 37, 38, 39]. In these attempts, CME is treated from a high-energy perspective and as we will see there is a fundamental difference in the interpretation of the effect compared to the condensed-matter analogue. Nonetheless, the discussion is rich and useful for a general brainstorming on the phenomenon.

As far as calculations are concerned, the free case is also the most convenient one as the f and g factors reduce to delta functions and analytic calculations can be performed. As we will show in Appendix A, the first term, containing derivatives of the f and g factors, is vanishing in the static limit for free Weyl fermions. Hence, in this section we shall concentrate only on the second term.

2.5.1 Right chiral contribution

Let us first concentrate on the right chiral fermion and recall that

$$\mathcal{G}_0^+(k_\mu)=-\frac{k_0+b_0}{(k_0+b_0+i\epsilon)^2-k^2}\qquad \mathcal{G}_z^+(k_\mu)=\frac{k_z}{(k_0+b_0+i\epsilon)^2-k^2}, \tag{2.59}$$

which can be further decomposed as

$$\begin{aligned}\mathcal{G}_0^+(k_\mu)&=-\frac{k_0+b_0}{(k_0+b_0+i\epsilon)^2-k^2}=-\frac{1}{2}\Big(\frac{1}{k_0+b_0-k+i\epsilon}+\frac{1}{k_0+b_0+k+i\epsilon}\Big)\\ \mathcal{G}_z^+(k_\mu)&=\frac{k_z}{(k_0+b_0+i\epsilon)^2-k^2}=\frac{1}{2k}\Big(\frac{1}{k_0+b_0-k+i\epsilon}-\frac{1}{k_0+b_0+k+i\epsilon}\Big)k_z.\end{aligned} \tag{2.60}$$

Then, using the identity

$$\lim_{\epsilon\to0}\frac{1}{x+i\epsilon}=PV(\frac{1}{x})-i\pi\delta(x), \tag{2.61}$$

we can easily see that the spectral functions read

$$\begin{aligned}\mathcal{A}_0^+(k_\mu) &= -\frac{1}{\pi}\mathrm{Im}[\mathcal{G}_0^+] = -\frac{1}{2}(\delta(k_0+b_0-k)+\delta(k_0+b_0+k)) \\ \mathcal{A}_z^+(k_\mu) &= -\frac{1}{\pi}\mathrm{Im}[\mathcal{G}_z^+] = \frac{1}{2k}(\delta(k_0+b_0-k)-\delta(k_0+b_0+k))k_z.\end{aligned} \tag{2.62}$$

Thus, from eqs. (2.49), we can see directly that the f and g factors are simply

$$\begin{aligned}g^+(k_\mu) &= -\frac{1}{2}(\delta(k_0+b_0-k)+\delta(k_0+b_0+k) \\ f^+(k_\mu) &= \frac{1}{2k}(\delta(k_0+b_0-k)-\delta(k_0+b_0+k)),\end{aligned} \tag{2.63}$$

or using eq. (2.15)

$$\begin{aligned}g^+(\omega,k) &= -\frac{1}{2}(\delta(-\omega+b_0-k)+\delta(-\omega+b_0+k)) \\ f^+(\omega,k) &= \frac{1}{2k}(\delta(-\omega+b_0-k)-\delta(-\omega+b_0+k)).\end{aligned} \tag{2.64}$$

Next, we note that the product that appears in eq. (2.58) has four constituent terms that read

$$\begin{aligned}g^+(\omega^{'},k)f^+(\omega^{''},k) = -\frac{1}{4k}\{&\delta(-\omega^{'}+b_0-k)\delta(-\omega^{''}+b_0-k)-\delta(-\omega^{'}+b_0-k)\delta(-\omega^{''}+b_0+k) \\ &+\delta(-\omega^{'}+b_0+k)\delta(-\omega^{''}+b_0-k)-\delta(-\omega^{'}+b_0+k)\delta(-\omega^{''}+b_0+k)\}.\end{aligned} \tag{2.65}$$

After that, we perform the $\omega^{'}$ and $\omega^{''}$ integrals that can be easily carried out. As a result, we get four corresponding terms that read

$$\begin{aligned}\int_{-\infty}^{+\infty} d\omega^{'}d\omega^{''}\frac{N_f(\omega^{'})-N_f(\omega^{''})}{\omega^{'}-\omega^{''}}g^+(\omega^{'},k)f^+(\omega^{''},k) &= \\ = -\frac{1}{4k}\Big[&\frac{N_f(-k+b_0)-N_f(-k+b_0)}{-k+b_0-(-k+b_0)}-\frac{N_f(-k+b_0)-N_f(k+b_0)}{-k+b_0-(k+b_0)} \\ &+\frac{N_f(k+b_0)-N_f(-k+b_0)}{k+b_0-(-k+b_0)}-\frac{N_f(k+b_0)-N_f(k+b_0)}{k+b_0-(k+b_0)}\Big].\end{aligned} \tag{2.66}$$

There are two comments at this point. Firstly the second and third terms in the above sum cancel each other. These are the interband contributions, that we will say more about in Chapter 3, and they appear not to be contributing in the static limit. Secondly, the first terms appear to be undefined since they lead to ambiguities of the form $\frac{0}{0}$. Correspondingly, these are the intraband contributions, which are eventually responsible for the CME conductivity in the model we are building. However, this ambiguity is raised if we recall that the corresponding ratio, is define within the Principal Value procedure. That simply amounts to examining what happens as $\omega^{''}$ approaches infinitesimally $\omega^{'}$ at the singular value. This is nothing else than the derivative of the underlying function, in our case the Fermi-Dirac distribution, evaluated at the singular value. Therefore the sum in eq. (2.66) simply reads

$$\frac{dN_f(x)}{dx}\Big|_{x=-k+b_0}-\frac{dN_f(x)}{dx}\Big|_{x=k+b_0} = -\delta(-k+b_0)+\delta(k+b_0). \tag{2.67}$$

In the last step, we took the extra approximation that we are working in the zero temperature limit. In this limit, the Fermi-Dirac distribution simplifies greatly as it reduces to a step function, namely $N_f(x) = \theta(-x)$. Therefore, its derivative is a delta function with a negative sign due to the form of the step function, i.e.

$$\frac{dN_f(x)}{dx} = -\delta(x). \tag{2.68}$$

Finally, we may perform the momentum integral that can also be easily calculated since we have reduced it to an integral of two delta functions. Namely, we have

$$\int_0^\infty dk k^2 (-\frac{1}{4k}) \left(-\delta(-k+b_0) + \delta(k+b_0) = \frac{b_0}{4}. \right. \tag{2.69}$$

2.5.2 Left chiral contribution

The above result, denotes the contribution to the conductivity arising only from the right chiral cone. To get the full result, we need to follow the same procedure for the left chiral cone and add up the two contributions. Since the two procedures are nearly identical, we will present the derivation for conductivity of the left chiral fermion only in a brief and sketchy manner.

Our starting point is the components of the propagator of the left chiral fermion that read

$$\mathcal{G}_0^-(k) = -\frac{k_0 - b_0}{(k_0 - b_0 + i\epsilon)^2 - k^2} \qquad \mathcal{G}_z^-(k) = -\frac{k_z}{(k_0 - b_0 + i\epsilon)^2 - k^2}. \tag{2.70}$$

Following the steps of the previous analysis, one easily sees that the f and g factors for the left chiral fermion simply read

$$\begin{aligned} g^-(\omega, k) &= -\frac{1}{2}(\delta(-\omega - b_0 - k) + \delta(-\omega - b_0 + k)) \\ f^-(\omega, k) &= -\frac{1}{2k}(\delta(-\omega - b_0 - k) - \delta(-\omega - b_0 + k)). \end{aligned} \tag{2.71}$$

The two difference from the corresponding equations for the right chiral fermion, eq. (2.64), is a minus sign in front of b_0 due to the opposite chirality, as well as an extra minus sign for the f factor due to the the corresponding minus sign in the $\mathcal{G}_z^-$ component of the propagator.

Then, in complete analogy with the right chiral fermion, we can perform the $\omega^{'}$ and $\omega^{''}$ integrals that will again lead to two delta functions of the form

$$\frac{dN_f(x)}{dx}\Big|_{x=-k-b_0} - \frac{dN_f(x)}{dx}\Big|_{x=k-b_0} = -\delta(-k-b_0) + \delta(k-b_0), \tag{2.72}$$

and the momentum integral will read

$$\int_0^\infty dk k^2 \frac{1}{4k} \left(-\delta(-k-b_0) + \delta(k-b_0) = \frac{b_0}{4}. \right. \tag{2.73}$$

As symmetry considerations might have led us believe, eqs. (2.69) and (2.73) imply that the two cones contribute equally to the conductivity. Then, replacing the two contributions in eq. (2.58), we see that the DC and uniform CME conductivity of a pair of chiral fermions separated in energy by $2b_0$, in the static limit, reads

$$\boxed{\sigma^x = \frac{e^2}{2\pi\hbar} b_0} \tag{2.74}$$

2.6 Uniform limit

In this section we will try to use a second limiting procedure to get to a DC and uniform CME conductivity. Contrary to path we took in the previous sections we will now attempt to take first any spatial fluctuations of the magnetic field to zero and then go to the DC limit. For obvious reasons, we will refer to this procedure as the uniform limit and the current this procedure describes is a non-equilibrium property of the system. Rather it is the DC limit of a transport phenomenon.

Looking again at the general CME conductivity formula in eq. (2.46), one sees that the $q_z \to 0$ limit is again problematic due to the presence of q_z in the denominator of the fraction. Thus, we will resort again to Taylor expansion of the spectral function term. However, in this limit order the term involving Fermi-Dirac distribution is no longer symmetric in the exchange of frequencies $\omega^{'} \leftrightarrow \omega^{''}$. In any case, let us proceed with the Taylor expansion as in the static limit case. Omitting, for the time being, any chirality index, and adopting the same form for the spectral functions as in eq. (2.49), we have

$$\begin{aligned}
&\frac{N_f(\omega^{'}) - N_f(\omega^{''})}{\omega^{+} + \omega^{'} - \omega^{''}} \Big(\mathcal{A}_0(\omega^{'}, \vec{k}) \mathcal{A}_z(\omega^{''}, \vec{k} + \vec{q}) - \mathcal{A}_z(\omega^{'}, \vec{k}) \mathcal{A}_0(\omega^{''}, \vec{k} + \vec{q}) \Big) \\
=&\frac{N_f(\omega^{'}) - N_f(\omega^{''})}{\omega^{+} + \omega^{'} - \omega^{''}} \Big(g(\omega^{'}, |\vec{k}|) f(\omega^{''}, |\vec{k} + \vec{q}|)(k_z + q_z) - f(\omega^{'}, |\vec{k}|) g(\omega^{''}, |\vec{k} + \vec{q}|) k_z \Big) \\
=&\frac{N_f(\omega^{'}) - N_f(\omega^{''})}{\omega^{+} + \omega^{'} - \omega^{''}} \Big(g(\omega^{'}, |\vec{k}|) f(\omega^{''}, |\vec{k} + \vec{q}|) - f(\omega^{'}, |\vec{k}|) g(\omega^{''}, |\vec{k} + \vec{q}|) \Big) k_z \\
&+ \frac{N_f(\omega^{'}) - N_f(\omega^{''})}{\omega^{+} + \omega^{'} - \omega^{''}} \Big(g(\omega^{'}, |\vec{k}|) f(\omega^{''}, |\vec{k} + \vec{q}|) \Big) q_z
\end{aligned} \tag{2.75}$$

As before, we try to Taylor expand the first term in the sum of eq. (2.75), namely

$$\frac{N_f(\omega^{'}) - N_f(\omega^{''})}{\omega^{+} + \omega^{'} - \omega^{''}} \Big(g(\omega^{'}, |\vec{k}|) f(\omega^{''}, |\vec{k} + \vec{q}|) - f(\omega^{'}, |\vec{k}|) g(\omega^{''}, |\vec{k} + \vec{q}|) \Big) k_z. \tag{2.76}$$

Using the power series from eq. (2.51), we can expand again the f and g factors as

$$\begin{aligned}
f(\omega, |\vec{k} + \vec{q}|) &= f(\omega, k) + q_z f^{'}(\omega, k) \frac{k_z}{k} + \mathcal{O}(q_z^2) \\
g(\omega, |\vec{k} + \vec{q}|) &= g(\omega, k) + q_z g^{'}(\omega, k) \frac{k_z}{k} + \mathcal{O}(q_z^2).
\end{aligned} \tag{2.77}$$

In this case, we need at first retain explicitly the frequency dependence of the two factors as in one factor g depends on $\omega^{'}$, while in the other it depends on $\omega^{''}$. This feature cannot change simply by an exchange of the dummy integration variables, $\omega^{'}$ and $\omega^{''}$, as the Fermi-Dirac distribution is no longer symmetric under the exchange of the two. Therefore we need to be careful with the different frequency arguments. Then using the expansions from eq. (2.77) we get

$$\begin{aligned}
g(\omega^{'}, |\vec{k}|) f(\omega^{''}, |\vec{k} + \vec{q}|) &= g(\omega^{'}, k) f(\omega^{''}, k) + q_z \frac{k_z}{k} g(\omega^{'}, k) f^{'}(\omega^{''}, k) + \mathcal{O}(q_z^2) \\
f(\omega^{'}, |\vec{k}|) g(\omega^{''}, |\vec{k} + \vec{q}|) &= f(\omega^{'}, k) g(\omega^{''}, k) + q_z \frac{k_z}{k} f(\omega^{'}, k) g^{'}(\omega^{''}, k) + \mathcal{O}(q_z^2).
\end{aligned} \tag{2.78}$$

Subtracting the two equations, we get

$$k_z\Big[g(\omega^{'},|\vec{k}|)f(\omega^{''},|\vec{k}+\vec{q}|)-f(\omega^{'},|\vec{k}|)g(\omega^{''},|\vec{k}+\vec{q}|)\Big]= \\ = k\cos\theta\Big[g(\omega^{'},k)f(\omega^{''},k)-f(\omega^{'},k)g(\omega^{''},k)\Big] \\ + q_z k\cos^2\theta\Big[g(\omega^{'},k)f^{'}(\omega^{''},k)+f(\omega^{'},k)g^{'}(\omega^{''},k)\Big] \\ + \mathcal{O}(q_z^2) \tag{2.79}$$

Now, recalling that eventually we want to take the limit $\lim_{q_z\to 0}\frac{1}{q_z}$, let us focus on each term in the above expansion. Obviously, second and higher order terms vanish in the limit so we do not have to worry about them. Next, the linear order contribution reads

$$k\cos^2\theta\frac{N_f(\omega^{'})-N_f(\omega^{''})}{\omega^{+}+\omega^{'}-\omega^{''}}\Big(g(\omega^{'},k)f^{'}(\omega^{''},k)-f(\omega^{'},k)g^{'}(\omega^{''},k)\Big), \tag{2.80}$$

while the zeroth order one is given by

$$k\cos\theta\frac{1}{q_z}\frac{N_f(\omega^{'})-N_f(\omega^{''})}{\omega^{+}+\omega^{'}-\omega^{''}}\Big(g(\omega^{'},k)f(\omega^{''},k)-f(\omega^{'},k)g(\omega^{''},k)\Big) \tag{2.81}$$

The second term in eq. (2.75) is linear in q_z and therefore the $\lim_{q_z\to 0}\frac{1}{q_z}$ can be taken straightforwardly giving

$$\frac{N_f(\omega^{'})-N_f(\omega^{''})}{\omega^{+}+\omega^{'}-\omega^{''}}g(\omega^{'},k)f(\omega^{''},k). \tag{2.82}$$

Eqs. (2.80), (2.81) and (2.82) are the three contributions to the CME conductivity in the uniform limit. Evidently, the 0th order term as given by eq. (2.81) is problematic. If the uniform limit is to be taken upon this term, we readily see that we end up with a divergent term. On the contrary, in the static limit this term vanishes, in accord with our previous analysis. Therefore, this analysis shows that CME must be an equilibrium property of the system, rather than the DC limit of a transport phenomenon. In Chapter 3 we will have to say more about this result, its interpretation as well as the objections that it gives rise to.

Chapter 3

CME Part II: Resolving the controversy

3.1 Introduction

Among the various interesting properties that emerge out of the topological character of the WSM, the chiral magnetic effect (CME) bears great significance and a big part of the thesis is devoted to it. In the field theory model we constructed in the previous chapter to model WSM, CME was indeed found to be present. Nonetheless, the result we get appears to depend on the limiting procedure we use. It is the purpose of this chapter to try and clarify the ambiguities that arise and provide a self consistent and physically acceptable framework for CME. In the end, we turn to the final judge of every physical theory and briefly explore an experimental attempt to capture CME.

3.2 Ambiguous limit order

As we saw in the previous chapter, the result for the CME conductivity depends crucially on the limiting procedure that we use. Nonetheless, this non-analyticity of $\sigma(\vec{q},\omega)$ near the point $(\vec{q},\omega) = (\vec{0},0)$ is not a peculiarity unique to WSM. Many other response functions are known to behave non-analytically in the neighbourhood of zero frequency and zero momentum. Two prominent situations where a non-analytical behaviour is present, are the static current-current correlation function of superfluids as well as the dielectric response function of an electron gas.

The key in understanding non-analyticity lies in the interpretation of the results. To put it differently, different limiting procedures describe different physical processes in the system. Consequently, a priori, there is no physical law that indicates which limit is the "correct" one; in principle, both are equally acceptable. However, the physics that these two limits describe are different and it is up to the physicist to determine which limit he/she should take based on the effect that he wants to study and possibly on extra considerations that allow or prohibit one.

So, how does all that apply in our situation? The field theory model that we set up clearly suggests that the CME current is an equilibrium property. What led us to this interpretation is precisely the limiting procedure we chose. Setting first $\omega \to 0$, means that we have removed all time dependence from our problem, turning it into a static one, and then see what happens when also any spatial variations of the external magnetic field are absent.

Is there, then, a problem with CME being an equilibrium current? Actually, yes! And there are two simple arguments to understand why this is the case, that are nicely put forward in [40]. The first one stems from a simple energy consideration. Suppose that the system is in

global equilibrium and in the presence of a magnetic field, along say the x-axis, an electric current appears along the same direction, in accord with the CME formula. Next, suppose I turn on also an electric field. Then, from ordinary electrodynamics, the energy input/output in the system, will be given by

$$\frac{dP}{dt} = \vec{J} \cdot \vec{E} \propto \vec{E} \cdot \vec{B}, \tag{3.1}$$

where P denotes the energy transfer[1] in the system. However, what this formula suggests is that by placing the electric field in the opposite direction of the magnetic field, I could extract energy from the system. However, this means that at zero temperature we can extract energy from a system in global equilibrium. And this directly contradicts the definition of a global equilibrium as the ground state of your system; as the state of lowest energy.

The same thing can be viewed in a different way. Recall again, that we chose to model WSM as two independent chiral fermions that are split in energy. And it was in this context that we found the existence of CME. However, in high energy physics the infinite Dirac sea of **both** fermions is assumed to be filled. The condensed matter analogue of this situation can be seen in Fig. 3.1(b). In this case, both Weyl cones are filled up to the touching points, but since the two cones are split in energy, different fillings is equivalent to different chemical potential for each cone. But the necessity for two chemical potentials and the absence of a Fermi level in the system is exactly what makes the situation an non-equilibrium one. Equilibrium is depicted in Fig. 3.1(a). There a Fermi level is established in the system and the two cones are filled up to the same level. Although the cones are still separated in energy, what is important in the formula are the levels up to which each cone is filled. Therefore in the static case, we should expect a zero CME current.

A a last remark on the resulting ambiguity, let us say this. On the one hand, the field theory model indeed describes an equilibrium situation. An equilibrium as viewed from a high-energy physics point of view where the infinitely filled Dirac seas make sense. However, in condensed-matter systems, this model cannot describe an equilibrium situation. By construction it leads to a non-equilibrium situation whose stability must be ensured by some external mechanism. Otherwise, the system will tend to find its proper equilibrium in which case no CME current can be observed. In the end of the chapter, we will see how nicely this picture is verified by the experimental attempt to capture CME.

3.3 Full band models give a puzzling answer

From the previous discussion it was clear that if CME is to exist in a condensed matter context, then it should be a transport rather than an equilibrium property of the system we are studying. However, the theoretical model we have constructed, and indeed predicts CME, suggests the latter interpretation. Therefore, there is clearly something that we are missing in the analysis.

As we have concluded in the last section, the problem arises due to the mismatch between the characteristics of the theoretical model and the actual physical properties of the system that is being modelled. To be more specific, the field theory model that we are using requires that the two fermions in the model are independent and there is by no means any coupling between them. Equivalently, the "Dirac sea" associated to each chiral fermion is infinitely deep and the two dispersion cones never meet. However, in real systems there is no such thing and the two cones inevitably meet at some point. In other words, the description of WSM as two fermions of opposite chirality is only valid in the low energy regime. In higher energies the quasiparticles' dispersion relations meet and the model breaks down. It is precisely these deviations from the realistic case that lead to a misinterpretation of the CME, as we will shortly see.

[1] Either input or output.

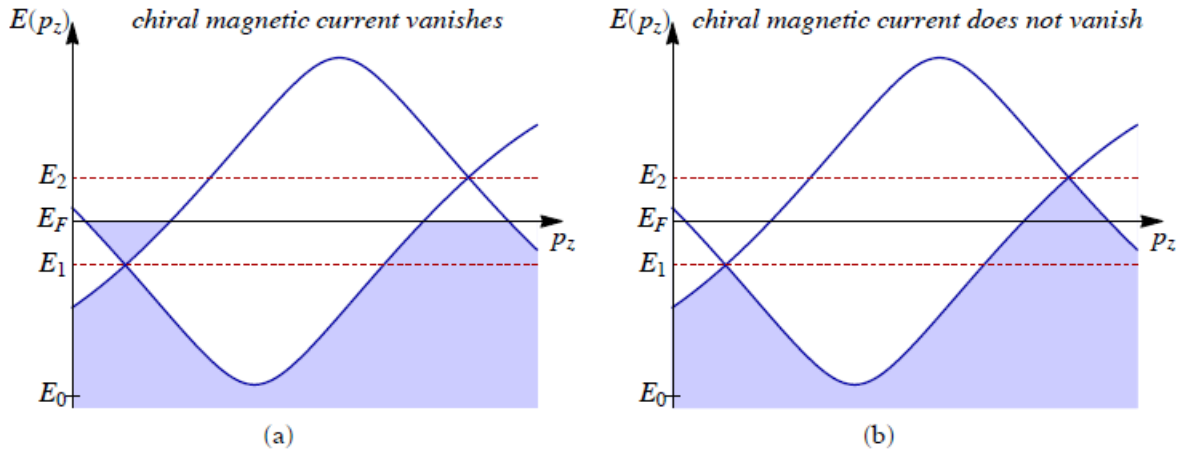

Figure 3.1: Physical condition for a non-vanishing CME. In the left panel, a global equilibrium has been established and the two cones are filled up the Fermi level. In this case the chiral chemical potential is evidently vanishing, $\mu_5 = 0$. In the right panel, the two cones are kept at different fillings and the system is out of equilibrium. Therefore, $\mu_5 = \frac{E_2 - E_1}{2} \neq 0$. The figure is borrowed from [40].

For a more realistic model to be constructed, the system's full band structure needs to be taken into account. People have been working on such models, but neither there could a unanimous answer be found. A.A Burkov and L. Balents were the first to pave the way in this line of research by constructing a multilayer periodic structure of Topological and Normal Insulators that could support Weyl fermions [41]. Building upon this model Burkov's group proposed the existence of CME as a non-dissipative, equilibrium current in Weyl semi-metals [42]. A few months later, Vazifeh and Franz performed an equilibrium calculation in their full band structure model and they showed that, up to numerical accuracy, CME was actually absent [32]. Convinced for their discovery, the former group came back with a new paper [43]. There, they showed that although Vazifeh and Franz were indeed right in their discovery, this was the case only because they were performing an equilibrium calculation. They managed to prove analytically that indeed in the static limit there should be no CME, in accord with the findings of Vazifeh and Franz. However, when the uniform limit is taken, then their analysis resulted in a non-zero CME conductivity that reads

$$\sigma_{cme} = -\frac{e^2 \Delta\epsilon}{4\pi^2}. \tag{3.2}$$

As it appeared, the crucial point to unlock the mysteries of CME was its non-equilibrium nature. Once this feature was properly taken into account, a full band structure model proved indeed that in equilibrium there is no CME current, while in the uniform limit a CME exists.

3.4 The remark to resolution

Although Burkov's results verified our physical intuition, the puzzle remained; if not got bigger. And the reason for the puzzle was simple. An ideal calculation gave us a certain result in an unphysical limit, while a full band structure theory gave the same result in the more physical one; albeit with a minus sign difference. Then the question was, how can an ideal calculation in the wrong limit provide, nearly, the correct result?

The answer to the above question, came with a recent paper[2] by Chang and Yang [44]. The crucial point that this paper puts forward is the distinction between intra and inter band

[2] I am thankful to Joel Moore for pointing out this paper.

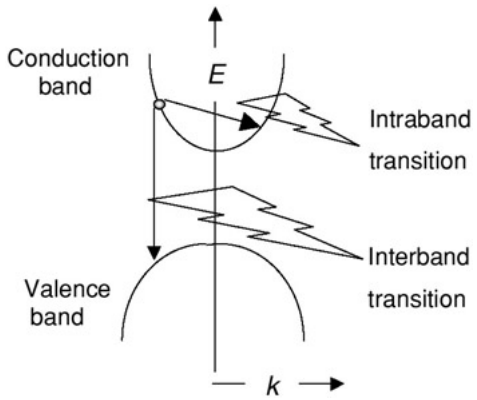

Figure 3.2: Conductivity can be attributed to two types of electron transitions. Either electrons moving within partially filled bands, intraband transitions, or electrons moving between the valence and conduction band, interband transition. In the figure the two bands are depicted exhibiting a band gap, yet the interpretation is similar for the general case.

contributions in the CME conductivity. The term intraband contributions refers to electron transitions within the same energy band. Instead, interband contributions refer to electron transitions within different bands. The situation is nicely depicted in Fig. 3.2. For presentation purposes, the bands shown have an energy gap. Therefore, interband transitions cannot occur at zero frequency and zero momentum. However, in the case of WSM the bands touch at a point. Thus, there and there only interband transitions are allowed even at the zero frequency zero momentum limit.

Their findings suggest that the interband and intraband components of CME conductivity behave differently in zero momentum, zero frequency limit. On the one hand, interband conductivity behaves analytically in the dc and uniform limit. On the other, the intraband part is limit dependend; vanishes in the uniform limit while it gives a non-zero result in the static limit. However, when both contributions are taken into account, it is the static limit that vanishes while in the uniform a net current appears. Clearly, this suggests that the interband contribution exactly cancels out the intraband one in the static limit, while it is the only one that survives in the the static. This interpretation explains also the difference in the sign in the CME formula between the ideal and the full band structure model.

To sum up, our current understanding that appears to reconcile the two pictures, is that our model is incapable of capturing the interband part of the conductivity. This appears to be the reason we end up with an unphysical interpretation of the current. Nonetheless, it seems that these contribution behave in such a way that using an ideal model and an unphysical limit, we can indeed get the correct result that a full band structure model would give in the physical limit[3]. This concluding remark is comforting and reassuring as it justifies our choice of using field theory results in our attempt to introduce holographic interactions in WSM.

3.5 Chiral anomaly

As we mentioned, this chapter will conclude with a short discussion related to experimental evidence supporting the existence of CME. But before going any deeper into the experiment, we need to take a detour through chiral anomaly[4]. Apart from being a vital element in the experiment to follow, chiral anomaly is interesting on its own right as it is a typical example of contradictions between the classical and quantum mathematical description of a system.

[3]Up to a sign difference as we have already mentioned.

[4]This detour will be short and will focus on the physics governing the anomaly. For a mathematically thorough walk, the reader could address to [45, 46] as well as references therein.

Chiral anomaly is a field theoretical concept. As with all anomalies it describes the non-conservation of a classically conserved quantity, when quantum corrections come into play. To understand chiral anomaly we need to recall the two currents that correspond to the two global symmetries of our Lagrangian. For clarity we simply note that these currents read

$$\begin{aligned} j_V^\mu &= \bar{\psi}\gamma^\mu\psi \\ j_A^\mu &= \bar{\psi}\gamma^\mu\gamma^5\psi. \end{aligned} \tag{3.3}$$

To give a more physical interpretation of these currents, suppose that the Dirac fermion ψ is decomposed into its chiral, 2-component spinors ψ_+ and ψ_-. Then, it is easy to see that the vector and axial currents decompose as

$$\begin{aligned} j_V^\mu &= j_R + j_L \\ j_A^\mu &= j_R - j_L, \end{aligned} \tag{3.4}$$

where the currents j_R and j_L are related to the each individual chiral component separately. Conservation of the vector current implies that the sum of right and left chiral fermions remains constant, while conservation of the axial current is related to their difference. Classically, both currents are conserved and therefore the corresponding right and left charges are also conserved. Therefore, a classical description of the system of chiral fermions suggests that there is a well defined number of fermions of each chirality.

However, in the quantum mechanical description of the system, the above considerations are not valid any more. We shall not dwell on the mathematical details of why this is happening as it would go beyond the scope if the thesis. Nonetheless, we consider worth mentioning, that the problem lies in the non-trivial Jacobian that the path integral measure acquires upon a chiral transformation. Therefore, the partition function of the system will change under a chiral transformation because although the action remains indeed invariant, the measure is not. This non-trivial Jacobian is exactly the chiral anomaly term.

The problem, though, is not that none of these currents is conserved. Actually, a suitable choice of the renormalisation procedure, can lead to a consistent scheme that conserves any of the two. The problem arises when one attempts to conserve both currents simultaneously. A scheme that conserves the vector current has an anomalous axial one, and vice versa. Therefore it is up to the theorist to decide which current he/she will choose to save.

To be honest, in the end of the day it is not much of a choice as another principle, that we consider of fundamental importance, dictates that we must conserve the vector current. This principle is no other than charge conservation. Usually the gauge field that we couple the vector current to, is the $U(1)$ field of electromagnetism. Therefore fermions acquire electric charge, and the conservation of their total number simply denotes ekectric charge conservation. If we consider electric charge conservation, and we do, a cornerstone of physics, then we are left with no other option than abandon axial current conservation.

But what implications will this anomaly bring about? Well, it is again more instructive if we consider the anomaly in terms of the corresponding chiral vector currents. It can be shown that each current is on its own anomalous, with the anomalies being equal in magnitude but opposite in sign. Explicitly,[5] they read

$$\begin{aligned} \partial_\mu j_R^\mu &= \frac{e^2}{4\pi^2}\vec{E}.\vec{B} \\ \partial_\mu j_L^\mu &= -\frac{e^2}{4\pi^2}\vec{E}.\vec{B}. \end{aligned} \tag{3.5}$$

[5] In suitably chosen units.

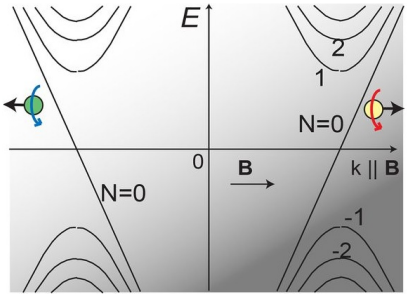

Figure 3.3: The presence of a magnetic field rearranges the linear dispersion of the Weyl nodes into Landau levels. Only the chiral 0-th order levels contribute to the anomaly.

The above equations make the physical meaning of the anomaly more than transparent. Namely, in the presence of a pair of non-orthogonal electric and magnetic fields, the number of right chiral fermions increases by a certain rate, given by Eq. (3.5) while the number of left chiral fermions decreases by the same amount. In other words, according to chiral anomaly, in the presence of a suitable configuration of the electromagnetic field, left chiral fermions disappear in the chiral vacuum with the simultaneous appearance of right chiral fermions from it. In the end, no charge is lost but the relative number of the two chiralities has changed.

All the above analysis is captured quite vividly in Fig. 3.5. There we see that the external magnetic field has rearranged the linear dispersion relations of the two Weyl nodes into Landau levels. The only levels that contribute to the chiral anomaly are the 0th order levels that cross zero energy. The crucial property of these levels is that they are chiral, meaning that their inclination (positive/negative) depends on the chirality they belong to (right/left). Therefore, if an electric field would create a right handed chiral fermion out of the infinite Dirac sea, a left one should at the same time sink into it. The pioneering paper that put forward the connection between the chiral anomaly and condensed matter systems captures the physics of the anomaly really vividly and the interested reader is eagerly encouraged to study it [47].

So as a concluding remark, due to chiral anomaly, a pair of non-orthogonal electric and magnetic fields drives an imbalance between right and left chiral fermions. This is exactly the point we will need to understand the experiment that follows.

3.6 Experimental evidence

And now comes the crucial question: "Can we check if the chiral magnetic effect is an actual physical phenomenon and not simply a theoretical artifact of our mathematical construction?". Our answer will try to describe the big picture regarding an experimental effort [48] without focusing on technical details and difficulties in the realisation of the experiment. For a deeper discussion, the interested reader is once again referred to the original paper and references therein. Similar experiments to broaden our understanding of Weyl semimetals are an on going process [49, 50].

As it is clear by now, a crucial property for the existence of chiral magnetic effect is a chiral imbalance between left and right handed fermions. The way this was achieved experimentally was via the chiral anomaly. At first, the system was in equilibrium and the two cones were located at the same energy level; the Fermi level of the system. Then, the experimentalist turned on a pair of parallel electric and magnetic fields and the analogue of chiral anomaly in condensed matter physics took place. As we have commented before, the magnetic field reorganised the cones into Landau levels and the electric field started to move the electrons in the zeroth mode. Due to their negative charge, electrons abandoned the right chiral cone and then populated the left one. The situation is clearly shown in Fig. 3.4.

There is a crucial point in this analysis. If this was the only mechanism taking place then

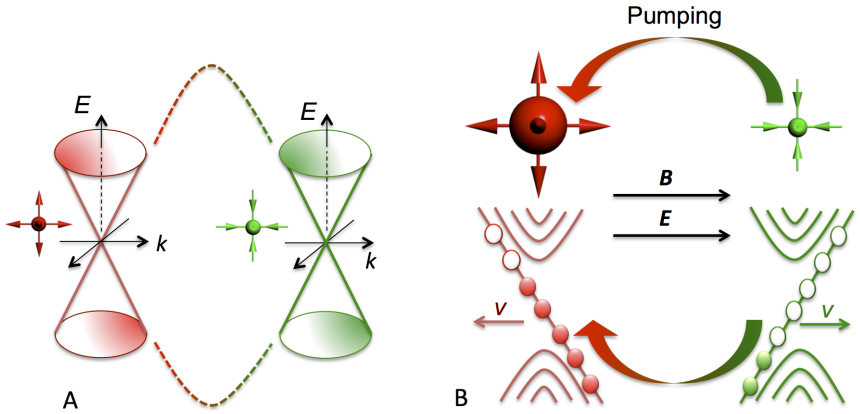

Figure 3.4: (A): Initially, the system is at equilibrium and both nodes are at the Fermi level of the system. (B): Parallel electric and magnetic fields pump electrons from the right chiral node to the left chiral one, via chiral anomaly, leading to a chiral imbalance that is dynamically preserved. The figure is borrowed from [49].

at some point all right chiral fermions would have turned into left and the whole model of the material would collapse. Besides, this picture ignores scattering phenomena that might turn some left handed fermions back to the right chiral cone. The theoretical model that they used took into account these processes by an additional term in the differential equation that determined the chiral charge ρ_5, which is related to the chiral chemical potential μ_5 via [35]

$$\rho_5 = \frac{\mu_5^3}{3\pi^2 v^3} + \frac{\mu_5}{3v^3}(T^2 + \frac{\mu^2}{\pi^2}), \tag{3.6}$$

through the differential equation

$$\frac{d\rho_5}{dt} = \frac{e^2}{4\pi^2\hbar^2 c}\vec{E}.\vec{B} - \frac{\rho_5}{\tau_V}, \tag{3.7}$$

where τ_V denotes the chirality changing scattering time. For $t >> \tau_V$, the chiral charge will have reached an equilibrium value and so will the chiral chemical potential, with the value of the latter being given by

$$\mu_5 = \frac{3v^3e^2}{4\pi^2\hbar^2 c}\frac{\vec{E}.\vec{B}}{T^2 + \frac{\mu^2}{\pi^2}}\tau_V. \tag{3.8}$$

What this means is that the system has reached a state of dynamical equilibrium with chiral imbalance. By the term dynamical equilibrium, I refer to the situation where the system is at steady state, but this stability of this state is supported by an external mechanism. In the case we are discussing, the role of this external mechanism is played by the electromagnetic field that drives chiral anomaly. If this input is turned off, the the system will reorganise itself in its proper ground state and then we can say that the system is at a static equilibrium. What happens physically, is that the system is characterised by a constant chiral imbalance because the rate of production of left chiral fermions due to the anomaly is balanced by the production rate of right chiral fermions due to scattering processes.

Now that we know have an understanding of this dynamical chiral imbalance, we turn to look for evidence of CME. The experimentalists looked for such evidence in the resistivity of a $ZrTe_5$ sample. The important feature that we need to remember for this material, is that it has an intrinsic positive magnetoresistance. In simple words, this means that its electric resistance

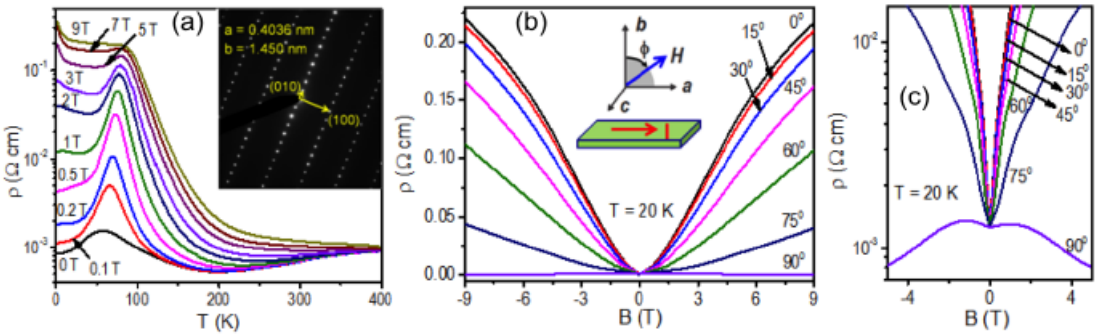

Figure 3.5: Left panel (a): Temperature dependence of resistivity for various values of the external magnetic field. Central panel (b): Positive magnetoresistance of $ZrTe_5$ at T=20K°due to dominance of Lorentz force for not aligned electric and magnetic fields. Right panel (c): Evidence of negative quadratic magnetoresistance at $\phi = 90°$. The figure is borrowed from [48].

changes in the presence of an external magnetic field in positive way; it increases with an increasing $\vec{B}$ field. This behaviour is depicted in Fig. 3.5(a). There we can see the temperature dependence of the resistivity of the sample for various values of the external magnetic field. Apart from the peak that all curves exhibit at a critical temperature, the important point to note here is that for increasing magnetic field th resistivity also increases.

With that in mind, they applied an electric field along one side of the sample, say along the $a-$axis as in Fig. 3.5(b) and a magnetic field at an angle ϕ with the axis perpendicular to the sample, say $b-$axis in the figure. Then measuring the current that appears in the same direction as the electric field, they get the resistivity curves that one can see in Figs. 3.5(b,c).

To better appreciate these figures, let us first understand why they measured resistivity. They assumed that if CME current was present, the total current along the $a-$axis should have two components. Namely the usual ohmic current, and an additional CME part

$$j_{tot} = j_{ohm} + j_{cme}. \tag{3.9}$$

Next supposing that the CME has indeed the theoretically predicted expression, $j_{cme} = \frac{e^2}{2h\pi^2}\mu_5$ and replacing μ_5 from eq. (3.8) it is easy to see that the current reads

$$j_{tot} = (\sigma_{ohm} + \lambda B^2)E, \tag{3.10}$$

where we have introduces a parameter $\lambda > 0$ to account for all numerical prefactors that are unimportant in this qualitative discussion. Inverting this proportionality factor, we see that the resistivity of the sample should have a dependence on the magnetic field of the form

$$\rho_{tot} = \frac{1}{\sigma_{ohm} + \lambda B^2}. \tag{3.11}$$

That means that if the chiral magnetic is there, and its expression is given by the theoretically predicted formula, we should expect a magntoresistance that depends inversely proportional to the magnetic field.

Let us then see what the experiment has shown. At an angle $\phi = 0°$, the two fields are perpendicular to each other and their inner product vanishes. As a result no chiral anomaly is expected. Indeed the black curve which corresponds to $\phi = 0°$ clearly shows the inherent positive magnetoresistance of $ZrTe_5$. As the angle ϕ increases, we see that the same qualitative behaviour persists, yet it appears to be weaker. The explanation for this result is that in the presence of non-orthogonal electric and magnetic fields, the chiral anomaly has started to show its presence. However, the inherent character of the material is strong enough to dominate its overall behaviour. This situation continues up to angles of $\phi = 75°$.

The situation changes drastically when $\phi = 90^\circ$ when the two fields are aligned in parallel. In that case two interesting things happen. On the one hand, chiral anomaly reaches its maximum value and therefore will have the maximum contribution to the composite behaviour of the material. More importantly, though, at $\phi = 90^\circ$ we are at the so called, Lorentz-force free regime because electrons move in the same direction as the magnetic field and therefore the Lorentz force on them vanishes. In Fig. 3.5(b), the resistivity for $\phi = 90^\circ$ appears to be nearly insensitive to the magnetic field. However, a closer look in this curve, as shown in Fig. 3.5(c), shows that this impression was simply a matter of scale. Upon closer examination we can see that the material exhibits negative magnetoresistance that to a pretty good approximation appears also to be quadratic.

To conclude, the experiment has clearly shown a quadratic negative magnetoresistance which can be elegantly described within the context of CME. Therefore, we have clear evidence that CME is an actual current that we can measure in an experiment, and not simply a mathematical artifact.

Chapter 4

A touch of interactions

In this chapter we will try to introduce interactions into the Weyl semimetals using the AdS/CFT correspondence. In essence what we do is construct an interacting Green's function for the system. The approach that we will take, follows the lines of semi-hoplography as was briefly discussed in Chapter 1. That means that we will deviate from a strict holographic framework by introducing an additional bulk field that will capture the fermionic natre of the system under study. A boundary term of this field, that will not alter its bulk equations of motion, will provide the free part of the Green's function we are after. In addition, the bulk contributions, will give rise to the self energy component of the Green's function. Interestingly enough, Weyl fermions shall appear rather straightforwardly in the model we will create, making holographic AdS/CFT an really interesting means of introducing interactions in systems with an effective description as Weyl fermions; a prominent example being of course WSM.

Several attempts have been made to construct a gravity dual to study CME and chiral anomaly [51, 52, 53, 54]. However, these efforts focus on a more pure AdS/CFT approach and the subtleties of CME need to be carefully taken into account. Instead, the semi-holographic path that we take, and builds upon previous similar work on fermionic systems [55, 56, 57, 58, 59], is inherently characterised by the chiral charge imbalance.

4.1 Introducing the model

It is the purpose of this section to introduce the gravitational dual model that will give rise to the interacting Green's function of our strongly interacting CFT. A defining working assumption of the correspondence is that the spacetime we will be working on should be AdS; meaning negatively curved, with a constant radius of curvature. Such a spacetime can be directly obtained simply by minimizing the Einstein-Hilbert action in 4+1 dimensions[1], with an additional negative cosmological constant, namely

$$S_{EH} = \int d^5x\sqrt{-g}(R - 2\Lambda), \tag{4.1}$$

where R denotes the Ricci scalar and Λ the cosmological constant. Solving the corresponding equations of motion, we find that the metric minimizing eq. (4.1), in a suitably chosen coordinate system, reads

$$ds^2_{AdS} = \frac{l^2}{r^2}dr^2 - \frac{r^2}{l^2}dt^2 + \frac{r^2}{l^2}d\vec{x}^2, \tag{4.2}$$

which is precisely the AdS space we were looking for, with l being the AdS radius that from now on we set to unity. As we can see, the AdS bulk in d+1 dimensions, can be thought of as a

[1] We shall henceforth restrict to the case d=4.

collection of flat Miknowski surfaces of one dimension less. Each such slice is scaled with the extra coordinate r, with $r \to \infty$ corresponding to the boundary of the AdS bulk. It is exactly at this boundary that our CFT will live in.

As a next step, we want to encode the physical characteristics of the strongly coupled field theory we are about to study in the gravity dual description. The first important feature we need to consider is that it describes a system at a constant temperature. As the AdS/CFT dictionary suggests, and is arguably an easy first guess, the way this is achieved is by introducing a black hole of equal Hawking temperature in the bulk. Strictly speaking, because of the special structure of the AdS spacetime as a collection of Minkowski surfaces, we no longer talk about a black hole but rather of a black brane. The second ingredient that our boundary theory should contain, is a constant chemical potential. Recall, that a crucial requirement for the existence of CME was that the two chiral cones are filled up to different chemical potentials. Looking up again in the AdS/CFT dictionary, we find that to describe a constant scalar field on the boundary we need a gauge field in the bulk that will asymptotically tend to a constant value. Hence, both of our requirements can be met by the introduction of a U(1) gauge field in the bulk action.

It is a rather cumbersome procedure[2], to prove that the bulk configuration that satisfies the above requirements reads

$$g_{\mu\nu} = diag(-rf(r), \frac{1}{rf(f)}, r, r, r), \tag{4.3}$$

with

$$ds^2 = -r^2 f^2(r) dt^2 + \frac{1}{r^2 f^2(r)} dr^2 + r^2 d\vec{x}, \tag{4.4}$$

and $f(r)$ is the so called "emblackenning factor" defined in this case as

$$f(r) = 1 - \frac{Q^2}{r^4} + \frac{M}{r^6}. \tag{4.5}$$

Also, the gauge field reads

$$A_\mu = \mu(1 - \frac{r_h^2}{r^2})\delta^0_\mu, \tag{4.6}$$

where Q is the charge of the black brane, M its mass, r_h is the location of the horizon defined as the first zero of the emblackening factor, and μ a parameter that is related to its charge and will be the chemical potential of the boundary theory. Therefore, with the above scheme we have fully defined the bulk configuration.

The next step we will take, is based on the character of the system we want to describe on the boundary; i.e. a system of two Weyl fermions. As it has been shown in the literature, this can be achieved with the introduction of a Dirac fermion in the bulk. This extra field we add in the description of the system, is exactly what we have anticipated when we were discussing the semi-holographic approach.

Since the Dirac equation that describes a Dirac fermion is first order in time, a chiral fermion will arise almost naturally in the boundary theory. A crucial property of the Dirac fermion that we will introduce, is that it lives in the probe-limit. This condition simply means that the fermion will not back-react to the metric; i.e. its energy-momentum tensor will be assumed zero for all practical purposes and will not appear in the right hand side of the Einstein equations. On the contrary, we will allow the Dirac fermion to be charged under the U(1) gauge field and the coupling between the two fields is expressed in terms of a coupling constant e, the charge of the fermion. As we will see later, choosing fermions with opposite charge leads to a difference in the chemical potential for the two chiral fermions. It is precisely

[2]And not part of this thesis.

this difference that we are interested in because it is the crucial ingredient of CME. But we will have time to say more about this in due course.

For now, we only add a fermion in the bulk that couples to the gauge field with a coupling constant e. The coupling between the two fields is done in the usual procedure of minimal coupling. That means that we start from the free Dirac action for the fermion that has a global U(1) symmetry. According to Noether's theorem, this symmetry leads to a conserved current with which the gauge field couples simply by taking the inner product of the two. Explicit, yet trivial, mathematics show that in essence the coupling boils down to the replacement $D_M \to D_M - ieA_M$, where $D_M = \partial_M + \frac{1}{4}\omega_{M\underline{AB}}S^{\underline{AB}}$ denotes the covariant fermion derivative whose deviation from the ordinary partial derivative is due to the curvature of spacetime[3].

4.2 Right chiral fermion propagator

As we said, the first step to take, is to add a fermion field in the bulk. That simply amounts to adding a Dirac action in the total action of our theory. Such an action reads

$$\begin{aligned} S_F &= ig_f \int d^5x\sqrt{-g}\bar{\Psi}(\frac{1}{2}\overrightarrow{\not{D}} - \frac{1}{2}\overleftarrow{\not{D}} - M)\Psi \\ &= ig_f \int d^5x\sqrt{-g}\left(\frac{1}{2}\bar{\Psi}\Gamma^\mu D_\mu\Psi - \frac{1}{2}D_\mu\bar{\Psi}\Gamma^\mu\Psi - M\bar{\Psi}\Psi\right), \end{aligned} \tag{4.7}$$

where $\tilde{D}_\mu = \partial_\mu + \frac{1}{4}\omega_{\mu\underline{AB}}S^{\underline{AB}} - ieA_\mu$.

Varying S_F with respect to Ψ and $\Psi^\dagger$, we get the equations of motion for this field. Although we know what the equations of motion will be, obviously the Dirac equations, what will be of greater importance to us, are the boundary terms that will emerge. Hence, we have[4]

$$\begin{aligned} \delta S_F &= ig_f \int d^5x\sqrt{-g}\left(\frac{1}{2}\delta\bar{\Psi}\Gamma^\mu\tilde{D}_\mu\Psi + \frac{1}{2}\bar{\Psi}\Gamma^\mu\tilde{D}_\mu\delta\Psi - \frac{1}{2}\tilde{D}_\mu\delta\bar{\Psi}\Gamma^\mu\Psi - \frac{1}{2}\tilde{D}_\mu\bar{\Psi}\Gamma^\mu\delta\Psi - M\delta\bar{\Psi}\Psi - M\bar{\Psi}\delta\Psi\right) \\ &= ig_f \int d^5x\sqrt{-g}\Big[\frac{1}{2}\delta\bar{\Psi}\Gamma^\mu\tilde{D}_\mu\Psi + \frac{1}{2}\tilde{D}_\mu\left(\bar{\Psi}\Gamma^\mu\delta\Psi\right) - \frac{1}{2}\tilde{D}_\mu\left(\bar{\Psi}\Gamma^\mu\right)\delta\Psi \\ &\qquad - \frac{1}{2}\tilde{D}_\mu(\delta\bar{\Psi}\Gamma^\mu\Psi) + \frac{1}{2}\delta\bar{\Psi}\tilde{D}_\mu(\Gamma^\mu\Psi) - \frac{1}{2}\tilde{D}_\mu\bar{\Psi}\Gamma^\mu\delta\Psi - M\delta\bar{\Psi}\Psi - M\bar{\Psi}\delta\Psi\Big] \\ &= ig_f \int d^5x\sqrt{-g}\Big[\frac{1}{2}\delta\bar{\Psi}\Gamma^\mu\tilde{D}_\mu\Psi + \frac{1}{2}\tilde{D}_\mu\left(\bar{\Psi}\Gamma^\mu\delta\Psi\right) - \frac{1}{2}\tilde{D}_\mu\bar{\Psi}\Gamma^\mu\delta\Psi \\ &\qquad - \frac{1}{2}\tilde{D}_\mu(\delta\bar{\Psi}\Gamma^\mu\Psi) + \frac{1}{2}\delta\bar{\Psi}\Gamma^\mu\tilde{D}_\mu\Psi - \frac{1}{2}\tilde{D}_\mu\bar{\Psi}\Gamma^\mu\delta\Psi - M\delta\bar{\Psi}\Psi - M\bar{\Psi}\delta\Psi\Big] \\ &= ig_f \int d^5x\sqrt{-g}\Big[\delta\bar{\Psi}(\Gamma^\mu\tilde{D}_\mu\Psi - M\Psi) - (\tilde{D}_\mu\bar{\Psi}\Gamma^\mu + M\bar{\Psi})\delta\Psi \\ &\qquad - \frac{1}{2}\tilde{D}_\mu(\delta\bar{\Psi}\Gamma^\mu\Psi) + \frac{1}{2}D_\mu\left(\bar{\Psi}\Gamma^\mu\delta\Psi\right)\Big]. \end{aligned} \tag{4.8}$$

In the above we could take the Γ-matrices outside the fermionic covariant derivative since

$$\begin{aligned} \tilde{D}_\mu(\Gamma^\mu\Psi) &= (D_\mu - ieA_\mu)(\Gamma^\mu\Psi) = D_\mu(\Gamma^\mu\Psi) - ieA_\mu\Gamma^\mu\Psi \\ &= D_\mu(\Gamma^a e^\mu_a\Psi) - ie\Gamma^\mu A_\mu\Psi = \Gamma^a e^\mu_a D_\mu\Psi - ie\Gamma^\mu A_\mu\Psi \\ &= \Gamma^\mu\tilde{D}_\mu\Psi. \end{aligned} \tag{4.9}$$

[3] A reader interested in following the mathematical derivations of this chapter should be familiar with the tetrad formulation of General Relativity. A well written review of the topic can be found in [60]

[4] For notational clarity, note that in the absence of a parenthesis, the derivative acts only in the factor that come after it.

There, we also used that the flat gamma matrices Γ^a are constant, that the tetrad postulate holds, namely $D_\mu e^\nu_a = 0$ and that $A_\mu \Gamma^\mu = \Gamma^\mu A_\mu$ since A_μ is not a matrix. In the above notation $\tilde{D}_\mu = D_\mu - ieA_\mu$, where D_μ is the fermionic covariant derivative due to the curvature of spacetime, while $\tilde{D}_\mu$ is the fermionic covariant derivative after the coupling with the gauge field.

Demanding $\delta S_f = 0$ we immediately get the two equations of motion for Ψ and $\bar{\Psi}$ which are indeed the Dirac equations as we expected in the first place, namely

$$\begin{aligned} \Gamma^\mu \tilde{D}_\mu \Psi - M\Psi = 0 \\ \tilde{D}_\mu \bar{\Psi}\Gamma^\mu + M\bar{\Psi} = 0. \end{aligned} \tag{4.10}$$

However, the on-shell variation of the action does not vanish as it is the case for a well posed variational problem. Instead we are left with two boundary terms,

$$\begin{aligned} \delta S_F &= ig_f \int d^5x\sqrt{-g}\Big[-\frac{1}{2}\tilde{D}_\mu(\delta\bar{\Psi}\Gamma^\mu\Psi) + \frac{1}{2}\tilde{D}_\mu\left(\bar{\Psi}\Gamma^\mu\delta\Psi\right)\Big] \\ &= ig_f \int d^5x\sqrt{-g}\Big[-\frac{1}{2}D_\mu(\delta\bar{\Psi}\Gamma^\mu\Psi) + \frac{1}{2}D_\mu\left(\bar{\Psi}\Gamma^\mu\delta\Psi\right) + ieA_\mu\delta\bar{\Psi}\Gamma^\mu\Psi) - ieA_\mu\bar{\Psi}\Gamma^\mu\delta\Psi\Big] \\ &= -\frac{1}{2}ig_f \int d^4x\sqrt{-h}n_\mu\Big[\delta\bar{\Psi}\Gamma^\mu\Psi - \bar{\Psi}\Gamma^\mu\delta\Psi\Big] = -\frac{1}{2}ig_f \int d^4x\sqrt{-h}\big[\delta\bar{\Psi}\Gamma^r\Psi - \bar{\Psi}\Gamma^r\delta\Psi\big]\Big|_{r=r_h}^{r=r_0} \\ &= -\frac{1}{2}ig_f \int_{r=r0} d^4x\sqrt{-h}\big[\delta\bar{\Psi}\Gamma^r\Psi - \bar{\Psi}\Gamma^r\delta\Psi\big]. \end{aligned} \tag{4.11}$$

In the fourth line, Stokes theorem was used which simply states

$$\int_V d^nx\sqrt{-g}\nabla_\mu J^\mu = \int_{\partial V} d^{n-1}x\sqrt{-h}n_\mu J^\mu, \tag{4.12}$$

where h is the induced metric and n_μ the normal vector on ∂V[5]. In this case V is the bulk AdS spacetime bounded by the flat hypersufaces at the horizon $r = r_h$ and at the boundary $r = r_0$. By definition of r_h, as the first zero of $f(r)$ we can easily see that the determinant of the induced metric vanishes at the horizon and that is why we are left only with the boundary term at $r = r_0$.

Next we decompose the Dirac fermion into its chiral components, and the various terms read

$$\begin{aligned} \delta\bar{\Psi}\Gamma^r\Psi &= \begin{pmatrix} \delta\Psi_+^\dagger & \delta\Psi_-^\dagger \end{pmatrix}\begin{pmatrix} 0 & 1 \\ 1 & 0 \end{pmatrix}\begin{pmatrix} \Psi_+ \\ \Psi_- \end{pmatrix} = \delta\Psi_+^\dagger\Psi_- + \delta\Psi_-^\dagger\Psi_+ \\ \bar{\Psi}\Gamma^r\delta\Psi &= \begin{pmatrix} \Psi_+^\dagger & \Psi_-^\dagger \end{pmatrix}\begin{pmatrix} 0 & 1 \\ 1 & 0 \end{pmatrix}\begin{pmatrix} \delta\Psi_+ \\ \delta\Psi_- \end{pmatrix} = \Psi_+^\dagger\delta\Psi_- + \Psi_-^\dagger\delta\Psi_+. \end{aligned} \tag{4.13}$$

Also, using the notation

$$\Psi = \Psi_R + \Psi_L = \begin{pmatrix} \Psi_+ \\ 0 \end{pmatrix} + \begin{pmatrix} 0 \\ \Psi_- \end{pmatrix} = \begin{pmatrix} \Psi_+ \\ \Psi_- \end{pmatrix}, \tag{4.14}$$

[5]Eq. (4.12) contains an important notational feature. As happens throughout the chapter, we do not use different types of indices to denote spaces of different dimension. Specifically, we used the μ index to denote coordinates both in space V and on its boundary ∂V. The reader should be able to infer from the context which the spacetime the index is referring to.

we have

$$\begin{aligned}
\delta\bar{\Psi}_R\Psi_L &= \begin{pmatrix} \delta\Psi_+^\dagger & 0 \end{pmatrix}\begin{pmatrix} 0 & -1 \\ 1 & 0 \end{pmatrix}\begin{pmatrix} 0 \\ \Psi_- \end{pmatrix} = -\delta\Psi_+^\dagger\Psi_- \\
\bar{\Psi}_R\delta\Psi_L &= \begin{pmatrix} \Psi_+^\dagger & 0 \end{pmatrix}\begin{pmatrix} 0 & -1 \\ 1 & 0 \end{pmatrix}\begin{pmatrix} 0 \\ \delta\Psi_- \end{pmatrix} = -\Psi_+^\dagger\delta\Psi_- \\
\delta\bar{\Psi}_L\Psi_R &= \begin{pmatrix} 0 & \delta\Psi_-^\dagger \end{pmatrix}\begin{pmatrix} 0 & -1 \\ 1 & 0 \end{pmatrix}\begin{pmatrix} \Psi_+ \\ 0 \end{pmatrix} = \delta\Psi_-^\dagger\Psi_+ \\
\bar{\Psi}_L\delta\Psi_R &= \begin{pmatrix} 0 & \Psi_-^\dagger \end{pmatrix}\begin{pmatrix} 0 & -1 \\ 1 & 0 \end{pmatrix}\begin{pmatrix} \delta\Psi_+ \\ 0 \end{pmatrix} = \Psi_-^\dagger\delta\Psi_+.
\end{aligned} \tag{4.15}$$

Hence, after straightforward replacement, we get

$$\begin{aligned}
\delta S_F &= -\frac{1}{2}ig_f\int_{r=r0} d^4x\sqrt{-h}\big[-\delta\bar{\Psi}_R\Psi_L + \delta\bar{\Psi}_L\Psi_R + \bar{\Psi}_R\delta\Psi_L - \bar{\Psi}_L\delta\Psi_R\big] \\
&= \frac{1}{2}ig_f\int_{r=r0} d^4x\sqrt{-h}\big[\delta\bar{\Psi}_R\Psi_L + \bar{\Psi}_L\delta\Psi_R - \delta\bar{\Psi}_L\Psi_R - \bar{\Psi}_R\delta\Psi_L\big].
\end{aligned} \tag{4.16}$$

Since the Dirac equation is a first order differential equation, we cannot impose $\delta\Psi_+ = \delta\Psi_- = 0$ simultaneously. Instead, only one of the two conditions can be chosen and the chirality of the boundary fermion will depend on this choice. In any case, there will be a leftover boundary term that we need to eliminate. To do so, we introduce by hand an additional boundary term in the action that will not affect the bulk equations of motion. This term can be easily seen that reads

$$S_\partial = \pm\frac{1}{2}ig_f\int_{r=r0} d^4x\sqrt{-h}\big[\bar{\Psi}_L\Psi_R + \bar{\Psi}_R\Psi_L\big]. \tag{4.17}$$

A small comment is in order here. Although the above choice of the boundary action will make the variational problem well posed, it doesn't come for free. What we are ultimately interested in, are interacting Green's functions on the boundary. In general we expect that the Green's function is complex and its imaginary part will give the spectral function of the system. However, the above choice renders the Green's function real and no information about the Green's function can be deduced. Interestingly enough, the solution to this problem is simply to drop one of the two terms in the boundary action according to which chirality we want to keep on the boundary [58]. In the end, the appropriate boundary term has the form

$$S_\partial = \begin{cases} \frac{1}{2}ig_f\int_{r=r0} d^4x\sqrt{-h}\big[\bar{\Psi}_R\Psi_L\big] & \text{if } \delta\Psi_+ = 0 \\ \\ -\frac{1}{2}ig_f\int_{r=r0} d^4x\sqrt{-h}\big[\bar{\Psi}_L\Psi_R\big] & \text{if } \delta\Psi_- = 0 \end{cases} \tag{4.18}$$

In essence, setting the variation of one chiral component of Ψ to zero on the boundary, will give us an effective field theory for it on the boundary.

Our ultimate goal is to have a semi-holographic description of WSM. In order to achieve this, we need two chiral fermions of opposite chirality on the boundary. Hence, as a starting point let us assume that for the first fermion that we put in the vacuum, we set $\delta\Psi_+ = 0$. This choice, will eventually amount to an effective description for a right-handed chiral fermion on the boundary. Once an interacting Green's function is obtained, then we will put a second Dirac fermion in the bulk with the boundary condition $\delta\Psi_- = 0$, that will give an interacting Green's function for a left-handed chiral fermion. But for now, we concentrate on the analysis for the first Dirac fermion.

Having set $\delta\Psi_+ = 0$ on the boundary, we can add more boundary terms that depend only on Ψ_+ without affecting the equations of motion in the bulk. We exploit this freedom to add a kinetic term for Ψ_+, namely

$$S_{kin} = iZ \int_{r=r_0} d^4x \sqrt{-h} \sqrt{g_{rr}} \bar{\Psi}_R \Gamma^\mu D_\mu \Psi_R. \tag{4.19}$$

It is precisely this term that will give the free part of the full, interacting Green's function. At the same time, such a term renders the Green's function obey ARPES sum rule, which is a crucial criterion for the Green's function to correspond to a single particle operator as we mentioned in Chapter 1 [59].

At this point we have all the necessary ingredients to build the first part of the semi-holographic dual theory of WSMs. As a recap, the total bulk action reads

$$S_{total} = S_{EHM} + S_F + S_\partial + S_{kin}. \tag{4.20}$$

Imposing the equations of motion, the on-shell boundary action reads

$$\begin{aligned} S_{on-shell}[\Psi_R, \Psi_L] &= S_{kin}[\Psi_R, \Psi_L] + S_\partial[\Psi_R, \Psi_L] \\ &= iZ \int_{r=r_0} d^4x \sqrt{-h} \sqrt{g_{rr}} \bar{\Psi}_R \tilde{\not{D}} \Psi_R + ig_f \int_{r=r_0} d^4x \sqrt{-h} \bar{\Psi}_R \Psi_L. \end{aligned} \tag{4.21}$$

In order to have an effective action for the boundary value of Ψ_R we need to eliminate Ψ_L. We can easily do so, recalling that the two chiral fields are related via the Dirac equation. Thus, if we write the Dirac operator as a matrix in the general form $\mathcal{D} = \begin{pmatrix} A & B \\ C & D \end{pmatrix}$ then

$$\mathcal{D}\Psi = \begin{pmatrix} A & B \\ C & D \end{pmatrix} \begin{pmatrix} \Psi_+ \\ \Psi_- \end{pmatrix} = 0 \quad \Rightarrow \quad \Psi_- = -i\xi\Psi_+, \tag{4.22}$$

where ξ is a 2×2 matrix that can be determined from the Dirac equation. For the moment, we ignore its exact form and we try to see what the effective action looks like after eliminating Ψ_L. After an expression for the interacting Green's function is obtained, we will return to the important question of how to determine this proportionality factor.

As usual, we are interested in the Green's function in momentum space. That means that the chiral spinor should be Fourier transformed. However, not all 5 coordinates, of our 5-dimensional bulk AdS spacetime, need to be transformed. After all, the fifth coordinate will not correspond to a physical coordinate of the 4d spacetime where the CFT lives in. That is why, we will Fourier transform the chiral field at constant r-slices. As a result, the components of the Fourier expansion will depend both on the 4-momentum k^μ but also on the given r-slice. This is a quite natural thing to do, as the physics we are trying to describe lives at the constant $r \to \infty$ slice. Therefore, we can write

$$\Psi_+(r, x) = \int \frac{d^4p}{(2\pi)^4} \tilde{\Psi_+}(r, k) e^{ik_\mu x^\mu}. \tag{4.23}$$

Using eqs. (4.22) and (4.23), the second term in eq. (4.21) reads

$$
\begin{aligned}
ig_f \int_{r=r_0} d^4x\sqrt{-h}\bar{\Psi}_R\Psi_L &= ig_f \int_{r=r_0} d^4x\sqrt{-h}\begin{pmatrix} \Psi_+^\dagger & 0 \end{pmatrix}\begin{pmatrix} 0 & -1 \\ 1 & 0 \end{pmatrix}\begin{pmatrix} 0 \\ \Psi_- \end{pmatrix} = -ig_f \int_{r=r_0} d^4x\sqrt{-h}\Psi_+^\dagger\Psi_- \\
&= -ig_f \int_{r=r_0} d^4x\sqrt{-h}\Psi_+^\dagger(-i\xi\Psi_+) = -g_f \int_{r=r_0} d^4x\sqrt{-h}\Psi_+^\dagger\xi\Psi_+ \\
&= -g_f \int d^4x\sqrt{-h}\{\int \frac{d^4p}{(2\pi)^4}\tilde{\Psi}_+^\dagger(r_0,p)e^{-ip.x}\}\xi\{\int \frac{d^4k}{(2\pi)^4}\tilde{\Psi}_+(r_0,k)e^{ik.x}\} \\
&= -g_f \int \frac{d^4pd^4k}{(2\pi)^8}\sqrt{-h}\tilde{\Psi}_+^\dagger(r_0,p)\xi\tilde{\Psi}_+(r_0,k)\{\int d^4x e^{-i(p_\mu-k_\mu)x^\mu}\} \\
&= -g_f \int \frac{d^4pd^4k}{(2\pi)^8}\sqrt{-h}\tilde{\Psi}_+^\dagger(r_0,p)\xi\tilde{\Psi}_+(r_0,k)(2\pi)^4\delta(p\mu - k\mu) \\
&= -g_f \int \frac{d^4p}{(2\pi)^4}\sqrt{-h}\tilde{\Psi}_+^\dagger(r_0,p)\xi\tilde{\Psi}_+(r_0,p).
\end{aligned}
\tag{4.24}
$$

In order to treat the kinetic term, we first need to find the expression of the covariant derivatives. It can be shown [30], that the metric of eq. (4.3) leads to a covariant derivate with components

$$
\begin{aligned}
\tilde{D}_r &= \partial_r \\
\tilde{D}_t &= \partial_t - \frac{1}{2}rf(r)\partial_r(rf(r))\Gamma^{\underline{t}}\Gamma^{\underline{r}} - ieA_t(r) \\
\tilde{D}_i &= \partial_i + \frac{1}{2}rf(r)\Gamma^{\underline{i}}\Gamma^{\underline{r}}.
\end{aligned}
\tag{4.25}
$$

Now that we know how to take the fermionic covariant derivative in this spacetime, let us have a closer look at the kinetic term. But before that, a simplifying remark will prove useful. Although the covariant derivatives seem to have a rather complicated form, we need to keep in mind that they are to be calculated on the boundary of the AdS spacetime. In other words we are calculating them for $r = r_0$ with the requirement $r_0 \to \infty$. This leads to great simplification, since in this limit the spin connection contribution vanishes and the gauge potential tends to its limiting value μ, as can be easily seen from its explicit form in eq. (4.6). In the end, the derivatives can be written as

$$
\begin{aligned}
\tilde{D}_r\Big|_{r_0\to\infty} &= \partial_r \\
\tilde{D}_t\Big|_{r_0\to\infty} &= \partial_t - ie\mu \\
\tilde{D}_i\Big|_{r_0\to\infty} &= \partial_i.
\end{aligned}
\tag{4.26}
$$

With an explicit form for the boundary covariant derivatives, we see that the kinetic term of

the Dirac field reads

$$\begin{aligned}
\bar{\Psi}_R\tilde{\not{D}}\Psi_R &= \begin{pmatrix} \Psi_+^\dagger & 0 \end{pmatrix}\Gamma^{\underline{t}}\Gamma^t(\partial_t - ie\mu)\begin{pmatrix} \Psi_+^\dagger \\ 0 \end{pmatrix} + \begin{pmatrix} \Psi_+^\dagger & 0 \end{pmatrix}\Gamma^{\underline{t}}\Gamma^i\partial_i\begin{pmatrix} \Psi_+^\dagger \\ 0 \end{pmatrix} \\
&= -e^t_{\underline{t}}(r_0)\Psi_+^\dagger(\partial_t - ie\mu)\Psi_+^\dagger - e^i_{\underline{i}}(r_0)\Psi_+^\dagger\sigma^{\underline{i}}\partial_i\Psi_+^\dagger \\
&= -\int\frac{d^4pd^4k}{(2\pi)^8}\Big\{e^t_{\underline{t}}(r_0)\tilde{\Psi}_+^\dagger(r_0,p)e^{-ip_\mu x^\mu}(\partial_t - ie\mu)\left(\tilde{\Psi}_+(r_0,k)e^{ik_\mu x^\mu}\right) \\
&\qquad\qquad + e^i_{\underline{i}}(r_0)\tilde{\Psi}_+^\dagger(r_0,p)e^{-ip_\mu x^\mu}\sigma^{\underline{i}}\partial_i\left(\tilde{\Psi}_+(r_0,k)e^{ik_\mu x^\mu}\right)\Big\} \\
&= -i\int\frac{d^4pd^4k}{(2\pi)^8}\Big\{e^t_{\underline{t}}(r_0)\tilde{\Psi}_+^\dagger(r_0,p)\tilde{k_0}\tilde{\Psi}_+(r_0,k) + e^i_{\underline{i}}(r_0)\tilde{\Psi}_+^\dagger(r_0,p)\sigma^{\underline{i}}k_i\tilde{\Psi}_+(r_0,k)\Big\}e^{-i(p_\mu-k_\mu)x^\mu} \\
&= -i\int\frac{d^4pd^4k}{(2\pi)^8}\Big\{e^\mu_a(r_0)\tilde{k}_\mu\tilde{\Psi}_+^\dagger(r_0,p)\sigma^a\tilde{\Psi}_+(r_0,k)\Big\}e^{-i(p_\mu-k_\mu)x^\mu}.
\end{aligned} \tag{4.27}$$

Also,we have that

$$\begin{aligned}
iZ\int_{r=r_0}d^4x\sqrt{-h}\sqrt{g_{rr}}\bar{\Psi}_R\tilde{\not{D}}\Psi_R &= Z\sqrt{-h}\sqrt{g_{rr}}\int\frac{d^4pd^4k}{(2\pi)^8}\Big\{e^\mu_a(r_0)\tilde{k}_\mu\tilde{\Psi}_+^\dagger(r_0,p)\sigma^a\tilde{\Psi}_+(r_0,k)\Big\}\int d^4xe^{-i(p_\mu-k_\mu)x^\mu} \\
&= Z\sqrt{-h}\sqrt{g_{rr}}\int\frac{d^4pd^4k}{(2\pi)^8}\Big\{e^\mu_a(r_0)\tilde{k}_\mu\tilde{\Psi}_+^\dagger(r_0,p)\sigma^a\tilde{\Psi}_+(r_0,k)\Big\}(2\pi)^4\delta(p_\mu-k_\mu) \\
&= Z\sqrt{-h}\sqrt{g_{rr}}\int\frac{d^4k}{(2\pi)^4}\Big\{e^\mu_a(r_0)\tilde{k}_\mu\tilde{\Psi}_+^\dagger(r_0,k)\sigma^a\tilde{\Psi}_+(r_0,k)\Big\}.
\end{aligned} \tag{4.28}$$

Hence, putting the two results from eqs. (4.24) and (4.28) together, we see that the on-shell action in momentum space for the right chiral component of the bulk Dirac fermion, eq. (4.21), reads

$$\begin{aligned}
S_{eff}[\Psi_+] &= -\int\frac{d^4k}{(2\pi)^4}\sqrt{-h}\sqrt{g_{rr}}\tilde{\Psi}_+^\dagger(r_0,k)\Big\{g_f\sqrt{g^{rr}}\xi(r_0,k) - Ze^\mu_a(r_0)\tilde{k}_\mu\sigma^a\Big\}\tilde{\Psi}_+(r_0,k) \\
&= -\int\frac{d^4k}{(2\pi)^4}r_0^3\tilde{\Psi}_+^\dagger(r_0,k)\Big\{g_fr_0f(r_0)\xi(r_0,k) - Z\frac{1}{r_0f(r_0)}\tilde{k}_0 - Z\frac{1}{r_0}\sigma^ik_i\Big\}\tilde{\Psi}_+(r_0,k) \\
&= -\int\frac{d^4k}{(2\pi)^4}\tilde{\Psi}_+^\dagger(r_0,k)\Big\{g_fr_0^4f(r_0)\xi(r_0,k) - Z\frac{r_0^2}{f(r_0)}\tilde{k}_0 - Zr_0^2\sigma^ik_i\Big\}\tilde{\Psi}_+(r_0,k) \\
&\to -\int\frac{d^4k}{(2\pi)^4}\tilde{\Psi}_+^\dagger(r_0,k)\Big\{-\tilde{k}_0 - f(r_0)\sigma^ik_i + g_fr_0^2f^2(r_0)Z^{-1}\xi(r_0,k)\Big\}\tilde{\Psi}_+(r_0,k) \\
&= \int\frac{d^4k}{(2\pi)^4}\tilde{\Psi}_+^\dagger(r_0,k)\Big\{\tilde{k}_0 + f(r_0)\sigma^ik_i - g_fr_0^2f^2(r_0)Z^{-1}\xi(r_0,k)\Big\}\tilde{\Psi}_+(r_0,k).
\end{aligned} \tag{4.29}$$

In the fourth line, we have performed a fermion rescaling of the form $\Psi_+ \to \sqrt{\frac{Z}{f(r_0)}}r_0\Psi_+$.

Finally, in order to take the limit $r_0 \to \infty$, we must be sure that all terms are well behaved. Of course the emblackening factor $f(r_0) \to 1$ as we approach the boundary of the AdS space-time; this was by construction what we wanted. As for the third term, we use the fact that for large r_0, $\xi \sim r_0^{-2M}$ and therefore $r_0^{2M}\xi \to constant$. To use this property, we introduce another parameter $g \equiv \frac{g_f}{Z}r_0^{2-2M}$ such that in the double limit $g \to \infty$ and $g_f \to 0$ this new parameter tends to a constant value. Then the third term in eq. (4.29) reads

$$\Sigma_+(k) \equiv -g\lim_{r_0\to\infty}r_0^{2M}\xi(r_0,k). \tag{4.30}$$

With these convention we can easily read the Green's function for the right chiral fermion as

$$G_+^{-1}(k) = -(\omega + e\mu) + \sigma^i k_i + \Sigma_+(k) = -(\omega + e\mu - \Sigma_0^+) + \sigma^i(k_i + \Sigma_i^+), \tag{4.31}$$

where we have performed an expansion of the self energy matrix in the Pauli matrices basis as

$$\Sigma_+(k) = \Sigma_0^+ \mathbb{I} + \sigma^i \Sigma_i^+, \tag{4.32}$$

where, for presentation clarity, we have used upper indices to denote the chirality of the components of the self energy.

Finally, inverting eq. (4.31) we see that the interacting propagator reads

$$G_+(k) = -\frac{\left(\omega + e\mu - \Sigma_0^+\right)\mathbb{I} + \left(k_i + \Sigma_i^+\right)\sigma^i}{\left(\omega + e\mu - \Sigma_0^+\right)^2 - \left(k_i + \Sigma_i^+\right)^2}. \tag{4.33}$$

Nonetheless, in order to have a final answer for the interacting Green's function we need to compute the proportionality factor $\xi(k)$, that we introduced in eq. 4.22. We will turn our attention to this point right now.

4.2.1 Finding ξ

Here comes a crucial part of the calculations we are performing. Ultimately, we are using the AdS/CFT correspondance to model the interactions of the system. This information is encoded in the self energy term of the boundary fermion propagator, which in the AdS/CFT model we have created depends on the ξ proportionality factor. Of course here the word factor doesn't mean that ξ is a c-number. Instead, as we have commented before, $\Psi_\pm$ are 2-component spinors, so their proportionality factor is a 2×2 matrix. It is this matrix that we will try to determine using the Dirac equation in the bulk. Let us see how can we do this.

By definition of the ξ matrix, we have $\Psi_-(k) = -i\xi(k)\Psi_+(k)$. Now lets try to find a plane wave solution at a constant r-slice to the Dirac equation, i.e. a solution of the form

$$\Psi(r, x) = \Psi(r, k)e^{ik_\mu x^\mu}.$$

Hence,

$$\begin{aligned}(\tilde{\not{D}} - M)\Psi(r,x) &= (\tilde{\not{D}} - M)\Psi(r,k)e^{ik\mu x^\mu} \\ &= (\Gamma^r \tilde{D}_r + \Gamma^t \tilde{D}_t + \Gamma^i \tilde{D}_i)\Psi(r,k)e^{ik\mu x^\mu} \\ &= (\Gamma^{\underline{r}} e^r_{\underline{r}} \tilde{D}_r + \Gamma^{\underline{t}} e^t_{\underline{t}} \tilde{D}_t + \Gamma^{\underline{i}} e^i_{\underline{i}} \tilde{D}_i)\Psi(r,k)e^{ik\mu x^\mu}.\end{aligned} \tag{4.34}$$

Now lets see each term separately

$$\begin{aligned}\Gamma^{\underline{t}} e^t_{\underline{t}} \tilde{D}_t e^{ik\mu x^\mu} &= \Gamma^{\underline{t}} \frac{1}{rf(r)}(\partial_t - \frac{1}{2} rf(r)\partial_r(rf(r))\Gamma^{\underline{t}}\Gamma^{\underline{r}} - ieA_t(r))e^{ik\mu x^\mu} \\ &= \left(\Gamma^{\underline{t}} \frac{i\left(k_t - eA_t(r)\right)}{rf(r)} + \frac{1}{2}\partial_r(rf(r))\Gamma^{\underline{r}}\right) e^{ik\mu x^\mu} \\ &= \left(-\Gamma^{\underline{t}} \frac{i\left(\omega + eA_t(r)\right)}{rf(r)} + \frac{1}{2}\partial_r(rf(r))\Gamma^{\underline{r}}\right) e^{ik\mu x^\mu} \\ &= \left(-i\Gamma^{\underline{t}} \frac{\tilde{\omega}}{r} + \frac{1}{2}\partial_r(rf(r))\Gamma^{\underline{r}}\right) e^{ik\mu x^\mu},\end{aligned} \tag{4.35}$$

where $\tilde{\omega} \equiv \frac{\omega + eA_t(r)}{f(r)}$. This definition of $\tilde{\omega}$ will simplify some notations later on. Similarly

$$\begin{aligned}\Gamma^{\underline{i}} e^{i}_{\underline{i}} \tilde{D}_i e^{ik\mu x^\mu} &= \Gamma^{\underline{i}} \frac{1}{r}\left(\partial_i + \frac{1}{2} r f(r) \Gamma^{\underline{i}} \Gamma^{\underline{r}}\right) e^{ik\mu x^\mu} \\ &= \left(\Gamma^{\underline{i}} \frac{1}{r} i k_i + \frac{1}{2} f(r) \Gamma^{\underline{i}} \Gamma^{\underline{i}} \Gamma^{\underline{r}}\right) e^{ik\mu x^\mu},\end{aligned} \tag{4.36}$$

and quite trivially

$$\Gamma^{\underline{r}} e^{r}_{\underline{r}} D_r = \Gamma^{\underline{r}} r f(r) \partial_r. \tag{4.37}$$

Replacing the above relations in the Dirac equation we have

$$\begin{aligned}(\tilde{\not{D}} - M)\Psi(r,x) = \Big[&\Gamma^{\underline{r}} r f(r) \partial_r + \frac{i}{r}\left(\Gamma^{\underline{i}} k_i - \Gamma^{\underline{t}} \tilde{\omega}\right) \\ &+ \frac{1}{2}\Gamma^{\underline{r}} \partial_r (r f(r)) + \frac{1}{2}\Gamma^{\underline{r}} f(r)(d-1) - M\Big]\Psi(r,k) e^{ik\mu x^\mu}\end{aligned} \tag{4.38}$$

$$= \Big[\Gamma^{\underline{r}} r f(r) \partial_r + \frac{i}{r}\left(\Gamma^{\underline{i}} k_i - \Gamma^{\underline{t}} \tilde{\omega}\right) + \frac{1}{2}\Gamma^{\underline{r}} w(r) - M\Big]\Psi(r,k) e^{ik\mu x^\mu},$$

where $w(r) \equiv \partial_r(r f(r)) + (d-1) f(r)$.

Let us, next, introduce the spinor $\Phi(r)$, defined through the following decomposition of the Ψ-spinor

$$\Psi(r,k) = \Phi(r,k) \exp\{-\frac{1}{2}\int_0^r d\tilde{r} \frac{w(\tilde{r})}{\tilde{r} f(\tilde{r})}\}. \tag{4.39}$$

Then

$$\begin{aligned}\Gamma^{\underline{r}} r f(r) \partial_r \Psi(r,k) &= \Gamma^{\underline{r}} r f(r) (-\frac{1}{2}\frac{w(r)}{r f(r)}) \Phi(r,k) \exp\{-\frac{1}{2}\int_0^r d\tilde{r} \frac{w(\tilde{r})}{\tilde{r} f(\tilde{r})}\} \\ &\quad + \Gamma^{\underline{r}} r f(r) \partial_r(\Phi(r,k)) \exp\{-\frac{1}{2}\int_0^r d\tilde{r} \frac{w(\tilde{r})}{\tilde{r} f(\tilde{r})}\} \\ &= -\frac{1}{2}\Gamma^{\underline{r}} w(r) \Phi(r,k) \exp\{-\frac{1}{2}\int_0^r d\tilde{r} \frac{w(\tilde{r})}{\tilde{r} f(\tilde{r})}\} \\ &\quad + \Gamma^{\underline{r}} r f(r) \partial_r(\Phi(r,k)) \exp\{-\frac{1}{2}\int_0^r d\tilde{r} \frac{w(\tilde{r})}{\tilde{r} f(\tilde{r})}\}.\end{aligned} \tag{4.40}$$

Hence, instead of solving the Dirac equation for the spinor field Ψ we can solve the equivalent and slightly easier equation for Φ that after the above replacements reads

$$\left(\Gamma^{\underline{r}} r f(r) \partial_r + \frac{i}{r} \Gamma . \tilde{k} - M\right) \Phi(r,k) = 0, \tag{4.41}$$

where as before $\tilde{k} = (-\tilde{\omega}, \vec{k})$.

The above equation is simpler than the one we started with, but it would be nice if we could simplify it even further. To do so, we recall that the system we are working with is rotationally invariant. That means that we do not have to work with a vector $\vec{k}$ that has in principle aribitrary components. We can work in any given direction and the same result should apply to all other directions. In other words, spherical symmetry reduces the independent degrees of freedom of our system from 3 to 1; namely the distance from the origin of the system. That means that the result we will get, can only depend on the magnitude of the vector $\vec{k}$.

Having said that, lets assume that $\vec{k}$ points along the positive z-axis, i.e. $\vec{k} = (0,0,k_3)$ with $k_3 > 0$. Then we can recover the general result simply by replacing $k_3 \to |\vec{k}|$. Such a choice, is

rather convenient because the third Pauli matrix σ^3 is diagonal just like the unit matrix. We shal see why this is the case soon enough! With this assumption and recalling that

$$\Gamma^{\underline{t}} = \begin{pmatrix} 0 & -1 \\ 1 & 0 \end{pmatrix} \qquad \Gamma^{\underline{r}} = \begin{pmatrix} 1 & 0 \\ 0 & -1 \end{pmatrix} \qquad \Gamma^{\underline{i}} = \begin{pmatrix} 0 & \sigma^i \\ \sigma^i & 0 \end{pmatrix}, \tag{4.42}$$

we have

$$\left[\begin{pmatrix} r(rf(r)\partial_r - M) & 0 \\ 0 & -r(rf(r)\partial_r + M) \end{pmatrix} + i \begin{pmatrix} 0 & -1 \\ 1 & 0 \end{pmatrix} (-\tilde{\omega}) + i \begin{pmatrix} 0 & \sigma^3 \\ \sigma^3 & 0 \end{pmatrix} k_3 \right] \begin{pmatrix} \Phi_+(r,k) \\ \Phi_-(r,k) \end{pmatrix} = 0, \tag{4.43}$$

that reduces to two equations for the two 2-component spinors $\Phi_\pm$

$$\begin{aligned} \mathcal{A}(M)\Phi_+ + i(\tilde{\omega} + \sigma^3 k_3)\Phi_- = 0 \\ -\mathcal{A}(-M)\Phi_- - i(\tilde{\omega} - \sigma^3 k_3)\Phi_+ = 0, \end{aligned} \tag{4.44}$$

where for notational convenience we have defined $\mathcal{A}(M) \equiv r(rf(r)\partial_r - M)$.

It is exactly at this point that the convenience of the choice for the momentum vector becomes transparent. The above are differential equations that relate the two spinors $\Phi\pm$. The matrices that relate them are diagonal and hence the ξ matrix should itself be diagonal. That means, that we can write

$$\Psi_- = -i \begin{pmatrix} \xi_+ & 0 \\ 0 & \xi_- \end{pmatrix} \Psi_+. \tag{4.45}$$

Note that here we might have some notational abuse. To make matters clear, the $\pm$ indices in the diagonal components of ξ have nothing to do with chirality[6]. It is just a label for the upper left and lower right components of the ξ matrix. Maybe an unfortunate, but still just a labelling!.

Then, we further decompose the Weyl spinors as $\Psi_\pm = \begin{pmatrix} \tilde{u}_\pm \\ \tilde{d}_\pm \end{pmatrix}$ to get

$$\xi_+ = i\frac{\tilde{u}_-}{\tilde{u}_+} \qquad \xi_- = i\frac{\tilde{d}_-}{\tilde{d}_+}. \tag{4.46}$$

A similar decomposition of the $\Phi_\pm$ spinors as $\Phi_\pm = \begin{pmatrix} u_\pm \\ d_\pm \end{pmatrix}$ leads to 4 equations relating the 4 components $u_\pm$ and $d_\pm$. Namely,

$$\begin{aligned} \mathcal{A}(M)u_+ + i(\tilde{\omega} + k_3)u_- = 0 \\ \mathcal{A}(M)d_+ + i(\tilde{\omega} - k_3)d_- = 0 \\ -\mathcal{A}(-M)u_- - i(\tilde{\omega} - k_3)u_+ = 0 \\ -\mathcal{A}(-M)d_- - i(\tilde{\omega} + k_3)d_+ = 0. \end{aligned} \tag{4.47}$$

From the definition of the Φ we can see that the ratios between components of Φ equal the ratio of the corresponding components of the Ψ field. In other words

$$\xi_+ = i\frac{\tilde{u}_-}{\tilde{u}_+} = i\frac{u_-}{u_+} \qquad \xi_- = i\frac{\tilde{d}_-}{\tilde{d}_+} = i\frac{d_-}{d_+}. \tag{4.48}$$

[6] At least not in principle.

We will now try to solve this system for the two ratios that are of interest to us. Solving the system for these ratios ammounts to obtaining differential equations where the unknown functions are these ratios. With that in mind, we have

$$r^2 f(r)\partial_r \xi_+ = r^2 f(r)\partial_r \left(i\frac{u_-}{u_+} \right) = +i\frac{r^2 f(r)\partial_r u_-}{u+} - i\frac{r^2 f(r) u_- \partial_r u_+}{u_+^2}, \tag{4.49}$$

with

$$\begin{aligned} i\frac{r^2 f(r)\partial_r u_-}{u_+} &= -irM\frac{u_-}{u_+} + (\tilde{\omega} - k_3) = -rM\xi_+ + (\omega - k_3) \\ i\frac{r^2 f(r) u_- \partial_r u_+}{u_+^2} &= (\tilde{\omega} + k_3)\left(\frac{u_-}{u_+}\right)^2 + irM\frac{u_-}{u_+} = -(\tilde{\omega} + k_3)\xi_+^2 + rM\xi_+. \end{aligned} \tag{4.50}$$

Hence, the differential equation for ξ_+ reads

$$r^2 f(r)\partial_r \xi_+ + 2rM\xi_+ = (\tilde{\omega} - k_3) + (\tilde{\omega} + k_3)\xi_+^2 \tag{4.51}$$

from which one can easily deduce the form that the differential equation should have for an arbitrary $\vec{k}$, namely

$$\boxed{r^2 f(r)\partial_r \xi_+ + 2rM\xi_+ = (\tilde{\omega} - |\vec{k}|) + (\tilde{\omega} + |\vec{k}|)\xi_+^2} \tag{4.52}$$

In a similar manner we can find the corresponding differential equation for ξ_-. Once again, we have

$$r^2 f(r)\partial_r \xi_- = r^2 f(r)\partial_r \left(i\frac{d_-}{d_+} \right) = +i\frac{r^2 f(r)\partial_r d_-}{d+} - i\frac{r^2 f(r) d_- \partial_r d_+}{d_+^2}, \tag{4.53}$$

with

$$\begin{aligned} i\frac{r^2 f(r)\partial_r d_-}{d_+} &= -irM\frac{d_-}{d_+} + (\tilde{\omega} + k_3) = -rM\xi_- + (\tilde{\omega} + k_3) \\ i\frac{r^2 f(r) d_- \partial_r d_+}{d_+^2} &= (\tilde{\omega} - k_3)\left(\frac{d_-}{d_+}\right)^2 + irM\frac{d_-}{d_+} = -(\tilde{\omega} - k_3)\xi_-^2 + rM\xi_-. \end{aligned} \tag{4.54}$$

The differential equation for ξ_- reads

$$r^2 f(r)\partial_r \xi_- + 2rM\xi_- = (\tilde{\omega} + k_3) + (\tilde{\omega} - k_3)\xi_-^2, \tag{4.55}$$

and the one for arbitrary $\vec{k}$ is

$$\boxed{r^2 f(r)\partial_r \xi_- + 2rM\xi_- = (\tilde{\omega} + |\vec{k}|) + (\tilde{\omega} - |\vec{k}|)\xi_-^2} \tag{4.56}$$

where $\tilde{\omega} = \frac{\omega + eA_t(r)}{f(r)}$. In what follows we shall use k to denote the magnitude of $\vec{k}$ but for the sake of simplicity we will assume that the only non-vanishing component is along the z-axis.

It is clear that we can map eq. (4.52) to eq. (4.56), with the substitution $k \leftrightarrow -k$. Therefore,

$$\xi_+(k) = \xi_-(-k). \tag{4.57}$$

In other words we don't need to solve both equations; as soon as we have ξ_+ we can easily find ξ_- and vice-versa.

Then the ξ-matrix reads

$$\begin{aligned}\xi = \begin{pmatrix} \xi_+(k) & 0 \\ 0 & \xi_-(k) \end{pmatrix} = \begin{pmatrix} \xi_+(k) & 0 \\ 0 & \xi_+(-k) \end{pmatrix} = \begin{pmatrix} \xi_+^s(k)+\xi_+^a(k) & 0 \\ 0 & \xi_+^s(k)-\xi_+^a(k) \end{pmatrix} \\ = \xi_+^s(k)\begin{pmatrix} 1 & 0 \\ 0 & 1 \end{pmatrix} + \xi_+^a(k)\begin{pmatrix} 1 & 0 \\ 0 & -1 \end{pmatrix} \\ = \xi_+^s(k)\mathbb{I} + \xi_+^a(k)\sigma^3,\end{aligned} \tag{4.58}$$

where

$$\begin{aligned}\xi_+^s(k) &= \frac{1}{2}\left(\xi_+(k)+\xi_+(-k)\right) \\ \xi_+^a(k) &= \frac{1}{2}(\xi_+(k)-\xi_+(-k)).\end{aligned} \tag{4.59}$$

Therefore, solving eq. (4.22) for the unknown function $\xi_+(k)$ we can calculate the coefficients $\xi_+^{s/a}$ of the ξ matrix when decomposed in the Pauli matrices via eq. (4.59). Consequently, we can also calculate the coefficients of the decomposition of the self energy matrix via

$$\begin{aligned}\Sigma_0^+(k) &= -g\lim_{r_0\to\infty} r_0^{2M}\xi_+^s(r_0,k) \\ \Sigma_3^+(k) &= -g\lim_{r_0\to\infty} r_0^{2M}\xi_+^a(r_0,k)\end{aligned} \tag{4.60}$$

4.3 Adding a second fermion

What we did in the previous chapter, was to introduce a free Dirac fermion in the bulk that could interact with the gauge field via a coupling constant e. This construction led to an effective description of an interacting right handed chiral fermion whose chemical potential is proportional to that coupling constant.

However, to describe WSM we need two fermions of opposite chirality. Therefore, the next step we need to take is rather straightforward and trivial up to a point. We simply add a second Dirac fermion in the bulk that will interact with the gauge field with a different coupling constant, say e_2. In this case, though, we impose a different boundary condition, namely $\delta\Psi_-\Big|_{r=r_0} = 0$, that in complete analogy with the previous section, will lead to an effective description of a chiral fermion of left chirality.

Nonetheless, in the previous chapters our attention was mostly focused on the unique property of WSM which is CME. We saw, that a crucial condition for the existence of CME was the separation of the two chiralities in energy. Therefore, if we want to discuss CME in a holographic context we need to find a way to implement this separation. As we noted the chemical potential for the right chiral fermion was proportional to the coupling constant between the Dirac fermion and the gauge field. Hence, it is easy to see that choosing a different coupling constant for the second Dirac fermion that we put in the bulk, results in a different chemical potential for the boundary chiral fermion! Since our field theoretical analysis adopted a symmetric separation, where the positive chirality was shifted by $+b_0$ and the negative by $-b_0$, we will maintain this approach in the AdS/CFT calculation by setting $e_2 = -e$.

4.3.1 Left chiral fermion propagator

The procedure we will follow resembles to a large extend the one we followed to introduce the first Dirac fermion. For simplicity we shall omit putting indices, e.g. $1, 2$, to distinguish between the two fermions. It is clear that Ψ in the previous section meant Ψ_1, i.e. the bulk Dirac fermion

that led to a boundary right-handed chiral fermion, while in this section Ψ means Ψ_2, i.e. the bulk Dirac fermion that will lead to a boundary left-handed chiral fermion. In complete analogy with the previous chapter we start from the on-shell action

$$\begin{aligned} S_{on-shell}[\Psi_R,\Psi_L] &= S_{kin}[\Psi_R,\Psi_L] + S_{\partial}[\Psi_R,\Psi_L] \\ &= iZ\int_{r=r_0} d^4x\sqrt{-h}\sqrt{g_{rr}}\bar{\Psi}_L\tilde{\not{D}}\Psi_L - ig_f\int_{r=r_0} d^4x\sqrt{-h}\bar{\Psi}_L\Psi_R. \end{aligned} \tag{4.61}$$

In this case, the boundary kinetic term, analogue of eq. (4.19), involves the left chiral component Ψ_L and the boundary term that we include to have a well posed variational problem, is the appropriate one according to eq. (4.18).

Again we proceed with each term separately. Hence,

$$\begin{aligned} -ig_f\int_{r=r_0} d^4x\sqrt{-h}\bar{\Psi}_L\Psi_R &= -ig_f\int_{r=r_0} d^4x\sqrt{-h}\begin{pmatrix} 0 & \Psi_-^\dagger \end{pmatrix}\begin{pmatrix} 0 & -1 \\ 1 & 0 \end{pmatrix}\begin{pmatrix} \Psi_+ \\ 0 \end{pmatrix} = -ig_f\int_{r=r_0} d^4x\sqrt{-h}\Psi_-^\dagger\Psi_+ \\ &= -ig_f\int_{r=r_0} d^4x\sqrt{-h}\Psi_-^\dagger(i\xi^{-1}\Psi_-) = g_f\int_{r=r_0} d^4x\sqrt{-h}\Psi_-^\dagger\xi^{-1}\Psi_- \\ &= g_f\int d^4x\sqrt{-h}\{\int\frac{d^4p}{(2\pi)^4}\tilde{\Psi}_-^\dagger(r_0,p)e^{-ip.x}\}\xi^{-1}\{\int\frac{d^4k}{(2\pi)^4}\tilde{\Psi}_-(r_0,k)e^{ik.x}\} \\ &= g_f\int\frac{d^4pd^4k}{(2\pi)^8}\sqrt{-h}\tilde{\Psi}_-^\dagger(r_0,p)\xi^{-1}\tilde{\Psi}_-(r_0,k)\{\int d^4xe^{-i(p_\mu-k_\mu)x^\mu}\} \\ &= g_f\int\frac{d^4pd^4k}{(2\pi)^8}\sqrt{-h}\tilde{\Psi}_-^\dagger(r_0,p)\xi^{-1}\tilde{\Psi}_-(r_0,k)(2\pi)^4\delta(p\mu-k\mu) \\ &= g_f\int\frac{d^4p}{(2\pi)^4}\sqrt{-h}\tilde{\Psi}_-^\dagger(r_0,p)\xi^{-1}\tilde{\Psi}_-(r_0,p), \end{aligned} \tag{4.62}$$

and

$$\begin{aligned} \bar{\Psi}_L\tilde{\not{D}}\Psi_L &= \begin{pmatrix} 0 & \Psi_-^\dagger \end{pmatrix}\Gamma^{\underline{t}}\Gamma^t(\partial_t+ie\mu)\begin{pmatrix} 0 \\ \Psi_- \end{pmatrix} + \begin{pmatrix} 0 & \Psi_-^\dagger \end{pmatrix}\Gamma^{\underline{t}}\Gamma^i\partial_i\begin{pmatrix} 0 \\ \Psi_- \end{pmatrix} \\ &= -e^t_{\underline{t}}(r_0)\Psi_+^\dagger(\partial_t+ie\mu)\Psi_- + e^i_{\underline{i}}(r_0)\Psi_-^\dagger\sigma^{\underline{i}}\partial_i\Psi_- \\ &= -\int\frac{d^4pd^4k}{(2\pi)^8}\Big\{e^t_{\underline{t}}(r_0)\tilde{\Psi}_-^\dagger(r_0,p)e^{-ip_\mu x^\mu}(\partial_t+ie\mu)\left(\tilde{\Psi}_-(r_0,k)e^{ik_\mu x^\mu}\right) \\ &\qquad - e^i_{\underline{i}}(r_0)\tilde{\Psi}_-^\dagger(r_0,p)e^{-ip_\mu x^\mu}\sigma^{\underline{i}}\partial_i\left(\tilde{\Psi}_-(r_0,k)e^{ik_\mu x^\mu}\right)\Big\} \\ &= -i\int\frac{d^4pd^4k}{(2\pi)^8}\Big\{e^t_{\underline{t}}(r_0)\tilde{\Psi}_-^\dagger(r_0,p)\tilde{k_0}\tilde{\Psi}_-(r_0,k) - e^i_{\underline{i}}(r_0)\tilde{\Psi}_-^\dagger(r_0,p)\sigma^{\underline{i}}k_i\tilde{\Psi}_-(r_0,k)\Big\}e^{-i(p_\mu-k_\mu)x^\mu} \\ &= -i\int\frac{d^4pd^4k}{(2\pi)^8}\Big\{e^\mu_a(r_0)\tilde{k}_\mu\tilde{\Psi}_-^\dagger(r_0,p)\tilde{\sigma}^a\tilde{\Psi}_-(r_0,k)\Big\}e^{-i(p_\mu-k_\mu)x^\mu}, \end{aligned} \tag{4.63}$$

where $\tilde{k}_0 = k_0 + e\mu = -\omega + e\mu$ and $\tilde{\sigma}^a = (\mathbb{I}, -\vec{\sigma})$. Therefore,

$$
\begin{aligned}
iZ\int_{r=r_0} d^4x\sqrt{-h}\sqrt{g_{rr}}\bar{\Psi}_L\tilde{\not{D}}\Psi_L &= Z\sqrt{-h}\sqrt{g_{rr}}\int\frac{d^4pd^4k}{(2\pi)^8}\Big\{e_a^\mu(r_0)\tilde{k}_\mu\tilde{\Psi}_-^\dagger(r_0,p)\tilde{\sigma}^a\tilde{\Psi}_-(r_0,k)\Big\}\int d^4x e^{-i(p_\mu-k_\mu)x^\mu}\\
&= Z\sqrt{-h}\sqrt{g_{rr}}\int\frac{d^4pd^4k}{(2\pi)^8}\Big\{e_a^\mu(r_0)\tilde{k}_\mu\tilde{\Psi}_-^\dagger(r_0,p)\tilde{\sigma}^a\tilde{\Psi}_-(r_0,k)\Big\}(2\pi)^4\delta(p_\mu-k_\mu)\\
&= Z\sqrt{-h}\sqrt{g_{rr}}\int\frac{d^4k}{(2\pi)^4}\Big\{e_a^\mu(r_0)\tilde{k}_\mu\tilde{\Psi}_-^\dagger(r_0,k)\tilde{\sigma}^a\tilde{\Psi}_-(r_0,k)\Big\}.
\end{aligned}
\tag{4.64}
$$

Putting together eqs. (4.62) and (4.62), the effective, on-shell boundary action for the left handed chiral fermion, eq. (4.61) reads

$$
\begin{aligned}
S_{eff}[\Psi_-] &= \int\frac{d^4k}{(2\pi)^4}\sqrt{-h}\sqrt{g_{rr}}\tilde{\Psi}_-^\dagger(r_0,k)\Big\{g_f\sqrt{g^{rr}}\xi^{-1}(r_0,k)+Ze_a^\mu(r_0)\tilde{k}_\mu\tilde{\sigma}^a\Big\}\tilde{\Psi}_-(r_0,k)\\
&= \int\frac{d^4k}{(2\pi)^4}r_0^3\tilde{\Psi}_-^\dagger(r_0,k)\Big\{g_f r_0 f(r_0)\xi^{-1}(r_0,k)+Z\frac{1}{r_0 f(r_0)}\tilde{k}_0-Z\frac{1}{r_0}\sigma^i k_i\Big\}\tilde{\Psi}_-(r_0,k)\\
&= \int\frac{d^4k}{(2\pi)^4}\tilde{\Psi}_-^\dagger(r_0,k)\Big\{g_f r_0^4 f(r_0)\xi^{-1}(r_0,k)+Z\frac{r_0^2}{f(r_0)}\tilde{k}_0-Zr_0^2\sigma^i k_i\Big\}\tilde{\Psi}_-(r_0,k)\\
&\to \int\frac{d^4k}{(2\pi)^4}\tilde{\Psi}_-^\dagger(r_0,k)\Big\{\tilde{k}_0-f(r_0)\sigma^i k_i+g_f r_0^2 f^2(r_0)Z^{-1}\xi^{-1}(r_0,k)\Big\}\tilde{\Psi}_-(r_0,k).
\end{aligned}
\tag{4.65}
$$

As before, the last term in the brackets is of great importance and we want to calculate it in the double limit $g_f\to 0$ and $r_0\to\infty$. As we mentioned before, for large r_0, $\xi\sim r_0^{-2M}$. Hence $\xi^{-1}\sim r_0^{2M}$ and $\xi^{-1}r_0^{-2M}\to ct.$ We further define $g\equiv g_f r_0^2 f^2(r_0)Z^{-1}$ that remains constant in the above double limit. Then we can define, in analogy with the right chiral fermion

$$
\Sigma_-(k)\equiv -g\lim_{r_0\to\infty} r_0^{-2M}\xi^{-1}(r_0,k). \tag{4.66}
$$

Then the inverse Green's function for the boundary left handed chiral fermion reads

$$
G_-^{-1}(k) = -\omega+e\mu-\sigma^i k_i-\Sigma_-(k) = -\left(\omega-e\mu+\Sigma_0^-\right)-\left(k_i+\Sigma_i^-\right)\sigma^i, \tag{4.67}
$$

where the left chiral fermion's self energy component is expanded in complete analogy with eq. (4.32) as

$$
\Sigma_-(k)=\Sigma_a^-\sigma^a=\Sigma_0^-\mathbb{I}+\Sigma_i^-\sigma^i. \tag{4.68}
$$

Finally we can invert the propagator, and the interacting Green's function for the left handed chiral fermion reads

$$
G_-(k) = -\frac{\left(\omega-e\mu+\Sigma_0^-\right)\mathbb{I}-\left(k_i+\Sigma_i^-\right)\sigma^i}{\left(\omega-e\mu+\Sigma_0^-\right)^2-\left(k_i+\Sigma_i^-\right)^2}. \tag{4.69}
$$

4.3.2 Finding ξ^{-1}

Up to this point, the analysis was nearly identical to the one we performed for the first Dirac fermion we added in the bulk. Apart from a change in the coupling constant, that was trivially incorporated in the analysis with a change of a sign, the second point where the analysis is modified is eq. (4.66). Contrary to eq. (4.30), the self energy for the left chiral fermion is proportional to ξ^{-1} and not to ξ. Nonetheless, the proportionality factor is still defined through

$$
\Psi_- = -i\xi\Psi_+ = -i\begin{pmatrix}\xi_+ & 0\\ 0 & \xi_-,\end{pmatrix}\Psi_+. \tag{4.70}
$$

and thus

$$\xi^{-1} = \begin{pmatrix} \xi_+^{-1} & 0 \\ 0 & \xi_-^{-1} \end{pmatrix}. \tag{4.71}$$

Soon, we will see how the symmetries of the previously derived equations for the components $\xi_\pm$, namely eqs. (4.52) and (4.56), will help us draw conclusions for this case as well. For clarity, we rewrite these equations bearing in mind that now all parameters, such as the mass M, as well as the unknown functions$\xi_\pm$, refer to the second Dirac fermion

$$\begin{aligned} r^2 f(r)\partial_r \xi_+ + 2rM\xi_+ &= (\tilde{\omega} - k_3) + (\tilde{\omega} + k_3)\xi_+^2 r^2 f(r)\partial_r \xi_- \\ +2rM\xi_- &= (\tilde{\omega} + k_3) + (\tilde{\omega} - k_3)\xi_-^2, \end{aligned} \tag{4.72}$$

with $\tilde{\omega} = \frac{\omega - eA_t(r)}{f(r)}$.

To see how the symmetries can help us save some time from trying to find new differential equations for $\xi_\pm^{-1}$, we replace in eq. (4.52) $\xi_+ \to \xi_+^{-1}$ to get

$$\begin{aligned} r^2 f(r)\partial_r \xi_+^{-1} + 2rM\xi_+^{-1} &= (\tilde{\omega} - k_3) + (\tilde{\omega} + k_3)\xi_+^{-2} \\ -\frac{1}{\xi_+^2} r^2 f(r)\partial_r \xi_+ + 2rM\xi_+^{-1} &= (\tilde{\omega} - k_3) + (\tilde{\omega} + k_3)\xi_+^{-2} \\ -r^2 f(r)\partial_r \xi_+ + 2rM\xi_+ &= (\tilde{\omega} + k_3) + (\tilde{\omega} - k_3)\xi_+^2 \\ r^2 f(r)\partial_r \left(-\xi_+\right) + 2r\left(-M\right)\left(-\xi_+\right) &= (\tilde{\omega} + k_3) + (\tilde{\omega} - k_3)\xi_+^2 \end{aligned} \tag{4.73}$$

The last line clearly suggests that ξ_+^{-1} satisfies the same differential equation as $-\xi_+$ for $M \to -M$ and $k_3 \to -k_3$. In symbols

$$\xi_+^{-1}(r; M, \omega, k_3) = -\xi_+(r; -M, \omega, -k_3). \tag{4.74}$$

The dependence of ξ_+ on (M, ω, k_3) is because these parameters appear as coefficients in the differential equation that determines it as a function of r. In other words, for each set of parameters (M, ω, k), we get a different differential equation, the solution of which is ξ_+. In the same way, it is straightforward to see that the same relation holds for ξ_-^{-1}, namely

$$\xi_-^{-1}(r; M, \omega, k_3) = -\xi_-(r; -M, \omega, -k_3). \tag{4.75}$$

Lastly, using a previous symmetry from eq. (4.57), which in the current notation would read

$$\xi_-(r; M, \omega, k_3) = \xi_+(r; M, \omega, -k_3), \tag{4.76}$$

we get that

$$\xi_-^{-1}(r; M, \omega, k_3) = -\xi_-^{-1}(r; -M, \omega, k_3). \tag{4.77}$$

As we did in all previous cases when dealing with 2×2 matrices, we want to expand ξ^{-1} in terms of Pauli matrices. Therefore we have

$$\begin{aligned} \xi^{-1} = \begin{pmatrix} \xi_+^{-1}(M,k) & 0 \\ 0 & \xi_-^{-1}(M,k) \end{pmatrix} &= \begin{pmatrix} -\xi_+(-M,-k) & 0 \\ 0 & -\xi_+(-M,k) \end{pmatrix} \\ &= -\begin{pmatrix} \xi_+^s(-M,-k) + \xi_+^a(-M,-k) & 0 \\ 0 & \xi_+^s(-M,-k) - \xi_-^a(-M,-k) \end{pmatrix} \\ &= -\xi_+^s(-M,-k)\begin{pmatrix} 1 & 0 \\ 0 & 1 \end{pmatrix} - \xi_+^a(-M,-k)\begin{pmatrix} 1 & 0 \\ 0 & -1 \end{pmatrix} \\ &= -\xi_+^s(-M,-k)\mathbb{I} - \xi_+^a(-M,-k)\sigma^3, \end{aligned} \tag{4.78}$$

where we defined

$$\begin{aligned}\xi_+^s(-M,-k) &= \frac{1}{2}(\xi_+(-M,-k)+\xi_+(-M,k))\\ \xi_-^a(-M,-k) &= \frac{1}{2}(\xi_+(-M,-k)-\xi_+(-M,k)).\end{aligned} \tag{4.79}$$

Then the self energy matrix can itself be decomposed as

$$\begin{aligned}\Sigma_-(k) &= -g\lim_{r_0\to\infty} r_0^{-2M}\xi^{-1}(r_0,k)\\ &= g\lim_{r_0\to\infty} r_0^{-2M}\xi_+^s(-M,-k)\mathbb{I} + g\lim_{r_0\to\infty} r_0^{-2M}\xi_-^a(-M,-k)\sigma^3\\ &= \Sigma_0^-\mathbb{I}+\Sigma_3^-\sigma^3.\end{aligned} \tag{4.80}$$

where the self energy components are defined to be

$$\begin{aligned}\Sigma_0^- &= g\lim_{r_0\to\infty} r_0^{-2M}\xi_+^s(-M,-k)\\ \Sigma_3^- &= g\lim_{r_0\to\infty} r_0^{-2M}\xi_+^a(-M,-k).\end{aligned} \tag{4.81}$$

4.4 Boundary spectral functions

At this point, let us briefly recapture what we have accomplished so far. In order to describe a WSM on the boundary, we have placed two Dirac fermions in the bulk, coupled differently to the gauge field. Choosing suitable boundary conditions, each Dirac fermion will lead to a chiral fermion on the boundary of opposite chirality. The difference in the coupling constants will create different energy shifts in the boundary chiral fermions. Thus, quite straightforwardly, combining the two fermions into a single 4-component spinor[7] we can have an interacting propagator that effectively describes the boundary WSM.

To get the propagator, we neeed to solve the differential equation (4.52) for various values of the parameters. Unfortunately, eq. (4.52) cannot be solved analytically for arbitrary values of the parameters. Therefore, a closed form for the interacting propagator is not possible. For that reason, we turn to numerical calculations of the differential equation with the help of Mathematica.

In this section, we plot our numerical results for the spectral function of this composite object for various values of the model parameters. However, we need to be more rigorous here. The propagator of the 4-component composite, boundary fermion we have constructed is a 4×4 matrix. Hence, when we are talking about its spectral function we actually refer to the imaginary part of the trace of the propagator[8], i.e.

$$\rho(k,\omega) = -\frac{1}{\pi}\mathrm{Tr}\left[G(k,\omega)\right] = -\frac{1}{\pi}\mathrm{Tr}\begin{pmatrix} G_+(k) & 0\\ 0 & G_-(k)\end{pmatrix}. \tag{4.82}$$

Our main focus will be on the dependence of $\rho(k,\omega)$ on the masses of the two Dirac fermions we included in the bulk, and more importantly on their coupling constants with the bulk gauge field, that is related to the chemical potential of the boundary fermions. Our reference model will be the one shown in Fig. (4.1) where the model parameters take the values $M_1=-M_2=-\frac{1}{4}$ and $\mu_1=-\mu_2=-\sqrt{2}$.

[7] We choose the term 4-component spinor because this object is not a genuine Dirac spinor. It indeed consists of a right and a left chiral component, but these are constituent parts of two other unrelated Dirac spinors.

[8] We acknowledge the abuse in terminology and only use it for convenience.

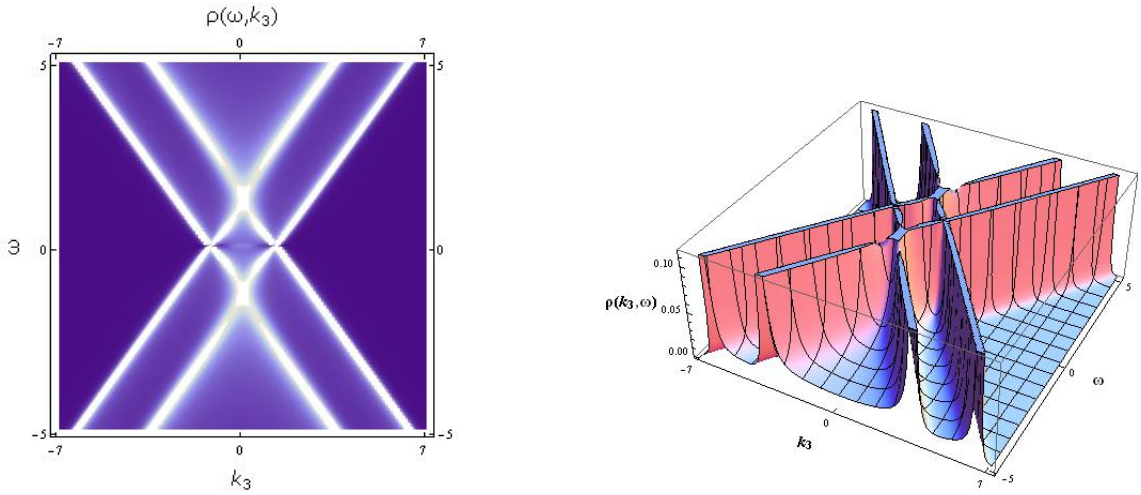

(a) Density Plot (b) 3D Plot

Figure 4.1: $M_1 = \frac{1}{4}, M_2 = -\frac{1}{4}$ and $\mu_1 = \sqrt{2}, \mu_2 = -\sqrt{2}$

With a first examination of these plots, we note that the dispersion relations of the two chiral fermions are clearly recognised. Therefore, the holographic model that we have set up is on the right track in the attempt to describe interacting WSM. Furthermore, the symmetry in the model results in Weyl fermions evenly separated in energy, as was initially expected. Changes in the values of the coupling constants lead to modifications of the interacting spectral function. We can see the behaviour of the response for a few choices of the chemical potentials in Figs. (4.5)-(4.4).

Two comments are in order. Firstly, we see that the values of the masses of the Dirac fermions do not affect the spectral function qualitatively. Rather, it appears that the relation between the masses and the chemical potentials affects the amplitude of the spectral function. As a general remark though, the masses of the Dirac fermions they don't seem to affect the result in a crucial way. Similarly, neither do the values of the chemical potential. Nonetheless, as it was expected, the latter are responsible for the energy separation of the Weyl. The dependence is positive in the sense that the higher the charge, the greater the separation is. Interestingly, when the chemical potentials are three times higher than their reference values, the form of the spectral function appears to change qualitatively with the appearance of extra structure that quite we shall call, in loose and vague sense for now, higher order peaks. Extra analysis required to specify whether this is a proper feature of the system or simply a numerical artifact. Eventually, it will be the actual system under study that will suggest which choice of parameter

4.4.1 Tuning the Dirac masses

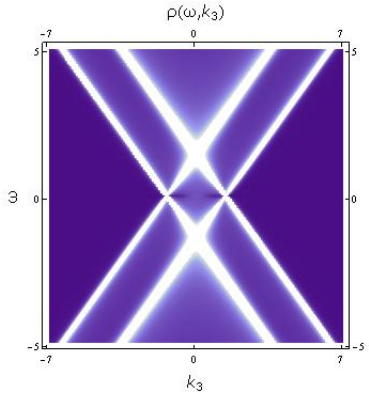

(a) Density Plot

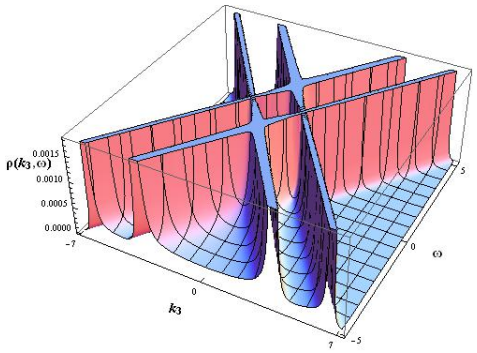

(b) 3D Plot

Figure 4.2: $M_1 = \frac{1}{2}, M_2 = -\frac{1}{2}$ and $\mu_1 = \sqrt{2}, \mu_2 = -\sqrt{2}$

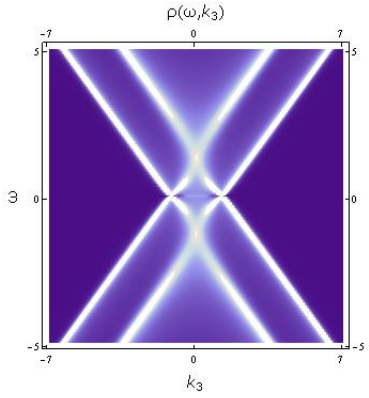

(a) Density Plot

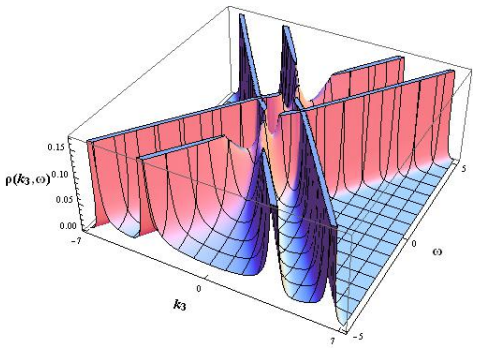

(b) 3D Plot

Figure 4.3: $M_1 = \frac{1}{8}, M_2 = -\frac{1}{8}$ and $\mu_1 = \sqrt{2}, \mu_2 = -\sqrt{2}$

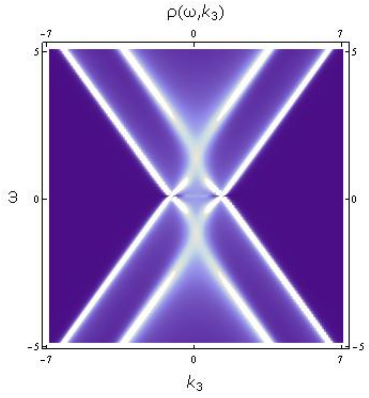

(a) Density Plot

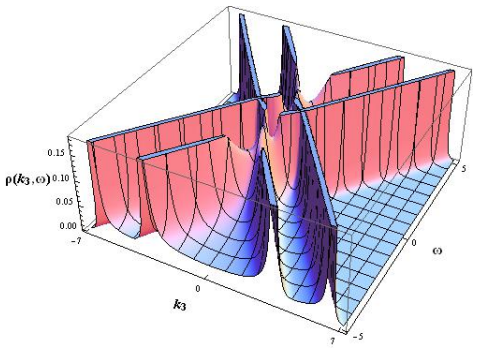

(b) 3D Plot

Figure 4.4: $M_1 = \frac{1}{12}, M_2 = -\frac{1}{12}$ and $\mu_1 = \sqrt{2}, \mu_2 = -\sqrt{2}$

4.4.2 Tuning chemical potentials

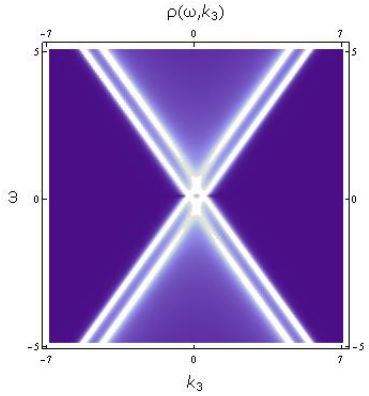

(a) Density Plot

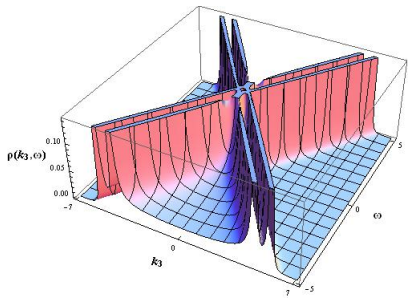

(b) 3D Plot

Figure 4.5: $M_1 = \frac{1}{4}, M_2 = -\frac{1}{4}$ and $\mu_1 = \frac{\sqrt{2}}{3}, \mu_2 = -\frac{\sqrt{2}}{3}$

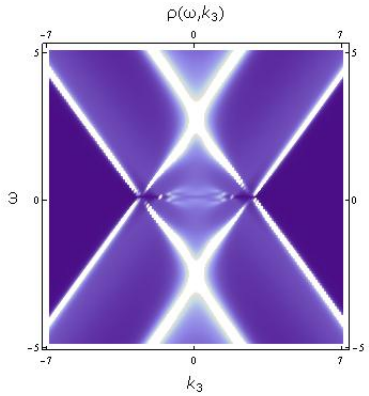

(a) Density Plot

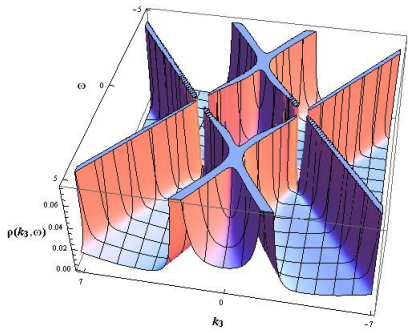

(b) 3D Plot

Figure 4.6: $M_1 = \frac{1}{4}, M_2 = -\frac{1}{4}$ and $\mu_1 = 2\sqrt{2}, \mu_2 = -2\sqrt{2}$

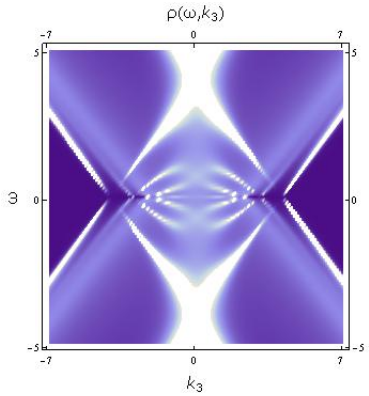

(a) Density Plot

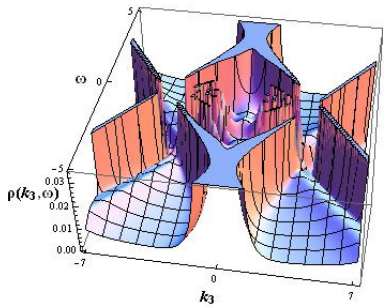

(b) 3D Plot

Figure 4.7: $M_1 = \frac{1}{4}, M_2 = -\frac{1}{4}$ and $\mu_1 = 3\sqrt{2}, \mu_2 = -3\sqrt{2}$

Chapter 5

Discussion and Outlook

Based on a phenomenological, field theory model, a general formula for CME conductivity was provided. This formula expresses σ in terms of the spectral functions of the model, which is also the novel feature of the derivation. Its validity was checked in the absence of electron interactions, and the CME formula found in the literature was derived. At the same time, a holographic model for interacting WSM was constructed from which interacting single-particle Green's functions were obtained.

A first further step, would be to combine the AdS/CFT data with the conductivity formula to study a holographic CME numerically. It will be rather interesting to see if holographic interactions change CME qualitatively, destroying its topological origin. At the same time, a parametric analysis will reveal how model parameters in the gravity dual theory affect CME response. As a second step towards better understanding WSM, will be to create a holographic model for Weyl cones separated in momentum. The suitable gravitational background that will effectively create such a split is far from trivial and is still under thorough research. Provided such a framework can be found, it will make it possible to study how holographic interactions may alter AHE.

On the condensed matter side, a debate related to the true nature of CME is still ongoing. In essence, the question resides on whether Berry phase or chiral anomaly is the main cause of CME. An important argument in favor of the former is the existence of CME even in cases where chirality cannot be accurately defined in the system. Moreover, it would be of considerable importance to check whether finite size and/or disorder effects alter the behavior of CME conductivity.

Appendices

Appendix A

Detailed calculation for a vanishing term

In this Appendix we will go through a detailed calculation of the term

$$\mathcal{I}=\int_0^{\infty}dkk^2\int_{-\infty}^{+\infty}\frac{N_f(\omega^{'})-N_f(\omega^{''})}{\omega+\omega^{'}-\omega^{''}}k\left(g(\omega^{'},k)f^{'}(\omega^{''},k)-f(\omega^{'},k)g^{'}(\omega^{''},k)\right). \tag{A.1}$$

The angular part in the momentum integration is trivial and gives rise only to numerical a prefactor. Since we shall prove that eq. (A.1) vanishes, this extra factor will not be of any importance. Following the steps we took in the main analysis, we will drop any chirality indices from the f and g factors and perform the calculation only for the right chiral fermion. Then the results we will get can be straightforwardly generalised in the case of a left chiral fermion.

Using eqs. (2.64) one can easily see that

$$\begin{aligned}g(\omega^{'},k)f^{'}(\omega^{''},k)&=-\frac{1}{2}(\delta(-\omega^{'}+b_0-k)+\delta(-\omega^{'}+b_0+k))\times\\&\times\left[\frac{1}{2k}(\delta^{'}(-\omega^{''}+b_0-k)-\delta^{'}(-\omega^{''}+b_0+k))-\frac{1}{2k^2}(-\delta(\omega^{''}+b_0-k)-\delta(-\omega^{''}+b_0+k))\right]\\&=-\frac{1}{4k}(-\delta(\omega^{'}+b_0-k)+\delta(-\omega^{'}+b_0+k))(\delta^{'}(-\omega^{''}+b_0-k)-\delta^{'}(-\omega^{''}+b_0+k))\\&+\frac{1}{4k^2}(\delta(-\omega^{'}+b_0-k)+\delta(-\omega^{'}+b_0+k))(\delta(-\omega^{''}+b_0-k)-\delta(-\omega^{''}+b_0+k)),\end{aligned} \tag{A.2}$$

and

$$g^{'}(\omega^{''},k)f(\omega^{'},k)=-\frac{1}{4k}(\delta^{'}(-\omega^{''}+b_0-k)+\delta^{'}(-\omega^{''}+b_0+k))(-\delta(\omega^{'}+b_0-k)-\delta(\omega^{'}+b_0+k)). \tag{A.3}$$

Then

$$
\begin{aligned}
&k[g(\omega^{'},k)f^{'}(\omega^{''}k) - f(\omega^{'},k)g^{'}(\omega^{''},k)] = \\
&= \frac{1}{2}\Big[(\delta(-\omega^{'}+b_0-k)\delta^{'}(-\omega^{''}+b_0+k)) - (\delta(-\omega^{'}+b_0+k)\delta^{'}(-\omega^{''}+b_0-k))\Big] \\
&+ \frac{1}{4k}\Big[(\delta(-\omega^{'}+b_0-k)+\delta(-\omega^{'}+b_0+k))(-\delta(\omega^{''}+b_0-k)-\delta(-\omega^{''}+b_0+k))\Big] \\
&= -g(\omega^{'},k)f(\omega^{''},k) + \frac{1}{2}\Big[\delta(-\omega^{'}+b_0-k)\delta^{'}(-\omega^{''}+b_0+k) - \delta(-\omega^{'}+b_0+k)\delta^{'}(-\omega^{''}+b_0-k)\Big].
\end{aligned}
\tag{A.4}
$$

Therefore, we can decompose the initial integral as

$$
\mathcal{I} = \mathcal{I}_1 + \mathcal{I}_2 \tag{A.5}
$$

with

$$
\begin{aligned}
\mathcal{I}_1 &= \int_0^{\infty} dk k^2 \int_{-\infty}^{+\infty} d\omega^{'} d\omega^{''} \frac{N_f(\omega^{'}) - N_f(\omega^{''})}{\omega+\omega^{'}-\omega^{''}} \Big(-g(\omega^{'},k)f(\omega^{''},k)\Big) \\
\mathcal{I}_2 &= \int_0^{\infty} dk k^2 \int_{-\infty}^{+\infty} d\omega^{'} d\omega^{''} \frac{N_f(\omega^{'}) - N_f(\omega^{''})}{\omega+\omega^{'}-\omega^{''}} \times \\
&\qquad \frac{1}{2}\Big[\delta(-\omega^{'}+b_0-k)\delta^{'}(-\omega^{''}+b_0+k) - \delta(-\omega^{'}+b_0+k)\delta^{'}(-\omega^{''}+b_0-k)\Big]
\end{aligned}
\tag{A.6}
$$

We have already calculated the first integral in eq. (A.6) and we have found that $\mathcal{I}_1 = -\frac{b_0}{4}$. Therefore we focus our attention in the second integral.

Treating the two terms inside $\mathcal{I}_2$ separately, we have

$$
\begin{aligned}
\mathcal{B} &= k^2 \frac{N_f(\omega^{'}) - N_f(\omega^{''})}{\omega+\omega^{'}-\omega^{''}} \delta(-\omega^{'}+b_0-k)\delta^{'}(-\omega^{''}+b_0+k) = k^2 \frac{N_f(b_0-k) - N_f(\omega^{''})}{\omega+b_0-k-\omega^{''}} \delta^{'}(-\omega^{''}+b_0+k) = \\
&= \frac{d}{dk}\left[k^2 \frac{N_f(b_0-k) - N_f(\omega^{''})}{\omega+b_0-k-\omega^{''}} \delta(-\omega^{''}+b_0+k)\right] - \frac{d}{dk}\left[k^2 \frac{N_f(b_0-k) - N_f(\omega^{''})}{\omega+b_0-k-\omega^{''}}\right] \delta(-\omega^{''}+b_0+k) = \\
&= \frac{d}{dk}\left[k^2 \frac{N_f(b_0-k) - N_f(b_0+k)}{\omega-2k}\right] - \frac{d}{dk}\left[k^2 \frac{N_f(b_0-k) - N_f(\omega^{''})}{\omega+b_0-k-\omega^{''}}\right] \delta(-\omega^{''}+b_0+k).
\end{aligned}
\tag{A.7}
$$

Similarly for the second term, we get

$$
\begin{aligned}
\mathcal{C} &= k^2 \frac{N_f(\omega^{'}) - N_f(\omega^{''})}{\omega+\omega^{'}-\omega^{''}} \delta(-\omega^{'}+b_0+k)\delta^{'}(-\omega^{''}+b_0-k) = \\
&= \frac{d}{dk}\left[k^2 \frac{N_f(b_0+k) - N_f(b_0-k)}{\omega+2k}\right] - \frac{d}{dk}\left[k^2 \frac{N_f(b_0+k) - N_f(\omega^{''})}{\omega+b_0+k-\omega^{''}}\right] \delta(-\omega^{''}+b_0-k).
\end{aligned}
\tag{A.8}
$$

Two comments are in order here related to the delta functions in the above expressions. Firstly, at some equalities the integrations over the frequency delta functions were implicitly performed. We believe that the reader will not have a problem identifying these equalities. Secondly, in order to perform these integrals the delta function and the test function should not be "separated" by a derivative operator. In other words either none of them contains a momentum derivative, or they are both under the same derivative operator.

The second term in eq. (A.7) can be further decomposed as

$$\begin{aligned}
&\frac{d}{dk}\left[k^2\frac{N_f(b_0-k)-N_f(\omega^{''})}{\omega+b_0-k-\omega^{''}}\right]\delta(-\omega^{''}+b_0+k)\\
&=\left[2k\frac{N_f(b_0-k)-N_f(\omega^{''})}{\omega+b_0-k-\omega^{''}}+k^2\frac{N_f^{'}(b_0-k)(\omega+b_0-k-\omega^{''})+N_f(b_0-k)-N_f(\omega'')}{(\omega+b_0-k-\omega^{''})^2}\right]\delta(-\omega^{''}+b_0+k)\\
&=\left[2k\frac{N_f(b_0-k)-N_f(b_0+k)}{\omega-2k}+k^2\frac{N_f^{'}(b_0-k)(\omega-2k)+N_f(b_0-k)-N_f(b_0+k)}{(\omega-2k)^2}\right],
\end{aligned} \tag{A.9}$$

and similarly for the second term in eq. (A.8) we get

$$\begin{aligned}
&\frac{d}{dk}\left[k^2\frac{N_f(b_0+k)-N_f(\omega^{''})}{\omega+b_0+k-\omega^{''}}\right]\delta(-\omega^{''}+b_0-k)\\
&=\left[2k\frac{N_f(b_0+k)-N_f(b_0-k)}{\omega+2k}+k^2\frac{N_f^{'}(b_0+k)(\omega+2k)-(N_f(b_0+k)-N_f(b_0-k))}{(\omega+2k)^2}\right],
\end{aligned} \tag{A.10}$$

To see how $\mathcal{I}_2$ behaves in the limit $\omega\to 0$ it is instructive to do some regrouping in the terms that we have found. We can start from the two terms in eqs. (A.7) and (A.8 containing total derivatives of k. Upon subtraction we get

$$\frac{d}{dk}\left[k^2\left(N_f(b_0-k)-N_f(b_0+k)\left(\frac{1}{\omega-2k}+\frac{1}{\omega+2k}\right)\right]=\frac{d}{dk}\left[2k^2\frac{N_f(b_0-k)-N_f(b_0+k)}{(\omega-2k)\,(\omega+2k)}\right]\omega. \tag{A.11}$$

In a similar manner, the first terms of eqs. (A.9) and (A.10) give again upon subtraction

$$2k\left(N_f(b_0-k)-N_f(b_0+k)\right)\left(\frac{1}{\omega-2k}+\frac{1}{\omega-2k}\right)=4k\frac{N_f(b_0-k)-N_f(b_0+k)}{(\omega-2k)(\omega+2k)}\omega \tag{A.12}$$

while the second ones give rise to two more terms that eventually read

$$8k^3\frac{N_f(b_0-k)-N_f(b_0+k)}{(\omega-2k)^2\,(\omega+2k)^2}\omega, \tag{A.13}$$

and

$$k^2\frac{N_f^{'}(b_0-k)-N_f^{'}(b_0+k)}{(\omega)^2-4k^2}\omega+2k^3\frac{N_f^{'}(b_0-k)+N_f^{'}(b_0+k)}{(\omega)^2-4k^2}. \tag{A.14}$$

It is obvious that in the limit $\omega\to 0$ only the very last term survives. Therefore, replacing the surviving term form eq. (A.14) into the second part of eq. A.6, we have

$$\mathcal{I}_2^{+}(\omega=0)=\int_0^{+\infty}dk\frac{k}{4}\left(N_f^{'}(b_0-k)+N_f^{'}(b_0+k)\right)=\frac{b_0}{4}. \tag{A.15}$$

In the last step, we took into account that we have assumed $b_0>0$ and also that we are working in the zero temperature limit, in which the Fermi Dirac distribution reduces to a step function. That means

$$N_f(b_0 - k) = \theta(k - b_0) \Rightarrow N_f^{'}(b_0 - k) = \delta(k - b_0). \tag{A.16}$$

Also, for reminding purposes, we have explicitly restored the chirality index in $\mathcal{I}_2$ to denote explicitly that this is the contribuion to the conductivity coming from only the right chiral fermion.

With simple arguments we can easily recover the analogous formula for the left chiral fermion. This is easily obtained from $\mathcal{I}_2^+$ by adding an extra overall minus sign due to the extra minus sign in the f^- factor, as well as by replacing b_0 by $-b_0$. Then we simply see that

$$\mathcal{I}_2^-(\omega = 0) = -\int_0^{+\infty} dk \frac{k}{4} \left(N_f^{'}(-b_0 - k) + N_f^{'}(-b_0 + k) \right) = \frac{b_0}{4}, \tag{A.17}$$

since in this case

$$N_f(-b_0 + k) = \theta(-k + b_0) \Rightarrow N_f^{'}(b_0 - k) = -\delta(k - b_0). \tag{A.18}$$

Therefore

$$\mathcal{I}_2 = \frac{b_0}{2} \tag{A.19}$$

which exactly cancels out the total contribution coming from $\mathcal{I}_1$ when both chiralities are taken into account.

To sum up, we have indeed shown that in the free case eq. (A.1) does not contribute to the conductivity.

Bibliography

[1] J. Bardeen and W. H. Brattain, "The transistor, a semi-conductor triode," *Physical Review*, vol. 74, no. 2, p. 230, 1948.

[2] C. L. Kane and E. J. Mele, "Z 2 topological order and the quantum spin Hall effect," *Physical review letters*, vol. 95, no. 14, p. 146802, 2005.

[3] S.-M. Huang, S.-Y. Xu, I. Belopolski, C.-C. Lee, G. Chang, B. Wang, N. Alidoust, G. Bian, M. Neupane, C. Zhang, *et al.*, "A weyl fermion semimetal with surface fermi arcs in the transition metal monopnictide taas class," *Nature communications*, vol. 6, 2015.

[4] S.-Y. Xu, I. Belopolski, N. Alidoust, M. Neupane, G. Bian, C. Zhang, R. Sankar, G. Chang, Z. Yuan, C.-C. Lee, *et al.*, "Discovery of a weyl fermion semimetal and topological fermi arcs," *Science*, vol. 349, no. 6248, pp. 613–617, 2015.

[5] M. V. Berry, "Quantal phase factors accompanying adiabatic changes," in *Proceedings of the Royal Society of London A: Mathematical, Physical and Engineering Sciences*, vol. 392, pp. 45–57, The Royal Society, 1984.

[6] J. Zak, "Berry's phase for energy bands in solids," *Physical review letters*, vol. 62, no. 23, p. 2747, 1989.

[7] A. Burkov, "Anomalous hall effect in weyl metals," *Physical review letters*, vol. 113, no. 18, p. 187202, 2014.

[8] G. Hooft, "Dimensional reduction in quantum gravity," *arXiv preprint gr-qc/9310026*, 1993.

[9] L. Susskind, "The world as a hologram," *Journal of Mathematical Physics*, vol. 36, no. 11, pp. 6377–6396, 1995.

[10] J. Maldacena, "The large-N limit of superconformal field theories and supergravity," *International journal of theoretical physics*, vol. 38, no. 4, pp. 1113–1133, 1999.

[11] J. D. Bekenstein, "Black holes and the second law," *Lettere Al Nuovo Cimento (1971-1985)*, vol. 4, no. 15, pp. 737–740, 1972.

[12] S. W. Hawking, "Particle creation by black holes," *Communications in mathematical physics*, vol. 43, no. 3, pp. 199–220, 1975.

[13] T. Faulkner and J. Polchinski, "Semi-holographic Fermi liquids," *Journal of High Energy Physics*, vol. 2011, no. 6, pp. 1–23, 2011.

[14] A. Mukhopadhyay and G. Policastro, "Phenomenological Characterization of Semiholographic Non-Fermi Liquids," *Physical review letters*, vol. 111, no. 22, p. 221602, 2013.

[15] E. Iancu and A. Mukhopadhyay, "A semi-holographic model for heavy-ion collisions," *arXiv preprint arXiv:1410.6448*, 2014.

[16] S. A. Hartnoll, J. Polchinski, E. Silverstein, and D. Tong, "Towards strange metallic holography," *Journal of High Energy Physics*, vol. 2010, no. 4, pp. 1–54, 2010.

[17] M. Z. Hasan and C. L. Kane, "Colloquium: topological insulators," *Reviews of Modern Physics*, vol. 82, no. 4, p. 3045, 2010.

[18] M. Z. Hasan, S.-Y. Xu, and M. Neupane, "Topological Insulators, Topological Crystalline Insulators, Topological Semimetals and Topological Kondo Insulators," *arXiv preprint arXiv:1406.1040*, 2014.

[19] G. Volovik, "Topology of quantum vacuum, Chapter in proceedings of the Como Summer School on analogue gravity," *arXiv preprint arXiv:1111.4627*.

[20] G. E. Volovik and G. Volovik, "The universe in a helium droplet," 2009.

[21] A. M. Turner, A. Vishwanath, and C. O. Head, "Beyond band insulators: topology of semi-metals and interacting phases," *Topological Insulators*, vol. 6, p. 293, 2013.

[22] P. Hosur and X. Qi, "Recent developments in transport phenomena in Weyl semimetals," *Comptes Rendus Physique*, vol. 14, no. 9, pp. 857–870, 2013.

[23] K. Landsteiner, "Anomalous transport of Weyl fermions in Weyl semimetals," *Physical Review B*, vol. 89, no. 7, p. 075124, 2014.

[24] A. Burkov, "Chiral anomaly and transport in Weyl metals," *Journal of Physics: Condensed Matter*, vol. 27, no. 11, p. 113201, 2015.

[25] O. Vafek and A. Vishwanath, "Dirac fermions in solids-from high Tc cuprates and graphene to topological insulators and Weyl semimetals," *arXiv preprint arXiv:1306.2272*, 2013.

[26] S. A. Hartnoll, "Lectures on holographic methods for condensed matter physics," *Classical and Quantum Gravity*, vol. 26, no. 22, p. 224002, 2009.

[27] J. McGreevy, "Holographic duality with a view toward many-body physics," *Advances in High Energy Physics*, vol. 2010, 2010.

[28] S. Sachdev, "Condensed matter and AdS/CFT," in *From Gravity to Thermal Gauge Theories: The AdS/CFT Correspondence*, pp. 273–311, Springer, 2011.

[29] Z. Sybesma, "Weyl Semimetals and Holography with a hint of Massive Spinors," Master's thesis, Institute of Theoretical Physics, Utrecht University, 2012.

[30] P. Borman, "Holographic Fermions: From Black Branes Towards Cold Atoms," Master's thesis, Institute of Theoretical Physics, Utrecht University, 2014.

[31] V. Jacobs, *Dirac and Weyl semimetals with holographic interactions*. PhD thesis, Utrecht University, 2015.

[32] M. Vazifeh and M. Franz, "Electromagnetic response of Weyl semimetals," *Physical review letters*, vol. 111, no. 2, p. 027201, 2013.

[33] H. T. Stoof, K. B. Gubbels, and D. B. Dickerscheid, *Ultracold quantum fields*, vol. 1. Springer, 2009.

[34] A. Altland and B. D. Simons, *Condensed matter field theory*. Cambridge University Press, 2010.

[35] K. Fukushima, D. E. Kharzeev, and H. J. Warringa, "Chiral magnetic effect," *Physical Review D*, vol. 78, no. 7, p. 074033, 2008.

[36] D. E. Kharzeev and H. J. Warringa, "Chiral magnetic conductivity," *Physical Review D*, vol. 80, no. 3, p. 034028, 2009.

[37] K. Fukushima, D. E. Kharzeev, and H. J. Warringa, "Electric-current susceptibility and the chiral magnetic effect," *Nuclear Physics A*, vol. 836, no. 3, pp. 311–336, 2010.

[38] D. E. Kharzeev, "The chiral magnetic effect and anomaly-induced transport," *Progress in Particle and Nuclear Physics*, vol. 75, pp. 133–151, 2014.

[39] K. Fukushima, "Views of the chiral magnetic effect," in *Strongly Interacting Matter in Magnetic Fields*, pp. 241–259, Springer, 2013.

[40] G. Başar, D. E. Kharzeev, and H.-U. Yee, "Triangle anomaly in Weyl semimetals," *Physical Review B*, vol. 89, no. 3, p. 035142, 2014.

[41] A. Burkov and L. Balents, "Weyl semimetal in a topological insulator multilayer," *Physical review letters*, vol. 107, no. 12, p. 127205, 2011.

[42] A. Zyuzin, S. Wu, and A. Burkov, "Weyl semimetal with broken time reversal and inversion symmetries," *Physical Review B*, vol. 85, no. 16, p. 165110, 2012.

[43] Y. Chen, S. Wu, and A. Burkov, "Axion response in Weyl semimetals," *Physical Review B*, vol. 88, no. 12, p. 125105, 2013.

[44] M.-C. Chang and M.-F. Yang, "Chiral magnetic effect in a two-band lattice model of Weyl semimetal," *Physical Review B*, vol. 91, no. 11, p. 115203, 2015.

[45] R. A. Bertlmann, *Anomalies in quantum field theory*, vol. 91. Oxford University Press, 2000.

[46] H. Banerjee, "Chiral anomalies in field theories," *arXiv preprint hep-th/9907162*, 1999.

[47] H. B. Nielsen and M. Ninomiya, "The Adler-Bell-Jackiw anomaly and Weyl fermions in a crystal," *Physics Letters B*, vol. 130, no. 6, pp. 389–396, 1983.

[48] Q. Li, D. E. Kharzeev, C. Zhang, Y. Huang, I. Pletikosic, A. Fedorov, R. Zhong, J. Schneeloch, G. Gu, and T. Valla, "Observation of the chiral magnetic effect in ZrTe5," *arXiv preprint arXiv:1412.6543*, 2014.

[49] C. Shekhar, F. Arnold, S.-C. Wu, Y. Sun, M. Schmidt, N. Kumar, A. G. Grushin, J. H. Bardarson, R. D. d. Reis, M. Naumann, *et al.*, "Large and unsaturated negative magnetoresistance induced by the chiral anomaly in the Weyl semimetal TaP," *arXiv preprint arXiv:1506.06577*, 2015.

[50] C. Zhang, S.-Y. Xu, I. Belopolski, Z. Yuan, Z. Lin, B. Tong, N. Alidoust, C.-C. Lee, S.-M. Huang, H. Lin, *et al.*, "Observation of the Adler-Bell-Jackiw chiral anomaly in a Weyl semimetal," *arXiv preprint arXiv:1503.02630*, 2015.

[51] H.-U. Yee, "Holographic chiral magnetic conductivity," *Journal of High Energy Physics*, vol. 2009, no. 11, p. 085, 2009.

[52] V. Rubakov, "On chiral magnetic effect and holography," *arXiv preprint arXiv:1005.1888*, 2010.

[53] A. Rebhan, A. Schmitt, and S. A. Stricker, "Anomalies and the chiral magnetic effect in the Sakai-Sugimoto model," *Journal of High Energy Physics*, vol. 2010, no. 1, pp. 1–36, 2010.

[54] A. Ballon-Bayona, K. Peeters, and M. Zamaklar, "A chiral magnetic spiral in the holographic Sakai-Sugimoto model," *Journal of High Energy Physics*, vol. 2012, no. 11, pp. 1–36, 2012.

[55] R. Contino and A. Pomarol, "Holography for fermions," *Journal of High Energy Physics*, vol. 2004, no. 11, p. 058, 2004.

[56] V. Jacobs, S. Vandoren, and H. Stoof, "Holographic interaction effects on transport in Dirac semimetals," *Physical Review B*, vol. 90, no. 4, p. 045108, 2014.

[57] N. Iqbal and H. Liu, "Real-time response in AdS/CFT with application to spinors," *Fortschritte der Physik*, vol. 57, no. 5-7, pp. 367–384, 2009.

[58] U. Gürsoy, V. Jacobs, E. Plauschinn, H. Stoof, and S. Vandoren, "Holographic models for undoped Weyl semimetals," *Journal of High Energy Physics*, vol. 2013, no. 4, pp. 1–59, 2013.

[59] U. Gürsoy, E. Plauschinn, H. Stoof, and S. Vandoren, "Holography and ARPES sum-rules," *Journal of High Energy Physics*, vol. 2012, no. 5, pp. 1–21, 2012.

[60] "Einstein's vierbein field theory of curved space, author=Yepez, Jeffrey," *arXiv preprint arXiv:1106.2037*, 2011.

[61] S. I. Adler, "Anomalies," *arXiv:hep-th/0411038v3*, 2004.

[62] A. Zyuzin and A. Burkov, "Topological response in Weyl semimetals and the chiral anomaly," *Physical Review B*, vol. 86, no. 11, p. 115133, 2012.

[63] M. O. Goerbig and G. Montambaux, "Dirac Fermions in condensed matter and beyond," *arXiv preprint arXiv:1410.4098*, 2014.

[64] C.-X. Liu, P. Ye, and X.-L. Qi, "Chiral gauge field and axial anomaly in a Weyl semimetal," *Physical Review B*, vol. 87, no. 23, p. 235306, 2013.

Acknowledgements

Writing this thesis was far from a personal accomplishment. On the contrary, quite a few people have contributed in the making either intentionally or not! First and foremost, I would like to thank my two supervisors, Henk Stoof and Vivian Jacobs for their firm guidance and influential presence during these 9 months. Henk, apart from a background in engineering and love for football, I am sure we share a headstrong character. For the sake of this thesis, I am glad we were, mostly, on the same side! I really enjoyed our fruitful and intense discussions. Vivian, I am totally grateful for your unstoppable assistance! Your devotion and tireless willingness to help me with every problem I faced, left me speechless. At the same time, I am also thankful for your time to carefully proofread my thesis thus helping me improve the final quality of my work. For all that, and even more, THANK YOU VIVIAN! Moreover, I was privileged to have short but invaluable discussions with Vladimir Juricic, now assistant professor in Stockholm, Yan Liu, postdoc in Madrid, and Joel Moore, professor in Berkeley. Further, I would like to thank my fellow classmates for the stimulating discussions we had that have helped me overcome any difficulty I came across, one way or the other. Thank you guys, it has been a great pleasure working studying with you! Special thanks to my good friend Konstantinos Vlachoulis who, in really short notice, put his artistic mind into work and took good care of the cover of the thesis. Lastly, I express my gratitude to "State Scholarship Foundation" that supported me financially during the two years of my Master's programme. Completion of this thesis was co-funded through the "IKY Scholarships" project, using resources from the European program "Education and Lifelong Learning" of the European Social Fund of NSRF 2007-2013.

If I am writing these lines, then it means that a circle of my life is about to close. A circle that started a bit more than two years ago, when I decided to pursue a Master in theoretical physics in Utrecht, leaving Greece and electrical engineering behind. It was a tough choice, but it was worth it without the slightest doubt. The time I had here and most importantly the people I had this time with, made it so. Don't expect to read any names; I know it, they know it and this is enough. Nonetheless, it would be an unforgivable omission not to include my friends in Greece whose long range support and presence has always been around. Before I close this part, I should admit that I considered thanking your family a trivial thing to do. It appears, though, that as you grow older you tend to re-consider various things, for whatever the reason might be. I must admit, then, that I do owe a big "THANK YOU" to my family that has been supporting me, both morally and materially all these years of my studies. I will try to prove that this support was worth giving!